

# REPORT 1115

## DESIGN OF TWO-DIMENSIONAL CHANNELS WITH PRESCRIBED VELOCITY DISTRIBUTIONS ALONG THE CHANNEL WALLS <sup>1</sup>

By JOHN D. STANITZ

### SUMMARY

A general method of design is developed for two-dimensional unbranched channels with prescribed velocities as a function of arc length along the channel walls. The method is developed for both compressible and incompressible, irrotational, nonviscous flow and applies to the design of elbows, diffusers, nozzles, and so forth. Two types of compressible flow are considered: the general type, with the ratio of specific heats  $\gamma$  equal to 1.4, for example, and the linearized type, in which  $\gamma$  is  $-1.0$ . Two methods of solution are used: In part I solutions are obtained by relaxation methods; in part II solutions are obtained by a Green's function.

Five numerical examples are given in part I including three elbow designs with the same prescribed velocity as a function of arc length along the channel walls but with incompressible, linearized compressible, and compressible flow. It is concluded that if a nonviscous gas with arbitrary  $\gamma$  (1.4, for example) were to flow through a channel designed for linearized compressible flow ( $\gamma = -1.0$ ), the resulting velocity distribution along the channel walls would be nearly the velocity distribution prescribed for the linearized compressible flow.

One numerical example is presented in part II for an accelerating elbow with linearized compressible flow, and the time required for the solution by a Green's function in part II was considerably less than the time required for the same solution by relaxation methods in part I.

### INTRODUCTION

There are two general types of theoretical problem in two-dimensional fluid motion: (1) the direct problem, in which the distribution of velocity is determined for a prescribed shape of boundary, and (2) the inverse problem, in which the shape of boundary is determined for a prescribed distribution of velocity along the boundary. The direct problem is an analysis problem; the inverse problem is a design problem. This report is concerned with the inverse, or design, problem for two-dimensional, irrotational flow in unbranched channels with prescribed velocities as a function of arc length along the channel walls.

The design of channels with prescribed velocities is important because: (1) Boundary-layer separation losses can be avoided by prescribed velocities that do not decelerate rapidly enough to cause separation, (2) shock losses in com-

pressible flow and cavitation in incompressible flow can be avoided by prescribed velocities that do not exceed certain maximum values dictated by these phenomena, and (3) for compressible flow the desired flow rate can be assured by prescribed velocities that do not result in "choke flow" conditions.

Several methods of channel design have been developed for particular application (refs. 1 and 2, for example). In reference 1 a design method is developed for accelerating elbows in which the velocity increases monotonically along the channel walls. The method is developed for incompressible and linearized ( $\gamma = -1.0$ ) compressible flow. The velocity distribution along the channel walls is not arbitrary and the design method applies to elbows only. In reference 2 a design method is developed for straight, symmetrical channels with contracting or expanding walls. The method is developed for incompressible flow and the velocities are prescribed not as a function of arc length along the channel walls but as a function of circle angle in the transformed circle plane. A more general design is suggested in reference 3, but no attempt is made to develop and apply the method.

In the present report a general method of design is developed for two-dimensional, unbranched channels with prescribed velocities as a function of arc length along the channel walls. The method is developed for both compressible and incompressible, irrotational, nonviscous flow and applies to the design of elbows, diffusers, nozzles, and so forth. Two types of compressible flow are considered: the general type with arbitrary value of  $\gamma$  (1.4, for example) and the linearized type with  $\gamma$  equal to  $-1.0$ . In general, if the prescribed velocity along one channel-wall differs from that along the other, the channel turns so that the downstream flow direction is different from the upstream direction. This change in flow direction cannot be arbitrarily chosen but depends on the prescribed velocity distribution along the walls. Equations are developed for computing this change in flow direction for an arbitrary prescribed velocity distribution with incompressible or linearized compressible flow. Two methods of solution have been developed for the design method and are presented in separate parts of this report. In part I solutions are obtained by relaxation methods (ref. 4). This method of solution results in complete information concerning the distribution of flow conditions throughout the

<sup>1</sup> Supersedes NACA TN 2593, "Design of Two-Dimensional Channels with Prescribed Velocity Distributions Along the Channel Walls. I—Relaxation Solutions" by John D. Stanitz, 1952, and NACA TN 2595, "Design of Two-Dimensional Channels with Prescribed Velocity Distributions Along the Channel Walls. II—Solution by Green's Function" by John D. Stanitz, 1952.

channel and, in addition, can be used to obtain nonlinear solutions for compressible flow with arbitrary values of  $\gamma$ . In part II solutions are obtained by means of a Green's function. This method of solution is limited to incompressible and linearized ( $\gamma = -1.0$ ) compressible flow, but the method is more rapid than relaxation methods, provided information within the channel is not required.

The design method reported herein was developed at the NACA Lewis laboratory during 1950 and is part of a doctoral thesis conducted with the advice of Professor Ascher H. Shapiro of the Massachusetts Institute of Technology.

## PART I

### GENERAL THEORY AND SOLUTION BY RELAXATION METHODS

A general method of design is developed for two-dimensional, unbranched channels with prescribed velocities as functions of arc length along the channel walls. The method is developed for both incompressible and compressible, irrotational, nonviscous flow. Two types of compressible flow are considered: the general type with arbitrary value for the ratio of specific heats  $\gamma$  (1.4, for example), and the linearized type in which  $\gamma$  is equal to  $-1.0$ . The solutions in part I of this report are obtained by relaxation methods and give complete information concerning the flow throughout the channel. Five numerical examples are given, including three elbow designs with the same prescribed velocity as a function of arc length along the channel walls but with incompressible, linearized compressible, and compressible flow.

#### THEORY OF DESIGN METHOD

The design method is developed for two-dimensional channels with prescribed velocities along the channel walls. The prescribed velocity is arbitrary except that stagnation points cannot be prescribed. This exception limits the design method to unbranched channels.

#### PRELIMINARY CONSIDERATIONS

**Assumptions.**—The fluid is assumed to be nonviscous and either compressible or incompressible. The flow is assumed to be two dimensional and irrotational.

The assumption of two-dimensional, nonviscous, irrotational motion limits the design method in practice to channels with thin (negligible) boundary layers, such as exist near the entrance to the channel or after a rapid acceleration of the flow through a contraction in the channel. Even if the boundary layer is thin, the design method is limited to (and finds its most useful application for) prescribed velocity distributions that, from boundary-layer theory, do not decelerate fast enough to result in separation of the boundary layer, which separation alters the "effective" shape of the channel and completely changes the character of the flow.

In some channels with fully developed turbulent boundary layers, the design method might be expected to yield results that are satisfactory, although approximate, because for this

type of flow the rotational motion occurs primarily in regions close to the channel walls. In channel walls with thick or fully developed laminar boundary layers the design method cannot be used, because not only is the rotation of the flow important in most of the channel but, if the channel bends, important secondary flows develop that are not considered by the two-dimensional design method.

**Flow field.**—The flow field of the two-dimensional channel is considered to lie in the physical  $xy$ -plane where  $x$  and  $y$  are Cartesian coordinates expressed as ratios of a characteristic length equal to the constant channel width downstream at infinity. (All symbols are defined in appendix A.)

At each point in the channel (fig. 1) the velocity vector has a magnitude  $Q$  and a direction  $\theta$  where  $Q$  is the fluid velocity expressed as the ratio of a characteristic velocity equal to the constant channel velocity downstream at infinity. For convenience, the velocity  $Q$  is related to a velocity  $q$  by

$$q = Qq_d \quad (1)$$

where  $q$  is the velocity expressed as a ratio of the stagnation speed of sound and the subscript  $d$  refers to conditions downstream at infinity.

The flow direction  $\theta$  at each point in the channel is measured counterclockwise from the positive  $x$ -axis. From figure 1

$$dx = ds \cos \theta \quad (2a)$$

$$dy = ds \sin \theta \quad (2b)$$

where  $ds$  is a differential distance in the direction of  $Q$ , that is, along a streamline.

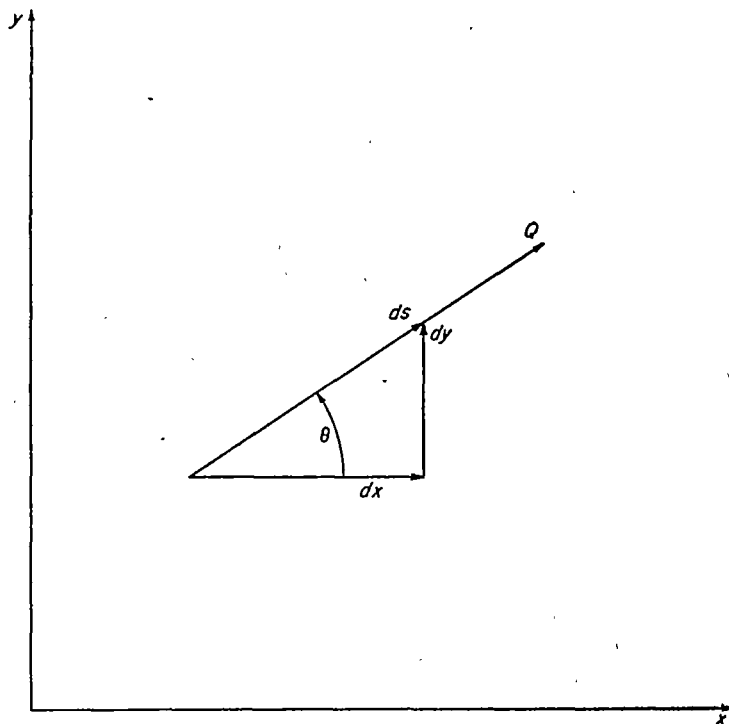


FIGURE 1.—Magnitude and direction of velocity at point in  $xy$ -plane.

Stream function and velocity potential.—If the condition of continuity is satisfied, a stream function  $\psi$  can be defined such that

$$d\psi = \rho Q \, dn \quad (3)$$

where  $\rho$  is the fluid density expressed as the ratio of a characteristic density equal to the stagnation density and where  $dn$  is a differential distance measured normal to the direction of  $Q$ , that is, normal to a streamline. Along a streamline,  $dn$  is zero so that from equation (3) the stream function  $\psi$  is constant.

If the condition of irrotational fluid motion is satisfied, a velocity potential  $\varphi$  can be defined such that

$$d\varphi = Q \, ds \quad (4)$$

Normal to a streamline,  $ds$  is zero so that from equation (4) the velocity potential  $\varphi$  is constant. Thus lines of constant  $\varphi$  and  $\psi$  are orthogonal in the physical  $xy$ -plane.

Outline of method.—Solutions of two-dimensional flow depend on known conditions imposed along the boundaries of the problem. In the inverse problem of channel design, the geometry of the channel walls in the physical  $xy$ -plane is unknown. This unknown geometry apparently precludes the possibility of solving the problem in the physical plane and necessitates the use of some new set of coordinates, that is, a transformed plane, in which to solve the problem. These new coordinates must be such that the geometric boundaries along which the velocities are prescribed are known in the transformed plane. It is also desirable, for mathematical simplicity, that the coordinate system in the transformed plane be orthogonal in the physical plane. A set of coordinates that satisfies these requirements is provided by  $\varphi$  and  $\psi$ , which are orthogonal in the physical  $xy$ -plane and for which the geometric boundaries are known constant values of  $\psi$  in the transformed  $\varphi\psi$ -plane. The distribution of velocity as a function of  $\varphi$  along these boundaries of constant  $\psi$  is known because, if

$$Q = Q(s)$$

is prescribed, equation (4) integrates to give

$$\varphi = \varphi(s)$$

from which equations,

$$Q = Q(\varphi)$$

The technique of the proposed method of channel design is therefore to obtain a differential equation for the distribution of velocity in the  $\varphi\psi$ -plane. The velocity distribution obtained from the solution of this equation is then used to obtain the distribution of flow direction, from which distribution the channel walls in the physical  $xy$ -plane are obtained directly. The differential equation for the distribution of velocity in the  $\varphi\psi$ -plane is nonlinear (for compressible flow with  $\gamma$  other than  $-1.0$ ) and is solved by numerical methods (relaxation methods).

#### DIFFERENTIAL EQUATION FOR DISTRIBUTION OF VELOCITY IN TRANSFORMED $\varphi\psi$ -PLANE

The differential equation for the distribution of velocity in the transformed  $\varphi\psi$ -plane is obtained from the equations for

continuity and irrotational fluid motion expressed in terms of the transformed coordinates  $\varphi$  and  $\psi$ .

Continuity.—The continuity equation expressed in terms of  $\varphi$  and  $\psi$  becomes (appendix B):

$$\frac{1}{\rho} \left( \frac{\partial \log_e \rho}{\partial \varphi} + \frac{\partial \log_e Q}{\partial \varphi} \right) + \frac{\partial \theta}{\partial \psi} = 0 \quad (5)$$

Irrotational fluid motion.—The equation for irrotational fluid motion, expressed in terms of  $\varphi$  and  $\psi$ , becomes (appendix B):

$$\rho \frac{\partial \log_e Q}{\partial \psi} - \frac{\partial \theta}{\partial \varphi} = 0 \quad (6)$$

Differential equation for distribution of velocity.—The second-order partial differential equation for the distribution of  $\log_e Q$  in the transformed  $\varphi\psi$ -plane is obtained by differentiating equations (5) and (6) with respect to  $\varphi$  and  $\psi$ , respectively, and combining to eliminate  $\frac{\partial^2 \theta}{\partial \varphi \partial \psi}$ . Thus,

$$\frac{\partial^2 \log_e \rho}{\partial \varphi^2} + \frac{\partial^2 \log_e Q}{\partial \varphi^2} - \frac{\partial \log_e \rho}{\partial \varphi} \left( \frac{\partial \log_e \rho}{\partial \varphi} + \frac{\partial \log_e Q}{\partial \varphi} \right) + \rho^2 \frac{\partial \log_e Q}{\partial \psi} \frac{\partial \log_e \rho}{\partial \psi} + \rho^2 \frac{\partial^2 \log_e Q}{\partial \psi^2} = 0 \quad (7)$$

Equation (7), together with a relation between  $\rho$ ,  $Q$ , and  $q_a$ , determines the distribution of  $\log_e Q$  in the  $\varphi\psi$ -plane for compressible flow with a given value of  $q_a$  and for arbitrarily prescribed variations in  $\log_e Q$  along the boundaries of constant  $\psi$ .

Density.—The density  $\rho$  is related to the velocity  $q$  by (ref. 5, p. 26, for example)

$$\rho = \left( 1 - \frac{\gamma - 1}{2} q^2 \right)^{\frac{1}{\gamma - 1}} \quad (8a)$$

which, from equation (1), becomes

$$\rho = \left( 1 - \frac{\gamma - 1}{2} Q^2 q_a^2 \right)^{\frac{1}{\gamma - 1}} \quad (8b)$$

Equation (8b) relates the density  $\rho$  to the velocity  $Q$  for a given value of  $q_a$ .

Incompressible flow.—For incompressible flow  $\rho$  is constant and equal to 1.0 so that equation (7) becomes

$$\frac{\partial^2 \log_e Q}{\partial \varphi^2} + \frac{\partial^2 \log_e Q}{\partial \psi^2} = 0 \quad (9)$$

Equation (9) determines the distribution of  $\log_e Q$  in the  $\varphi\psi$ -plane for incompressible flow.

#### CHANNEL-WALL GEOMETRY

After equation (7) or (9) has been solved to obtain the distribution of  $\log_e Q$  in the transformed  $\varphi\psi$ -plane (for the arbitrary specified variations in  $\log_e Q$  with  $\varphi$  along the boundaries of constant  $\psi$ ), the geometry of the channel walls in the physical  $xy$ -plane can be determined from the resulting distribution of flow direction  $\theta$ .

Flow direction  $\theta$ .—The distribution of flow direction  $\theta$  along a streamline (constant  $\psi$ ) is obtained from equation (6), which integrates to give

$$\theta = \int_{\psi} \rho \frac{\partial \log_e Q}{\partial \psi} d\psi \quad (10a)$$

where the subscript  $\psi$  indicates that the integration is taken along a line of constant  $\psi$  and where the constant of integration is selected to give a known value of  $\theta$  at one value of  $\psi$  along each streamline. The integrand in equation (10a) is obtained from the distribution of  $\log_e Q$ , which is known from the solution of equation (7) or (9).

The distribution of flow direction  $\theta$  along a velocity-potential line (constant  $\varphi$ ) is obtained from equation (5), which integrates to give

$$\theta = - \int_{\varphi} \frac{1}{\rho} \left( \frac{\partial \log_e \rho}{\partial \varphi} + \frac{\partial \log_e Q}{\partial \varphi} \right) d\varphi \quad (10b)$$

where the subscript  $\varphi$  indicates that the integration is taken along a line of constant  $\varphi$  and where the constant of integration is selected to give a known value of  $\theta$  at one value of  $\psi$  along each velocity-potential line. As for equation (10a), the integrand in equation (10b) is known from the distribution of  $\log_e Q$  obtained from the solution of equation (7) or (9).

Channel-wall coordinates.—The variation in  $x$  along a line of constant  $\psi$  in the  $\varphi\psi$ -plane is given by

$$\frac{\partial x}{\partial \varphi} = \left( \frac{dx ds}{ds d\varphi} \right)_{\psi}$$

which, combined with equations (2a) and (4), integrates to give

$$x = \int_{\psi} \frac{\cos \theta}{Q} d\psi \quad (11a)$$

Likewise,

$$x = - \int_{\varphi} \frac{\sin \theta}{\rho Q} d\varphi \quad (11b)$$

$$y = \int_{\psi} \frac{\sin \theta}{Q} d\psi \quad (11c)$$

$$y = \int_{\varphi} \frac{\cos \theta}{\rho Q} d\varphi \quad (11d)$$

where the constants of integration are selected to give known values of  $x$  or  $y$  at one value of  $\varphi$  along each streamline or at one value of  $\psi$  along each velocity-potential line. Equations (11a) to (11d) determine the distribution of  $x$  and  $y$  in the transformed  $\varphi\psi$ -plane or, which is the same thing, the shape of the streamlines and velocity-potential lines in the physical  $xy$ -plane. In particular, equations (11a) and (11c) when integrated along the boundaries of constant  $\psi$  in the  $\varphi\psi$ -plane determine the shape of the channel walls.

Turning angle.—In general, if the prescribed velocity distribution along one channel wall differs from the distribution along the other wall, the channel deflects an amount  $\Delta\theta$ , which is the difference in flow direction far downstream and far upstream of the region in which the prescribed velocity

distribution varies. In part II it is shown that for incompressible flow the turning angle  $\Delta\theta$  is given by

$$\begin{aligned} \Delta\theta &= \theta_a - \theta_u \\ &= - \int_{-\infty}^{\infty} \varphi \left[ \left( \frac{\partial \log_e Q}{\partial \varphi} \right)_{1.0} - \left( \frac{\partial \log_e Q}{\partial \varphi} \right)_0 \right] d\varphi \end{aligned} \quad (12)$$

where the subscript  $u$  refers to conditions upstream at infinity and where the subscripts 0 and 1.0 refer to the channel boundaries along which  $\psi$  equals 0 and 1.0, respectively. A similar equation will be given later for the case of linearized compressible flow.

#### LINEARIZED COMPRESSIBLE FLOW

The nonlinear differential equation (7) for the distribution of velocity in the  $\varphi\psi$ -plane with compressible flow becomes linear and is considerably simplified if a linear variation in pressure with specific volume ( $1/\rho$ ) is assumed. This linear relation between pressure and specific volume was first suggested by Chaplygin (ref. 6) in order to linearize the differential equations for two-dimensional compressible flow in the hodograph plane.

Density.—If a linear variation in pressure with specific volume is assumed, the density  $\rho^*$  is related to the velocity  $q^*$  by (appendix C)

$$\rho^* = (1 + q^{*2})^{-1/2} \quad (13)$$

where

$$\rho^* = k_1 \rho \quad (13a)$$

and

$$q^* = k_2 q \quad (13b)$$

where the constants  $k_1$  and  $k_2$  have been determined so that values of  $\rho$  given by equation (13) equal the values of  $\rho$  given by equation (8a) for any two selected values of  $q$  (designated by  $q_a$  and  $q_b$ ). Thus,

$$k_1 = \frac{1}{\rho_a} \sqrt{\frac{1 - \left( \frac{\rho_a q_a}{\rho_b q_b} \right)^2}{1 - \left( \frac{q_a}{q_b} \right)^2}} \quad (14a)$$

and

$$k_2 = \frac{1}{q_b} \sqrt{\frac{\left( \frac{\rho_a}{\rho_b} \right)^2 - 1}{1 - \left( \frac{\rho_a q_a}{\rho_b q_b} \right)^2}} \quad (14b)$$

where  $\rho_a$  and  $\rho_b$  are determined by equation (8a) for the selected values of  $q_a$  and  $q_b$ , respectively. A discussion of the selection of  $q_a$  and  $q_b$  is given in appendix C. It will be noted that, if  $\gamma$  is equal to  $-1.0$ , equation (8a) has the same form as equation (13).

Stream function and velocity potential.—For the case of linearized compressible flow it is convenient to define the stream function  $\psi^*$  and the velocity potential  $\varphi^*$  by

$$d\psi^* = \rho^* q^* dn \quad (15)$$

and

$$d\varphi^* = q^* ds \quad (16)$$

Continuity.—The continuity equation expressed in terms of  $\varphi^*$  and  $\psi^*$  becomes (appendix D)

$$\frac{\partial \log_e u}{\partial \varphi^*} + \frac{\partial \theta}{\partial \psi^*} = 0 \quad (17)$$

where

$$u = \frac{q^*}{1 + \sqrt{1 + q^{*2}}} \quad (18)$$

or, conversely,

$$q^* = \frac{2u}{1 - u^2} \quad (19)$$

Irrotational fluid motion.—The equation for irrotational fluid motion, expressed in terms of  $\varphi^*$  and  $\psi^*$ , becomes (appendix D)

$$\frac{\partial \log_e u}{\partial \psi^*} - \frac{\partial \theta}{\partial \varphi^*} = 0 \quad (20)$$

Differential equation for distribution of  $\log_e u$ .—The partial differential equation for the distribution of  $\log_e u$  in the  $\varphi^*\psi^*$ -plane is obtained by differentiating equations (17) and (20) with respect to  $\varphi^*$  and  $\psi^*$ , respectively, and combining to eliminate  $\frac{\partial^2 \theta}{\partial \varphi^* \partial \psi^*}$ . Thus

$$\frac{\partial^2 \log_e u}{\partial \varphi^{*2}} + \frac{\partial^2 \log_e u}{\partial \psi^{*2}} = 0 \quad (21)$$

Equation (21) determines the distribution of  $\log_e u$  in the  $\varphi^*\psi^*$ -plane for linearized compressible flow with a given value of  $q_a$  and for arbitrarily prescribed variations in  $\log_e Q$ , related to  $\log_e u$  by equations (1), (13b), and (18), along the boundaries of constant  $\psi^*$ . Equation (21) is linear and is, like equation (9) for the case of incompressible flow, the equation of Laplace. Thus an incompressible flow solution for the distribution of  $\log_e Q$  in the  $\varphi\psi$ -plane is also a linearized compressible flow solution for the distribution of  $\log_e u$  in the  $\varphi^*\psi^*$ -plane. The transformation from the  $\varphi\psi$ -plane is different, however, from the transformation from the  $\varphi^*\psi^*$ -plane so that different channel shapes result in the  $xy$ -plane.

Flow direction  $\theta$ .—The distribution of flow direction  $\theta$  along a streamline (constant  $\psi^*$ ) is obtained from equation (20), which integrates to give

$$\theta = \int_{\psi^*} \frac{\partial \log_e u}{\partial \psi^*} d\psi^* \quad (22a)$$

Likewise, the distribution of flow direction  $\theta$  along a velocity-potential line (constant  $\varphi^*$ ) is obtained from equation (17), which integrates to give

$$\theta = - \int_{\varphi^*} \frac{\partial \log_e u}{\partial \varphi^*} d\varphi^* \quad (22b)$$

Equations (22a) and (22b) for linearized compressible flow correspond to, and are used in the same manner as, equations (10a) and (10b) for the usual type of compressible or incompressible flow.

Channel-wall coordinates.—The variation in  $x$  along a line of constant  $\psi^*$  in the  $\varphi^*\psi^*$ -plane is given by

$$\frac{\partial x}{\partial \varphi^*} = \left( \frac{dx}{ds} \frac{ds}{d\varphi^*} \right)_{\psi^*}$$

which combined with equations (2a) and (16) integrates to give

$$x = \int_{\psi^*} \frac{\cos \theta}{q^*} d\varphi^* \quad (23a)$$

Likewise,

$$x = - \int_{\varphi^*} \frac{\sin \theta}{\rho^* q^*} d\psi^* \quad (23b)$$

$$y = \int_{\psi^*} \frac{\sin \theta}{q^*} d\varphi^* \quad (23c)$$

$$y = \int_{\varphi^*} \frac{\cos \theta}{\rho^* q^*} d\psi^* \quad (23d)$$

Equations (23a) to (23d) determine the distribution of  $x$  and  $y$  in the transformed  $\varphi^*\psi^*$ -plane or, which is the same thing, the shape of the streamline and velocity-potential lines in the physical  $xy$ -plane. In particular, equations (23a) and (23c), when integrated along the boundaries of constant  $\psi^*$  in the  $\varphi^*\psi^*$ -plane, determine the shape of the channel walls. Equations (23a) to (23d) for linearized compressible flow correspond to, and are used in the same manner as, equations (11a) to (11d) for the usual type of compressible or incompressible flow.

Turning angle.—In part II it is shown that for linearized compressible flow the turning angle, or difference in flow direction far downstream and far upstream of the region in which the prescribed velocity distribution varies along the channel walls, is given by

$$\Delta \theta = \frac{-1}{\Delta \psi^*} \int_{-\infty}^{\infty} \varphi^* \left[ \left( \frac{\partial \log_e u}{\partial \varphi^*} \right)_{\Delta \psi^*} - \left( \frac{\partial \log_e u}{\partial \varphi^*} \right)_0 \right] d\varphi^* \quad (24)$$

where  $\Delta \psi^*$  is the value of  $\psi^*$  along the left boundary (channel wall) when faced in the direction of flow if the value of  $\psi^*$  along the right boundary is zero, and where the subscript  $\Delta \psi^*$  refers to the boundary along which  $\psi^*$  is equal to  $\Delta \psi^*$ .

## NUMERICAL PROCEDURE

The channel design method in part I of this report was developed for three types of fluid flow: (1) compressible, (2) incompressible, and (3) linearized compressible. Although the numerical procedures of the design method are similar for each type of fluid, the procedures differ in detail and are therefore considered separately in this section.

### COMPRESSIBLE FLOW

The numerical procedure for channel design with compressible flow ( $\gamma=1.4$ , for example) is as follows:

(1) The velocity is specified as a function of arc length along that portion of the channel walls over which the velocity varies

$$q = q(s)$$

or  $q_a$  is specified and

$$Q=Q(s) \quad (25)$$

where  $s$  is arbitrarily equal to zero at that point along one channel wall where the velocity first begins to vary.

(2) The channel-wall boundaries of the flow field in the transformed  $\varphi\psi$ -plane are straight, parallel lines of constant  $\psi$  extending indefinitely far upstream and downstream between  $\varphi$  equals  $\pm\infty$ , where  $\varphi$  is arbitrarily equal to zero at that point on the channel wall at which  $s$  is equal to zero. The value of  $\psi$  along the right channel wall when faced in the direction of flow (direction of positive  $\varphi$ ) is arbitrarily set equal to zero in which case the value of  $\psi$  along the left channel wall ( $\Delta\psi$ ) is obtained by integrating equation (3) across the channel at a position far downstream where flow conditions are uniform

$$\Delta\psi=\rho_a \quad (26)$$

(3) The distribution of  $\log_e Q$  as a function of  $\varphi$  along the boundaries in the  $\varphi\psi$ -plane is obtained by integrating equation (4) between limits so that

$$\varphi=\int_0^s Q ds=\varphi(s) \quad (27)$$

which together with equation (25) gives the distribution of  $\log_e Q$  along the boundaries in the  $\varphi\psi$ -plane

$$\log_e Q=f(\varphi) \quad (28)$$

The integration indicated by equation (27) is carried out numerically for arbitrary distributions of  $Q$  as a function of  $s$ .

(4) If the velocities prescribed along one channel wall differ from those along the other wall, the channel will, in general, turn the flow. This turning angle cannot be determined exactly for compressible flow until the channel design is completed. However, it will be shown that this turning angle is only slightly greater than that resulting for linearized compressible flow with the same prescribed velocity and with a suitable selection for  $q_a$  and  $q_b$  in equations (14a) and (14b). This latter turning angle for linearized compressible flow is given by equation (24), which can be integrated numerically for the arbitrary distribution of  $\log_e u=f(\varphi)$  corresponding to equation (28).

(5) In order to solve equation (7) for the distribution of  $\log_e Q$  in the  $\varphi\psi$ -plane, it is convenient to eliminate the density terms from equation (7) by means of equation (8b). Thus, equation (7) becomes

$$A \frac{\partial^2 \log_e q}{\partial \varphi^2} + B \frac{\partial^2 \log_e q}{\partial \psi^2} + 4C \left( \frac{\partial \log_e q}{\partial \varphi} \right)^2 + 4D \left( \frac{\partial \log_e q}{\partial \psi} \right)^2 = 0 \quad (29)$$

where

$$A = \frac{1 - \frac{\gamma+1}{2} q^2}{\left(1 - \frac{\gamma-1}{2} q^2\right)^{\frac{\gamma+1}{\gamma-1}}}$$

$$B=1.0$$

$$4C = \frac{-q^2 \left(1 + \frac{\gamma+1}{2} q^2\right)}{\left(1 - \frac{\gamma-1}{2} q^2\right)^{\frac{2\gamma}{\gamma-1}}}$$

and

$$4D = \frac{-q^2}{1 - \frac{\gamma-1}{2} q^2}$$

Equation (29) is nonlinear, and it can be solved by relaxation methods (refs. 4 and 7, for example). A grid of equally spaced points, at each of which the value of  $\log_e Q$  is to be determined, is placed in the flow field between the channel-wall boundaries. The grid is extended upstream and downstream sufficiently far so that constant values of  $\log_e Q$  are obtained across the channel by the relaxation methods. In the numerical examples to be presented six or eight grid spaces were used across the channel. In example III the number of grid spaces was reduced from eight to four with negligible effect on the resulting channel design. The values of  $\log_e Q$  at each grid point were relaxed to five significant figures. If the same velocity distribution is prescribed along both walls, the channel is symmetrical so that the velocity distribution in only one half of the channel need be determined by relaxation methods.

(6) After  $\log_e Q$  has been determined at each grid point in the  $\varphi\psi$ -plane, the distribution of  $\theta$  is determined by equations (10a) and (10b), which are integrated numerically. The constants of integration in equations (10a) and (10b) are determined to give a specified value of  $\theta$  at one point in the channel (far upstream, for example). The integrands in equations (10a) and (10b) are determined by numerical methods (tables I to VII, ref. 4, for example) from the known values of  $\rho$  and  $\log_e Q$  at each of the grid points. If it is desired to know the flow direction along the channel-walls only, equation (10a) can be solved along the channel-wall boundaries  $\psi=0$  and  $\psi=\Delta\psi$  only. If it is desired to know  $\theta$  everywhere in the channel, the recommended procedure is to determine the variation in  $\theta$  along the mean streamline ( $\psi=(\Delta\psi)/2$ ) by equation (10a) and to determine the variation in  $\theta$  along each velocity-potential line from the previously determined values on the mean streamline by equation (10b).

(7) After the distributions of  $\log_e Q$  and  $\theta$  are known in the  $\varphi\psi$ -plane, the shapes of the streamlines and the velocity-potential lines in the physical  $xy$ -plane or, which is the same thing, the distributions of  $x$  and  $y$  in the transformed  $\varphi\psi$ -plane are determined by the numerical integration of equations (11a) to (11d). The constants of integration in these equations are determined so that specified values of  $x$  and  $y$  occur at one point in the flow field. The recommended procedure is to determine the variation in  $x$  and  $y$  along the mean streamline by equations (11a) and (11c) and to determine the variation in  $x$  and  $y$  along each velocity-potential line for the previously determined values on the mean streamline by equations (11b) and (11d). If it is desired to know the  $x$  and  $y$  coordinates for the channel walls only, equations (11a) and (11c) can be solved along the channel-wall boundaries  $\psi=0$  and  $\psi=\Delta\psi$  only.

## INCOMPRESSIBLE FLOW

The numerical procedure for channel design with incompressible flow ( $\rho=1$ ) is similar to that just outlined for compressible flow, but with the following differences:

- (1) The velocity is specified as a function of arc length by equation (25) alone.
- (2) The value of  $\psi$  along the left channel wall ( $\Delta\psi$ ) is equal to 1.0 instead of the value given by equation (26).
- (3) The distribution of  $\log_e Q$  as a function of  $\varphi$  along the channel-wall boundaries in the  $\varphi\psi$ -plane is the same as that obtained from equations (25) and (27) and given by equation (28).
- (4) The turning angle  $\Delta\theta$  of the channel is given by equation (12).
- (5) The distribution of  $\log_e Q$  in the  $\varphi\psi$ -plane is obtained from the solution of equation (9) by relaxation methods.
- (6) After  $\log_e Q$  has been determined at each grid point between the channel-wall boundaries in the  $\varphi\psi$ -plane, the distribution of  $\theta$  is determined by equations (10a) and (10b) as indicated previously for compressible flow, but with  $\rho$  equal to unity.
- (7) After the distributions of  $\log_e Q$  and  $\theta$  are known in the  $\varphi\psi$ -plane, the shapes of the streamlines and velocity-potential lines in the physical  $xy$ -plane are determined by equations (11a) to (11d) as indicated previously for compressible flow, but with  $\rho$  equal to unity.

## LINEARIZED COMPRESSIBLE FLOW

The numerical procedure for channel design with linearized compressible flow ( $\gamma=-1.0$ ) is similar to that previously outlined for compressible flow, but with the following differences:

- (1) The velocity  $q$  is specified as a function of arc length along the channel walls by  $q(s)$  or by  $q_a$  and equation (25). For each prescribed velocity, there are an infinite number of linearized compressible flow solutions depending on the selected values of  $q_a$  and  $q_b$  in equations (14a) and (14b). However, for values of  $q_a$  and  $q_b$  within the range of  $q$  prescribed along the channel walls (and therefore everywhere in the channel), the solutions, that is, channel shapes, probably differ only in small detail. The best solution is that most nearly like the nonlinear compressible solution with arbitrary value of  $\gamma$  (1.4, for example). In the numerical examples of this report it is shown that, if  $q_a$  and  $q_b$  are equal to the maximum and minimum values of  $q$ , a good solution results, at least if the ratio of these prescribed velocities is not too large (2:1 in the numerical examples). On the other hand, if continuity is to be satisfied for a gas with the correct value of  $\gamma$  (1.4, for example) upstream and downstream of the region of the channel in which the prescribed velocities vary, then  $q_a$  and  $q_b$  must equal  $q_u$  and  $q_d$ .

After  $q_a$  and  $q_b$  have been selected, the velocity distribution  $q(s)$  is expressed as  $q^*(s)$  by equation (13b) where  $k_2$  is given by equation (14b) so that

$$q^* = q^*(s) \quad (30)$$

The velocity  $q^*$  is then expressed as  $u$  by equation (18) so that

$$u = u(s) \quad (31)$$

In the particular case where the selected value of  $q_a$  is equal to  $q_b$ , the value of  $k_2$  is given by equation (C4b) in appendix C, where the significance of this particular case is also discussed.

- (2) The solution is obtained in the transformed  $\varphi^*\psi^*$ -plane where  $\varphi^*$  and  $\psi^*$  are defined by equations (16) and (15), respectively. If the value of  $\psi^*$  along the right channel wall when faced in the direction of  $q^*$  is zero, the value of  $\psi^*$  along the left wall ( $\Delta\psi^*$ ) is obtained by integrating equation (15) across the channel at a position far downstream where flow conditions are uniform

$$\Delta\psi^* = \rho_a^* q_a^* \quad (32)$$

- (3) The distribution of  $\log_e u$  as a function of  $\varphi^*$  along the channel-wall boundaries in the  $\varphi^*\psi^*$ -plane is obtained by integrating equation (16) between limits similar to those discussed previously for compressible flow so that

$$\varphi^* = \int_0^s q^* ds = \varphi^*(s) \quad (33)$$

which together with equation (31) determines the distribution of  $\log_e u$  along the channel-wall boundaries in the  $\varphi^*\psi^*$ -plane

$$\log_e u = f(\varphi^*) \quad (34)$$

- (4) The turning angle  $\Delta\theta$  of the channel is given by equation (24).
- (5) The distribution of  $\log_e u$  in the  $\varphi^*\psi^*$ -plane is obtained from the solution of equation (21) by relaxation methods.
- (6) After  $\log_e u$  has been determined at each grid point between the channel-wall boundaries in the  $\varphi^*\psi^*$ -plane, the distribution of  $\theta$  is determined by equations (22a) and (22b) in a manner similar to that outlined previously for compressible flow.
- (7) After the distributions of  $\log_e u$  and  $\theta$  are known in the  $\varphi^*\psi^*$ -plane, the shapes of the streamlines and the velocity-potential lines in the physical  $xy$ -plane are determined by equations (23a) to (23d) in a manner similar to that outlined previously for compressible flow. The velocities  $q^*$  in equations (23) are obtained from the known values of  $u$ , and the densities  $\rho^*$  are given by equation (13).

## NUMERICAL EXAMPLES

The channel design method has been applied in part I to the five examples listed below:

Examples	Type of channel	Type of flow
I	Reducing section	Incompressible
II	Converging section	Incompressible
III	Elbow	Incompressible
IV	Elbow	Linearized compressible
V	Elbow	Compressible ( $\gamma=1.4$ )

## EXAMPLE I

The first numerical example is the design of a reducing section in a straight channel such that the upstream velocity is half the downstream velocity. The solution is for incompressible flow.

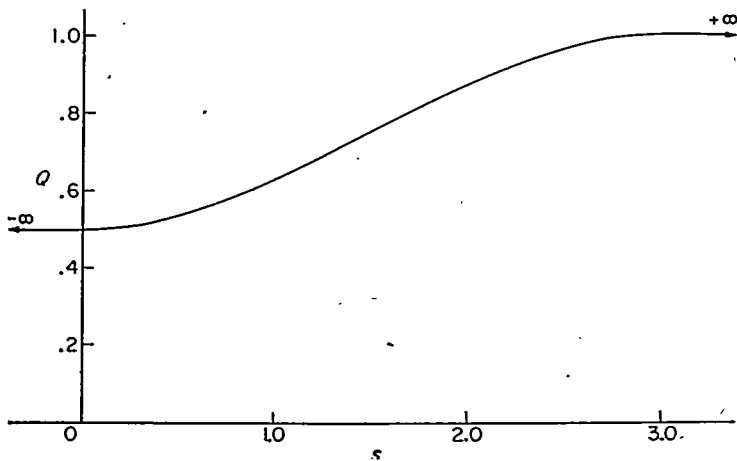


FIGURE 2.—Prescribed velocity distribution as function of arc length along channel wall for examples I, III, IV, and V. Equation (35).

Prescribed velocity distribution.—The prescribed velocity as a function of arc length  $s$  along both channel walls is given by

$$\left. \begin{aligned} Q &= 0.5 & (s \leq 0) \\ Q &= \frac{1}{2} + \frac{s^2}{6} - \frac{s^3}{27} & (0 \leq s \leq 3.0) \\ Q &= 1.0 & (s \leq 3.0) \end{aligned} \right\} \quad (35)$$

The prescribed velocity given by equation (35) is plotted in figure 2.

Equation (35) together with equation (27) results in

$$\left. \begin{aligned} \varphi &= 0.5s & (s \leq 0) \\ \varphi &= \frac{s}{2} + \frac{s^3}{18} - \frac{s^4}{108} & (0 \leq s \leq 3.0) \\ \varphi &= -0.75 + s & (s \leq 3.0) \end{aligned} \right\} \quad (36)$$

From equations (35) and (36),  $\log_e Q$  is a known function of  $\varphi$ , which function is plotted in figure 3.

Results.—The results of example I are presented in figures 4 to 7.

In figure 4, lines of constant velocity  $Q$  and flow direction  $\theta$  are plotted in the transformed  $\varphi\psi$ -plane. The flow direction  $\theta$  is constant and equal to zero along the mean streamline ( $\psi=0.5$ ), indicating that the center line of the channel is straight. The maximum absolute values of  $\theta$  occur along the channel walls. The solution is symmetrical about the mean streamline. The lines of constant  $Q$  and  $\theta$  are orthogonal.

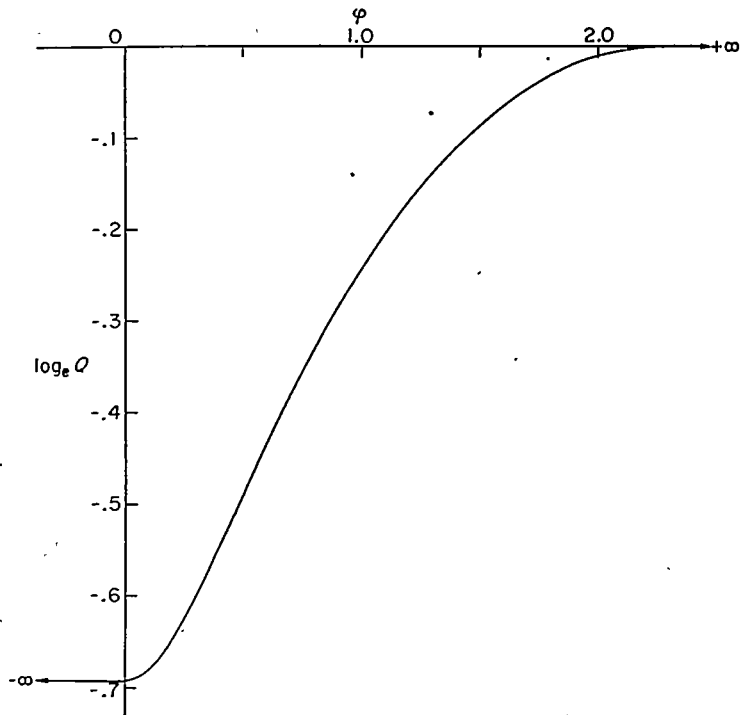


FIGURE 3.—Prescribed distribution of  $\log_e Q$  as function of  $\varphi$  along channel walls for example I.

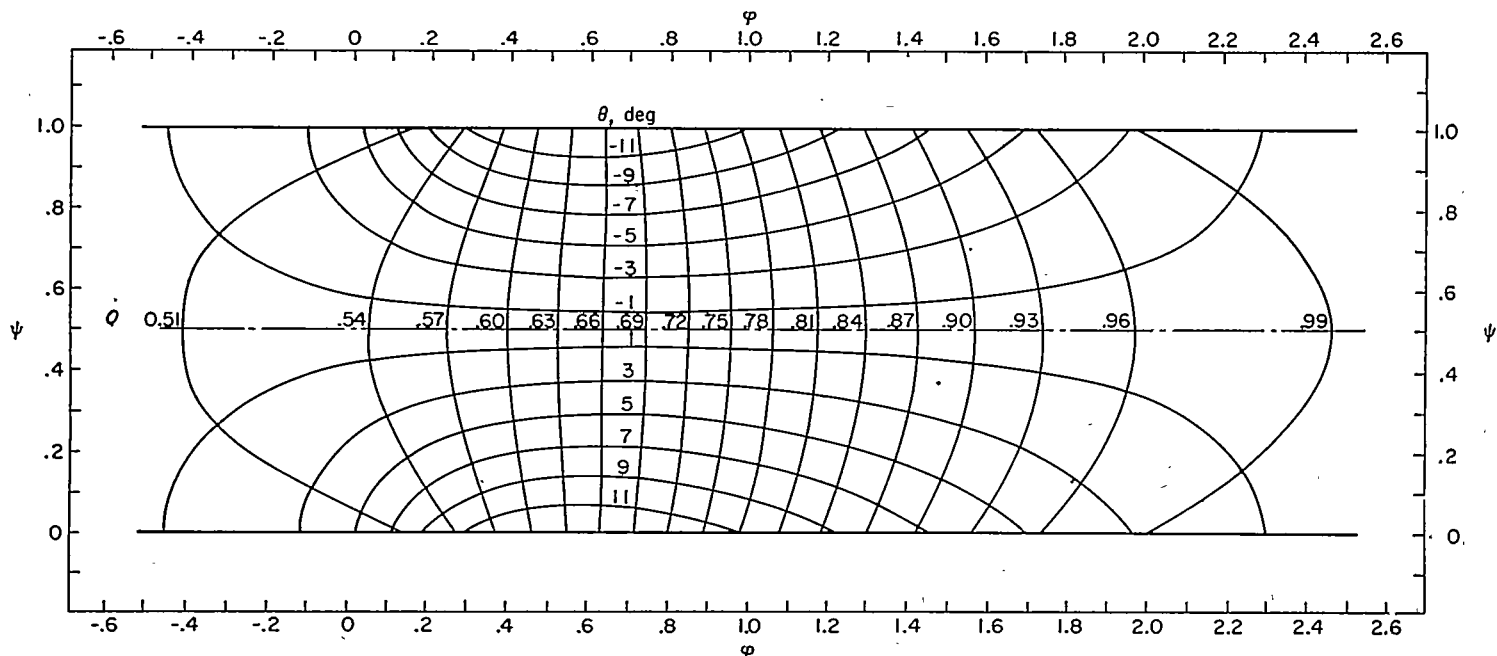


FIGURE 4.—Lines of constant velocity  $Q$  and flow direction  $\theta$  in transformed  $\varphi\psi$ -plane for example I. Incompressible flow; prescribed velocity given in figure 2.

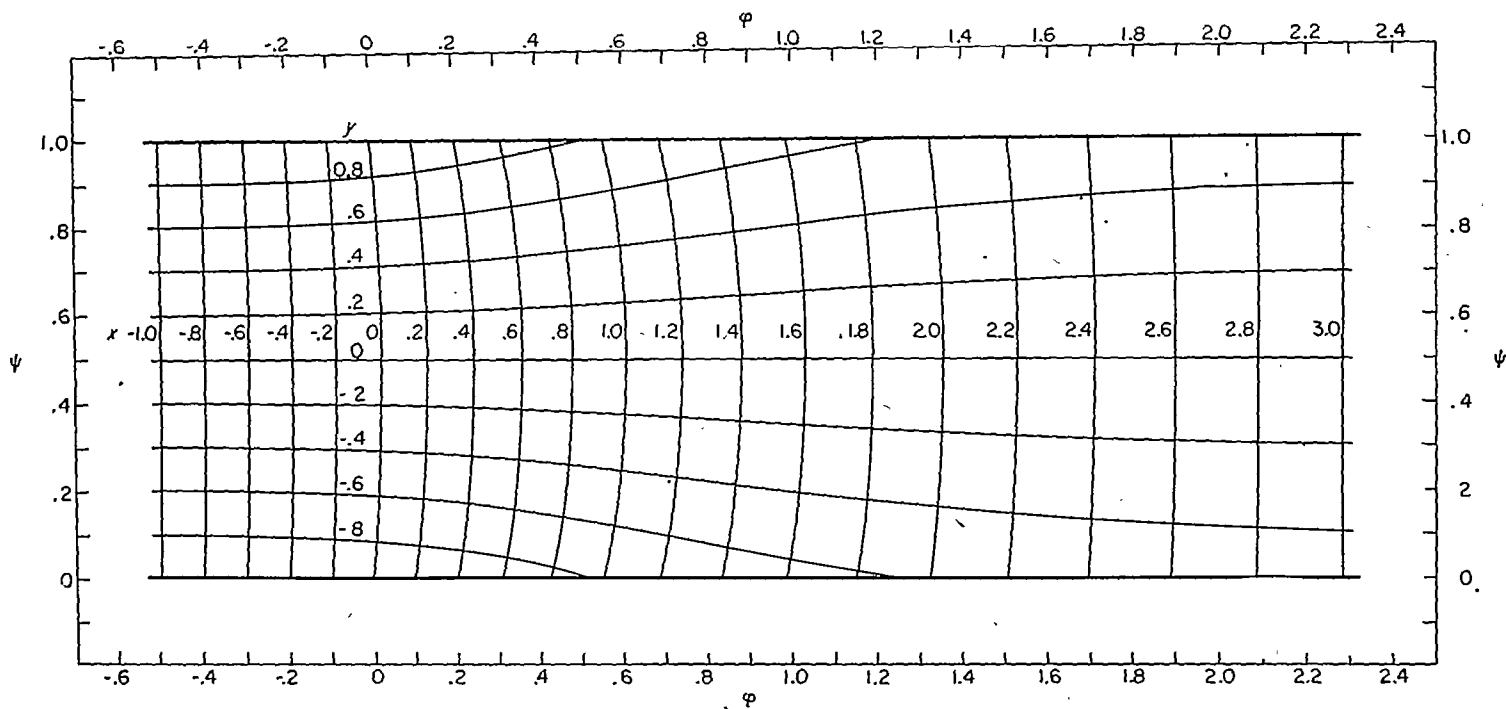


FIGURE 5.—Lines of constant  $x$  and  $y$  coordinates in transformed  $\phi\psi$ -plane for example I. Incompressible flow; prescribed velocity given in figure 2.

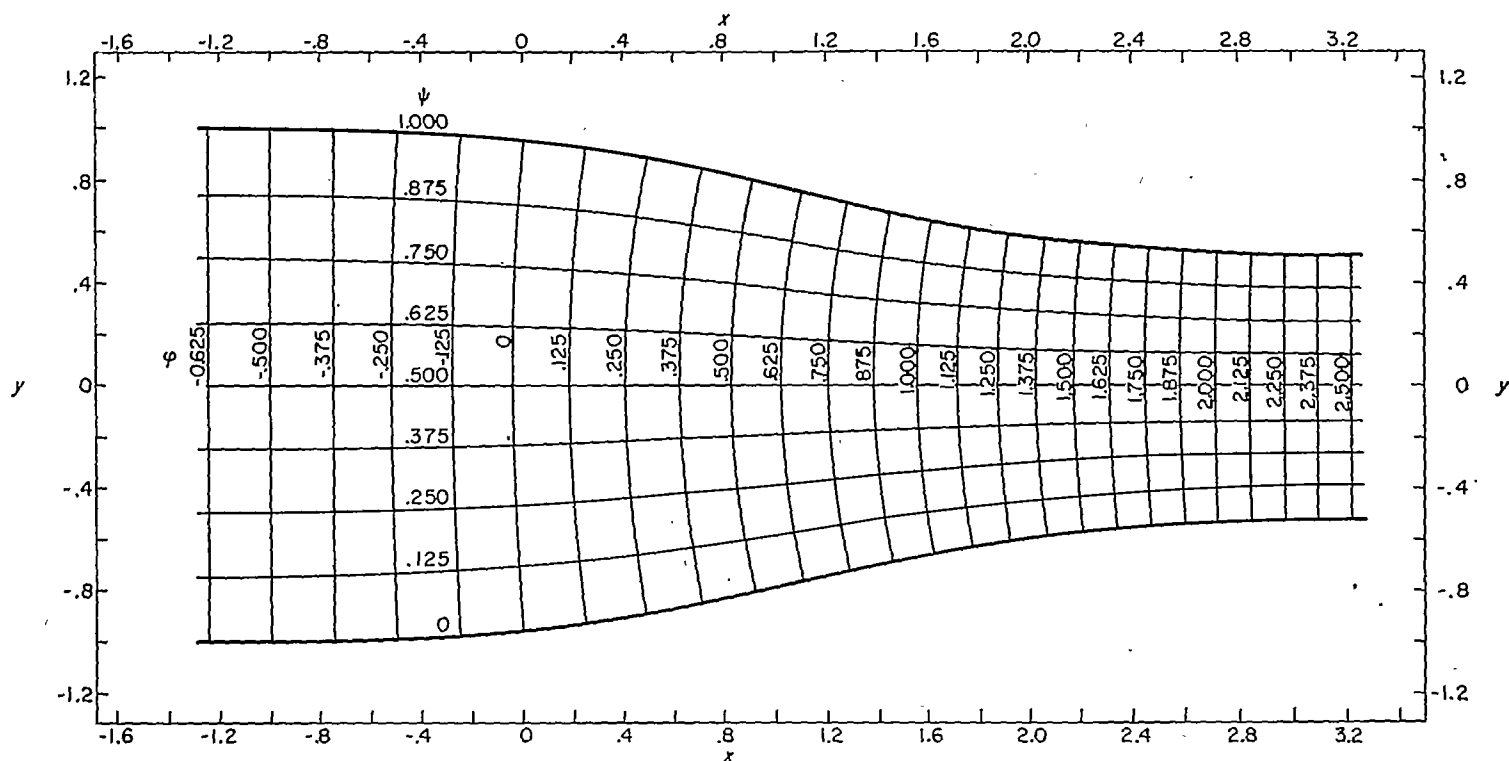


FIGURE 6.—Streamlines and velocity-potential lines on physical  $xy$ -plane for example I. Incompressible flow; prescribed velocity given in figure 2.

In figure 5, lines of constant  $x$  and  $y$  are plotted on the transformed  $\phi\psi$ -plane. Along the mean streamline ( $\psi=0.5$ ) the value of  $y$  is constant and equal to zero indicating, as before, that the center line of the channel is straight. The lines of constant  $x$  and  $y$  are orthogonal, and the system of curves forms a square network. The solution is symmetrical.

In figure 6, lines of constant  $\phi$  and  $\psi$  (velocity potential and streamlines, respectively) are plotted in the physical  $xy$ -plane. The shape of the channel walls is that required to result in the prescribed velocity distribution given by equation (35) and plotted in figure 2. The downstream channel width is 1.0 by definition. The upstream channel width is 2.0 in order that the upstream velocity be half the down-

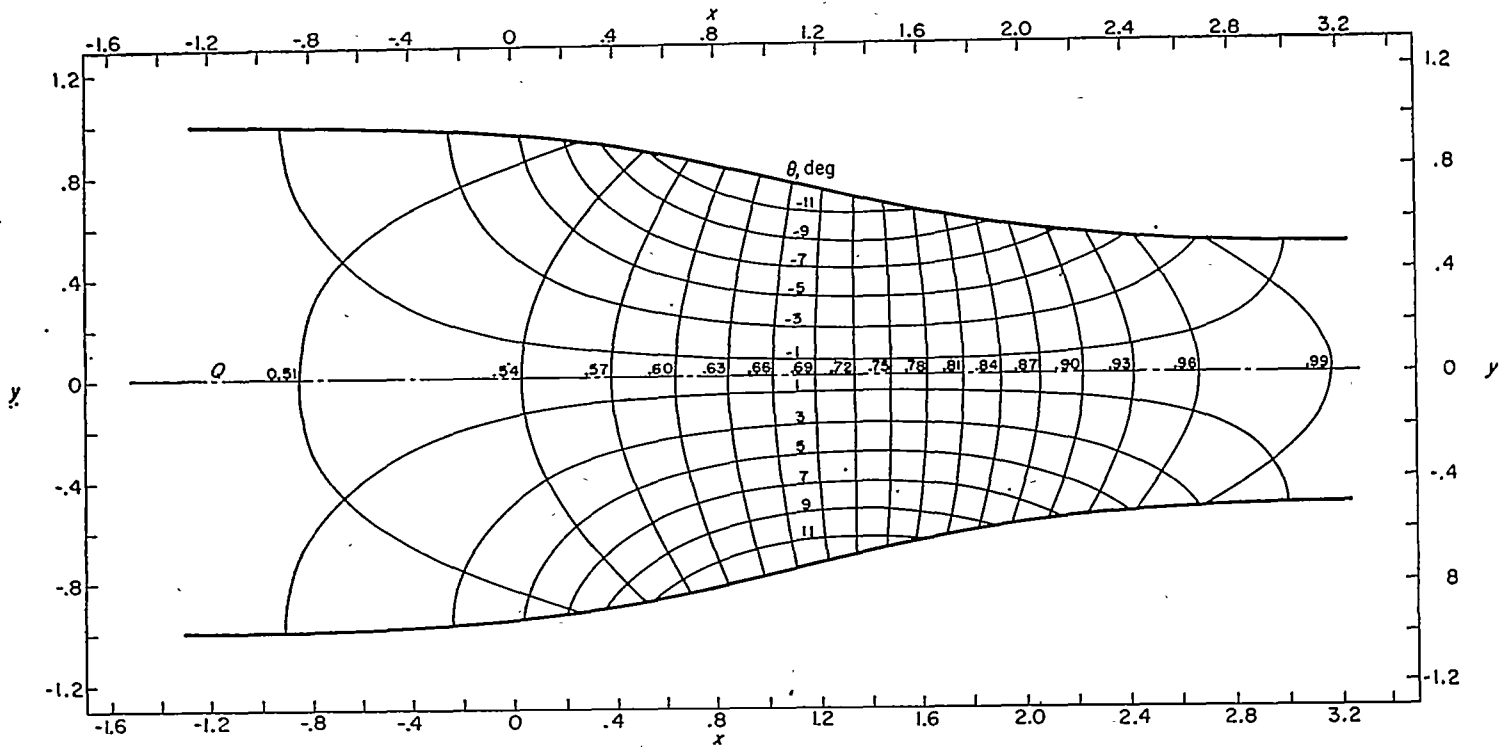


FIGURE 7.—Lines of constant velocity  $Q$  and flow direction  $\theta$  in physical  $xy$ -plane for example I. Incompressible flow; prescribed velocity given in figure 2.

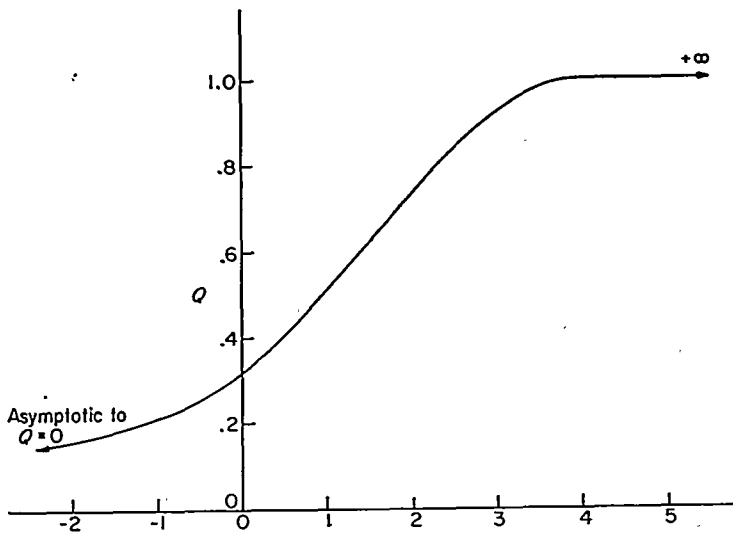


FIGURE 8.—Prescribed velocity distribution as function of arc length along channel wall for example II. Equation (38).

stream velocity. As usual, the streamlines and velocity potential lines are orthogonal and, with equal increments of  $\varphi$  and  $\psi$ , form a square network for incompressible flow.

In figure 7, lines of constant  $Q$  and  $\theta$  are plotted in the physical  $xy$ -plane. The lines of constant  $Q$  and  $\theta$  are orthogonal.

EXAMPLE II

The second numerical example is the design of a converging section that funnels the fluid from an infinite expanse into a

straight channel of unit width. Far upstream the channel walls are straight and converge at a  $90^\circ$  angle. The solution is for incompressible flow.

Prescribed velocity distribution.—The prescribed velocity as a function of arc length  $s$  along both channel walls is given by

$$\left. \begin{aligned} Q &= \frac{-2}{\pi(s-2)} & (s \leq 0) \\ Q &= \frac{1}{\pi} + \frac{1}{2\pi}s - \frac{1}{8} \left( \frac{7}{2\pi} - \frac{3}{2} \right) s^2 + \frac{1}{32} \left( \frac{2}{\pi} - 1 \right) s^3 & (0 \leq s \leq 4) \\ Q &= 1.0 & (s \geq 4) \end{aligned} \right\} (37)$$

The prescribed velocity given by equation (37) is plotted in figure 8.

Equation (37) together with equation (27) results in

$$\left. \begin{aligned} \varphi &= \frac{-2}{\pi} \log_e \left( 1 - \frac{s}{2} \right) & (s \leq 0) \\ \varphi &= \frac{1}{\pi} s + \frac{1}{2\pi} \frac{s^2}{2} - \frac{1}{8} \left( \frac{7}{2\pi} - \frac{3}{2} \right) \frac{s^3}{3} + \frac{1}{32} \left( \frac{2}{\pi} - 1 \right) \frac{s^4}{4} & (0 \leq s \leq 4) \\ \varphi &= \frac{8}{3\pi} - 2 + s & (s \geq 4) \end{aligned} \right\} (38)$$

From equations (37) and (38),  $\log_e Q$  is a known function of  $\varphi$ , which function is plotted in figure 9.

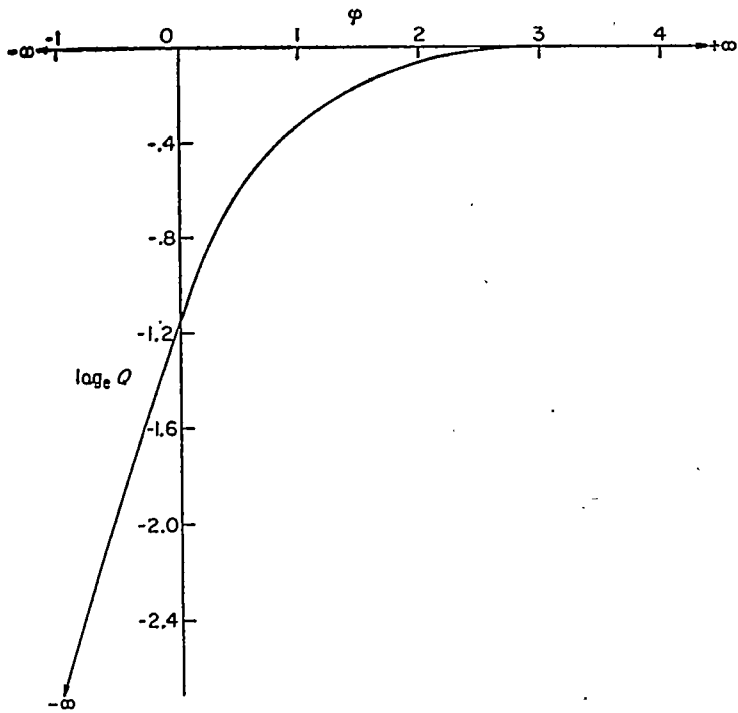


FIGURE 9.—Prescribed distribution of  $\log_e Q$  as function of  $\varphi$  along channel walls for example II.

**Results.**—The results of example II are presented in figures 10 to 12.

In figure 10, lines of constant velocity  $Q$  and flow direction  $\theta$  are plotted in the transformed  $\varphi\psi$ -plane. The flow direction  $\theta$  is constant and equal to zero along the mean streamline ( $\psi=0.5$ ), indicating that the center line of the channel is straight. The solution is symmetrical about the mean streamline. As for example I, the lines of constant  $Q$  and  $\theta$  are orthogonal.

In figure 11, lines of constant  $\varphi$  and  $\psi$  are plotted in the physical  $xy$ -plane. The shape of the channel walls is that

required to result in the prescribed velocity distribution given by equation (37) and plotted in figure 8. As usual, the streamlines and velocity-potential lines are orthogonal and, for incompressible flow with equal increments of  $\varphi$  and  $\psi$ , form a square network.

In figure 12, lines of constant  $Q$  and  $\theta$  are plotted in the physical  $xy$ -plane. The lines of constant  $Q$  and  $\theta$  are orthogonal.

**EXAMPLE III**

The third numerical example is the design of an elbow for which the upstream velocity is half the downstream velocity. The prescribed velocities are such that no deceleration occurs anywhere along the channel walls. The solution is for incompressible flow.

**Prescribed velocity distribution.**—Along both walls upstream of the elbow the velocity  $Q$  is equal to 0.5, and along both walls downstream of the elbow  $Q$  is equal to 1.0. The transition from  $Q$  equals 0.5 to 1.0 along both walls of the elbow will be the prescribed velocity distribution as a function of arc length given by equation (35) for example I and plotted in figure 2. In terms of  $\log_e Q$  as a function of  $\varphi$ , this prescribed velocity distribution is given by equation (36) and is plotted in figure 3. Although this velocity distribution is the same for both walls, the distribution on the outer wall (wall with larger radii of curvature) is shifted in the positive  $\varphi$  direction an amount equal to 2.25 relative to the distribution on the inner wall. Thus, a velocity difference exists on the two walls at equal values of  $\varphi$ , as shown in figure 13. The greater this difference in velocity and the greater the range in  $\varphi$  over which velocity differences exist, the greater is the elbow turning angle. For the prescribed velocity distribution given in figure 13, the elbow turning angle given by equation (12) was  $89.37^\circ$  compared with a value of  $89.36^\circ$  obtained from the relaxation solution.

**Results.**—The results of example III are presented in figures 14 to 16 and in tables I and II. (The numerical

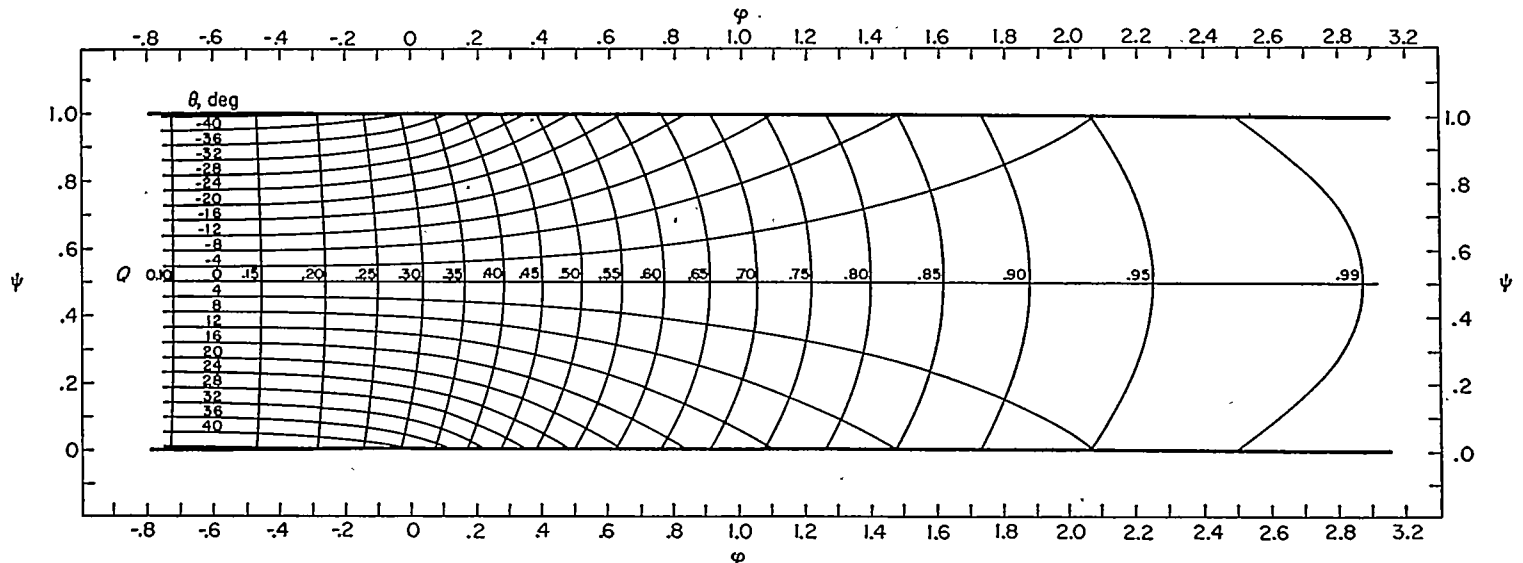


FIGURE 10.—Lines of constant velocity  $Q$  and flow direction  $\theta$  in transformed  $\varphi\psi$ -plane for example II. Incompressible flow; prescribed velocity given in figure 8.

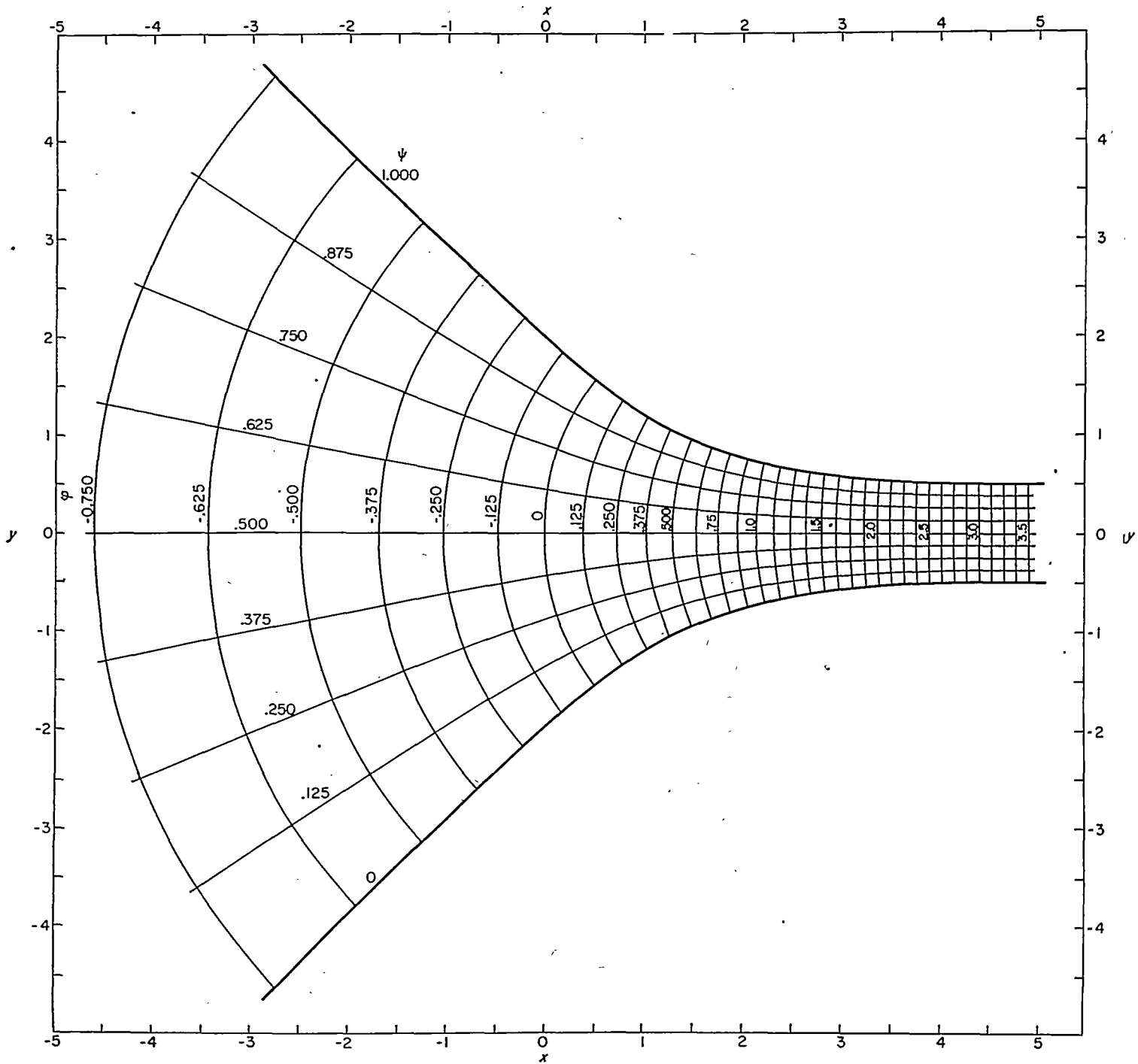


FIGURE 11.—Streamlines and velocity-potential lines in physical  $xy$ -plane for example II. Incompressible flow; prescribed velocity given in figure 8.

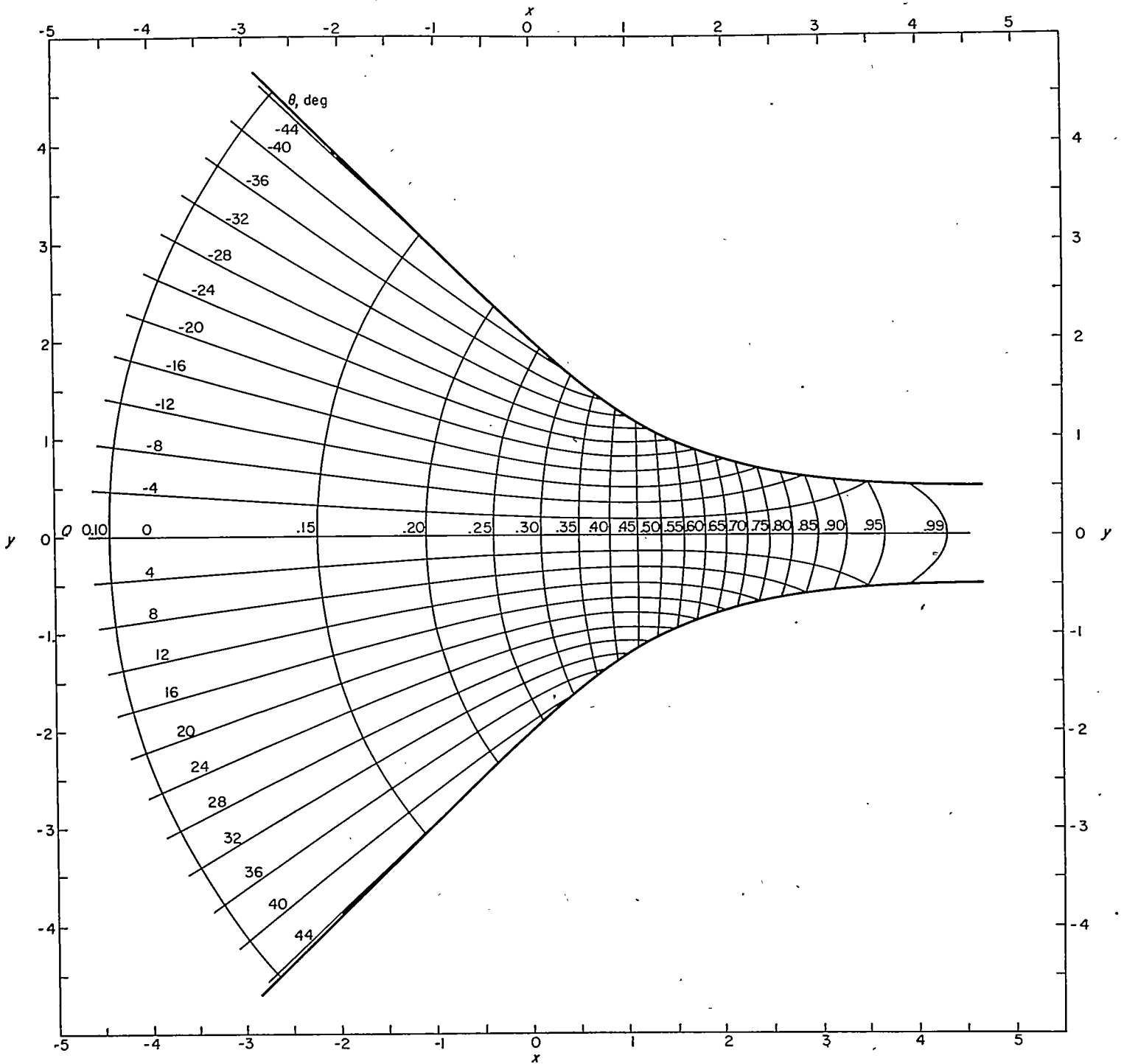


FIGURE 12.—Lines of constant velocity  $Q$  and flow direction  $\theta$  in physical  $xy$ -plane for example II. Incompressible flow; prescribed velocity given in figure 8.

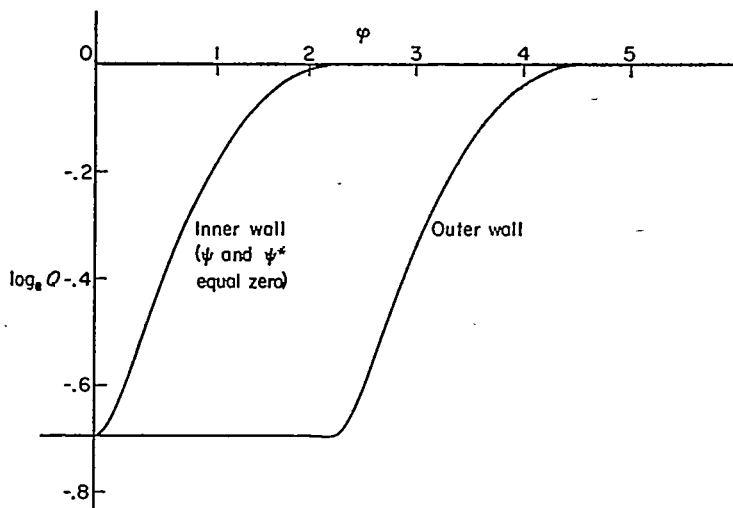


FIGURE 13.—Prescribed distribution of  $\log_{10} Q$  as function of  $\varphi$  along channel walls for examples III, IV, and V.

results for examples III, IV, and V are tabulated in tables I to VI to enable a detailed comparison of the three elbow designs with the same prescribed velocity  $Q$  distribution as a function of arc length but with incompressible (example III), linearized compressible (example IV), and compressible (example V) flow.)

In figure 14, lines of constant  $Q$  and  $\theta$  are plotted in the  $\varphi\psi$ -plane. The flow direction  $\theta$  varies along the mean streamline ( $\psi=0.5$ ), indicating that the channel is curved. The solution is unsymmetrical. As for examples I and II, the lines of constant  $Q$  and  $\theta$  are orthogonal.

In figure 15, lines of constant  $\varphi$  and  $\psi$  are plotted in the physical  $xy$ -plane. The shape of the channel walls is that required to result in the prescribed velocity distribution given by equations (35) and (36) and plotted in figures 2 and 13. The upstream channel width is twice the downstream width in order that the upstream velocity be half the downstream velocity. It is interesting to note that, before curving in the direction of the elbow turning angle, the inner wall first curves in the opposite direction. This behavior of the inner-wall geometry is necessary in order to

maintain the prescribed constant velocity along the outer wall where the velocity would otherwise decelerate because of the necessary curvature in the direction of elbow turning. This feature of the elbow geometry will also be noted in examples IV and V. As usual, the streamlines and velocity-potential lines are orthogonal and, for equal increments of  $\varphi$  and  $\psi$ , form a square network.

In figure 16, lines of constant  $Q$  and  $\theta$  are plotted in the physical  $xy$ -plane. The lines of constant  $Q$  and  $\theta$  are orthogonal.

EXAMPLE IV

The fourth numerical example is the design of an elbow with the same prescribed velocity  $Q$ , as a function of arc length, used in example III but for linearized compressible flow ( $\gamma=-1.0$ ).

**Prescribed velocity distribution.**—The prescribed velocity distribution  $Q$  is the same as that for example III and with  $q_a$  equal to 0.80176. The variation in  $Q$  with  $s$  along one channel wall is plotted in figure 2. The values of  $q_a$  and  $q_b$  in equations (14a) and (14b) are equal to  $q_*$  and  $q_a$ , or 0.40088 and 0.80176, respectively. For these values of  $q_a$  and  $q_b$  and for the prescribed velocity distribution with linearized compressible flow, the elbow turning angle given by equation (24) was  $104.08^\circ$  compared with a value of  $104.07^\circ$  obtained from the relaxation solution and a value of  $89.36^\circ$  obtained for incompressible flow (example III).

**Results.**—The results of example IV are presented in figures 17 to 19 and in tables III and IV.

In figure 17, lines of constant  $q$  and  $\theta$  are plotted in the transformed  $\varphi^*\psi^*$ -plane. The solution is unsymmetrical and the lines of constant  $q$  and  $\theta$  are orthogonal.

In figure 18, lines of constant  $\varphi^*/\Delta\psi^*$  and  $\psi^*/\Delta\psi^*$  are plotted in the physical  $xy$ -plane (where the constant  $\Delta\psi^*$  is given by equation (32) and is equal to 0.73782 for  $q_a$  equal to 0.80176). The shape of the channel walls is that required to result in the prescribed velocity distribution used in example III but with linearized compressible flow and for  $q_a$  equal to 0.80176. From continuity considerations the upstream channel width is 1.5385 times the downstream width. As in example III, the inner wall of the elbow first

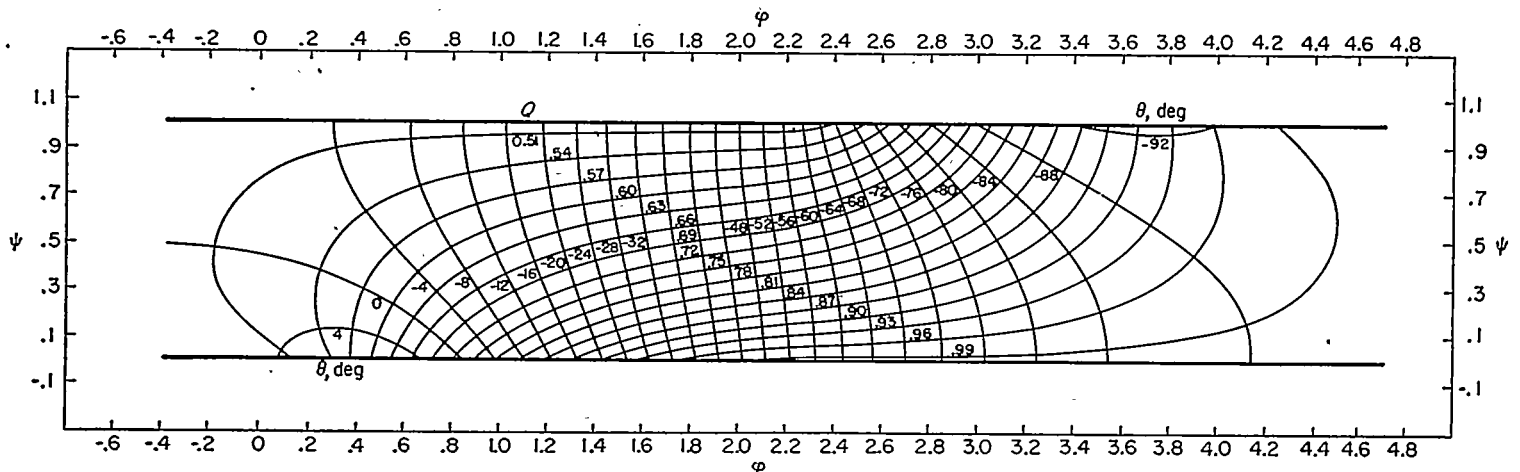


FIGURE 14.—Lines of constant velocity  $Q$  and flow direction  $\theta$  in transformed  $\varphi\psi$ -plane for example III. Incompressible flow; prescribed velocity given in figures 2 and 13.

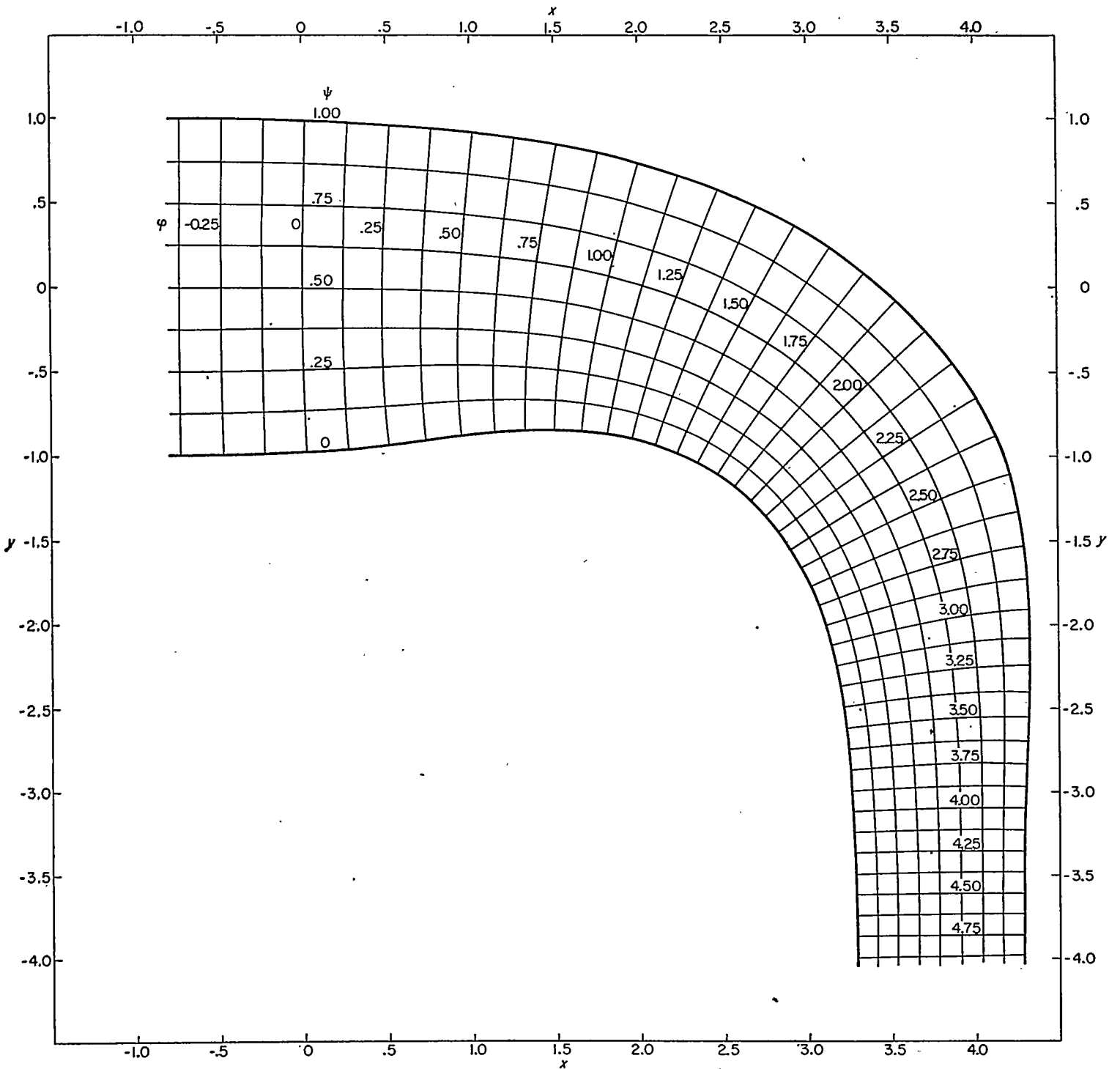


FIGURE 15.—Streamlines and velocity-potential lines in physical  $xy$ -plane for example III. Incompressible flow; prescribed velocity given in figures 2 and 13.

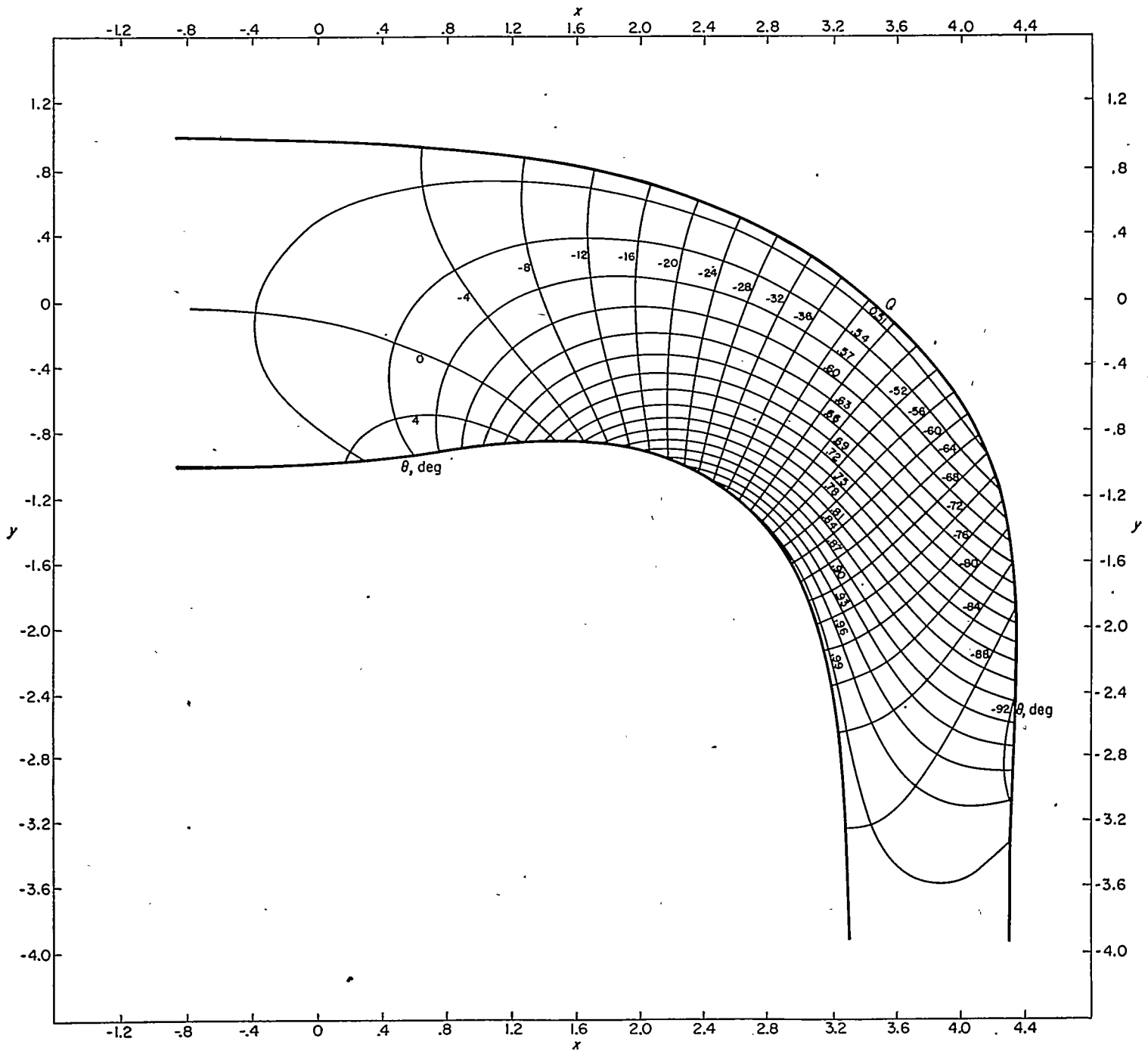


FIGURE 16.—Lines of constant velocity  $Q$  and flow direction  $\theta$  in physical  $xy$ -plane for example III. Incompressible flow; prescribed velocity given in figures 2 and 13.

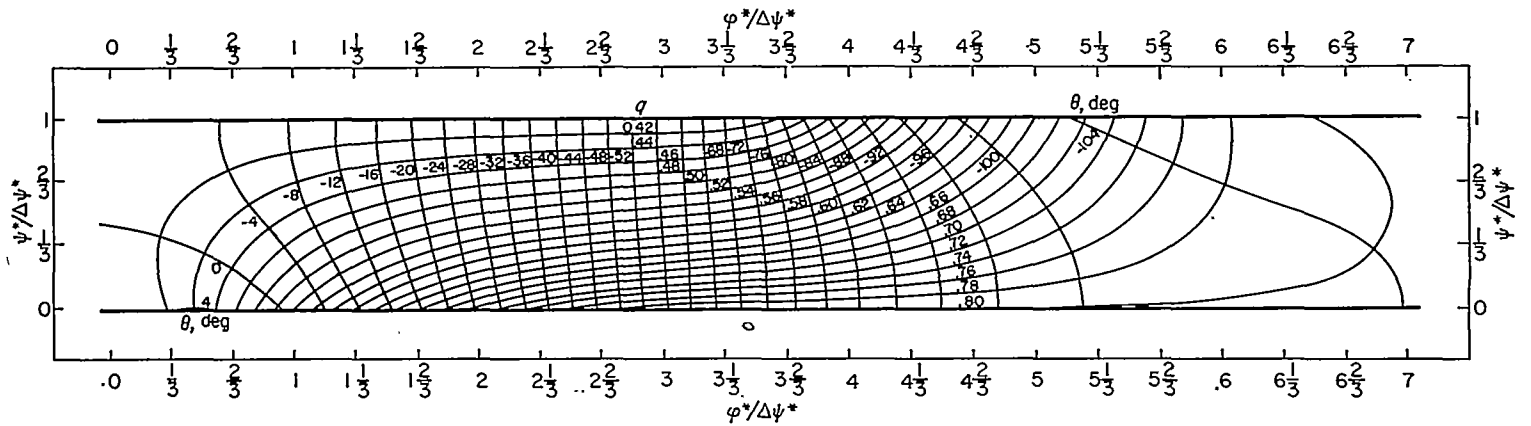


FIGURE 17.—Lines of constant velocity  $q$  and flow direction  $\theta$  in transformed  $\phi^*\psi^*$ -plane for example IV. Linearized compressible flow; prescribed velocity as function of arc length along channel walls same as for example III (fig. 2) and with  $q_a$  equal to 0.80176.

turns in the opposite direction to the elbow turning angle. As usual, the streamlines and velocity-potential lines are orthogonal.

In figure 19, lines of constant  $q$  and  $\theta$  are plotted in the physical  $xy$ -plane. The lines of constant  $q$  and  $\theta$  are not, in general, orthogonal.

EXAMPLE V

The fifth numerical example is the design of an elbow with the same prescribed velocity  $Q$ , as a function of arc length, used in examples III and IV but for compressible flow ( $\gamma=1.4$ ).

Prescribed velocity distribution.—The prescribed velocity distribution  $Q$  is the same as that for examples III and IV but with  $q_a$  equal to 0.79927. The variation in  $Q$  with  $s$  along one channel wall is plotted in figure 2.

Results.—The results of example V are presented in figures 20 and 21 and in tables V and VI.

In figure 20, lines of constant  $\phi/\Delta\psi$  and  $\psi/\Delta\psi$  are plotted in the physical  $xy$ -plane (where the constant  $\Delta\psi$  is given by equation (26) and is equal to 0.71054 for  $q_a$  equal to 0.79927). The shape of the channel walls is that required to result in the prescribed velocity distribution used in examples III and IV but with compressible flow ( $\gamma=1.4$ ) and for  $q_a$  equal to 0.79927. The upstream channel width is 1.5412 times the downstream width, and the turning angle is  $105.31^\circ$  compared with  $104.07^\circ$  for linearized compressible flow (example IV) and  $89.36^\circ$  for incompressible flow (example III). The streamlines and velocity-potential lines are orthogonal.

The shape of the elbow for compressible flow (example V, fig. 20) is nearly the same as the shape of the elbow for linearized compressible flow (example IV, fig. 18). Therefore, in figure 21 the contours of the walls for both examples are compared. The difference in contours is very small and it is concluded that, if a nonviscous gas with arbitrary  $\gamma$  (1.4, for example) were to flow through a channel designed for linearized compressible flow ( $\gamma=-1.0$ ), the resulting velocity distribution along the channel walls would be nearly the velocity distribution prescribed for the linearized compressible flow, at least if the linearized flow were selected (by the choice of  $q_a$  and  $q_b$ ) so that the densities were equal for both types of flow at the maximum and minimum velocities

and if the ratio of these prescribed velocities is not too large (2:1 in the numerical examples). This conclusion is important because the design method for linearized compressible flow is considerably faster than the design method for compressible flow with  $\gamma$  other than  $-1.0$ .

PART II

SOLUTION BY GREEN'S FUNCTION

In part II a method of solution for the design of two-dimensional channels with prescribed velocity distributions along the walls is developed by means of the appropriate Green's function. The method applies to incompressible and linearized compressible, irrotational flow. One numerical example is presented for an accelerating elbow with linearized compressible flow and with the same prescribed conditions as example IV of part I.

METHOD OF SOLUTION

The method of solution by Green's function is in conjunction with a formula derived from Green's theorem.

PRELIMINARY CONSIDERATIONS

Stream function  $\Psi$ .—In part II it is convenient to define the stream function by  $\Psi$ , where for incompressible flow

$$d\Psi = \frac{\pi}{2} d\psi \tag{39a}$$

and for linearized compressible flow ( $\gamma=-1.0$ )

$$d\Psi = \frac{\pi d\psi^*}{2\Delta\psi^*} \tag{39b}$$

For both types of flow  $\Psi$  varies from zero along the right side of the channel, when faced in the direction of flow, to  $\pi/2$  along the left side.

Velocity potential  $\Phi$ .—In part II it is convenient to define the velocity potential by  $\Phi$ , where for incompressible flow

$$d\Phi = \frac{\pi}{2} d\phi \tag{40a}$$

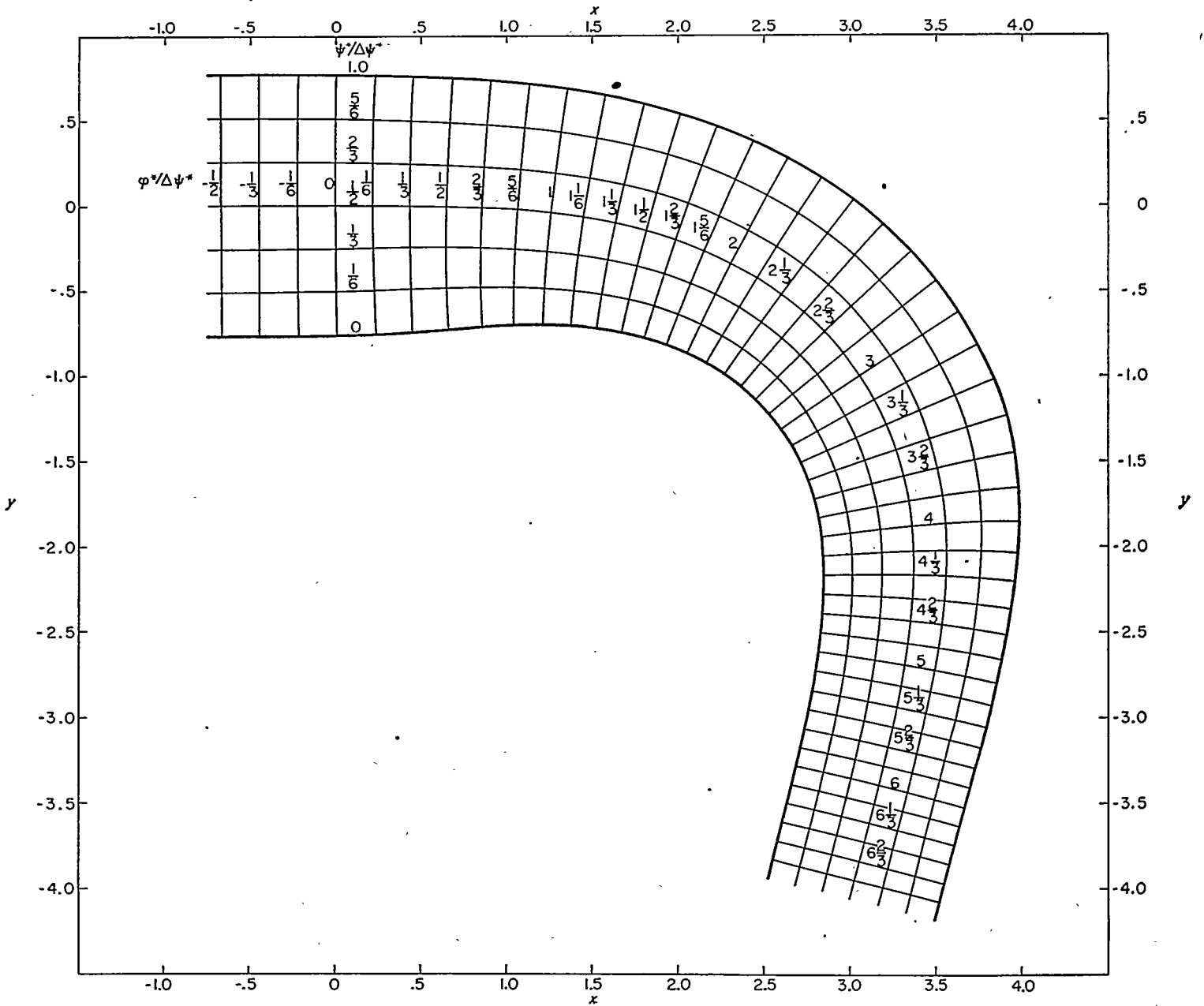


FIGURE 18.—Streamlines and velocity-potential lines in physical  $xy$ -plane for example IV. Linearized compressible flow; prescribed velocity as function of arc length along channel walls same as for example III (fig. 2) and with  $q_2$  equal to 0.80176.

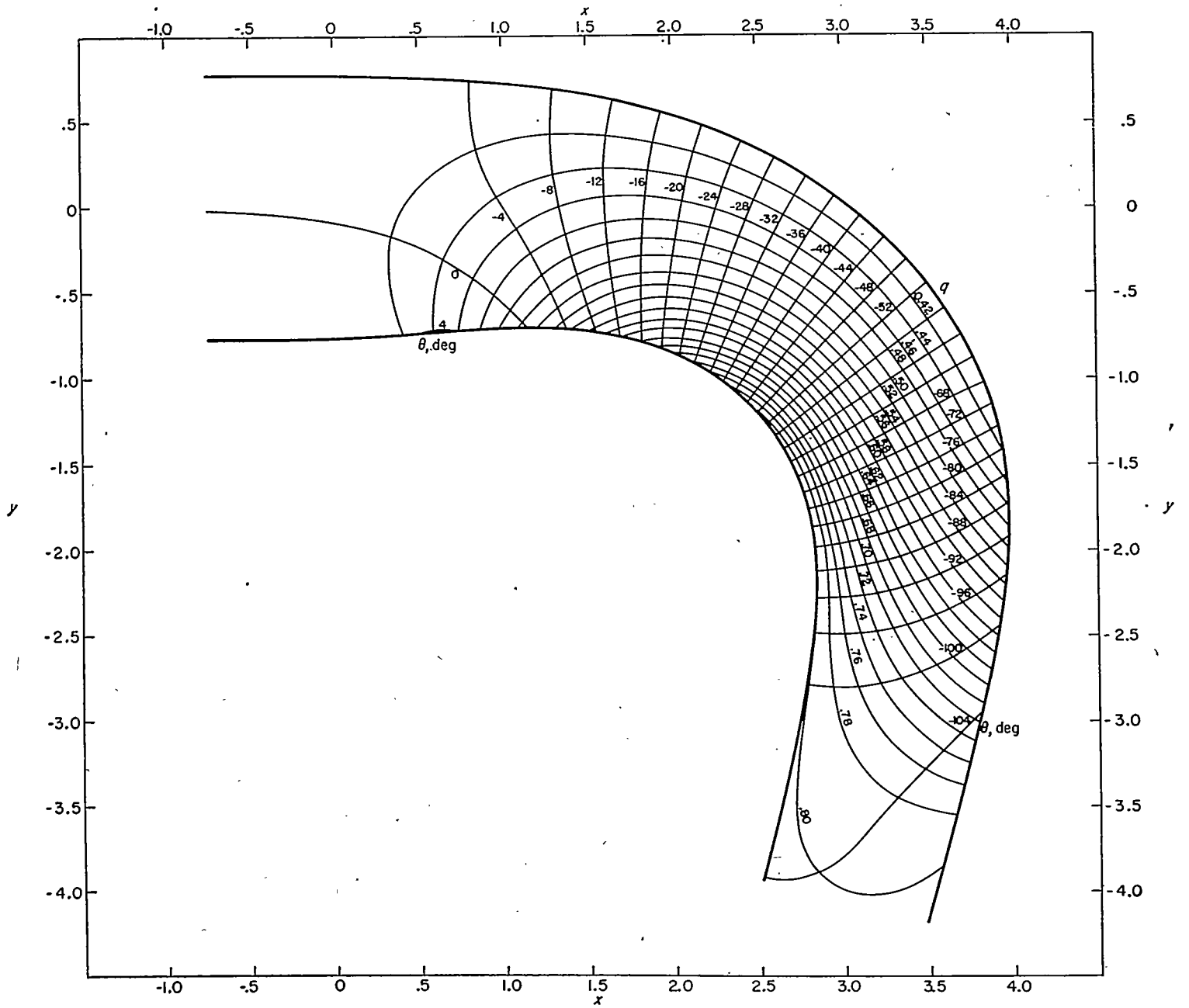


FIGURE 19.—Lines of constant velocity  $q$  and flow direction  $\theta$  in physical  $xy$ -plane for example IV. Linearized compressible flow; prescribed velocity as function of arc length along channel walls same as for example III (fig. 2) and with  $q_*$  equal to 0.80176.

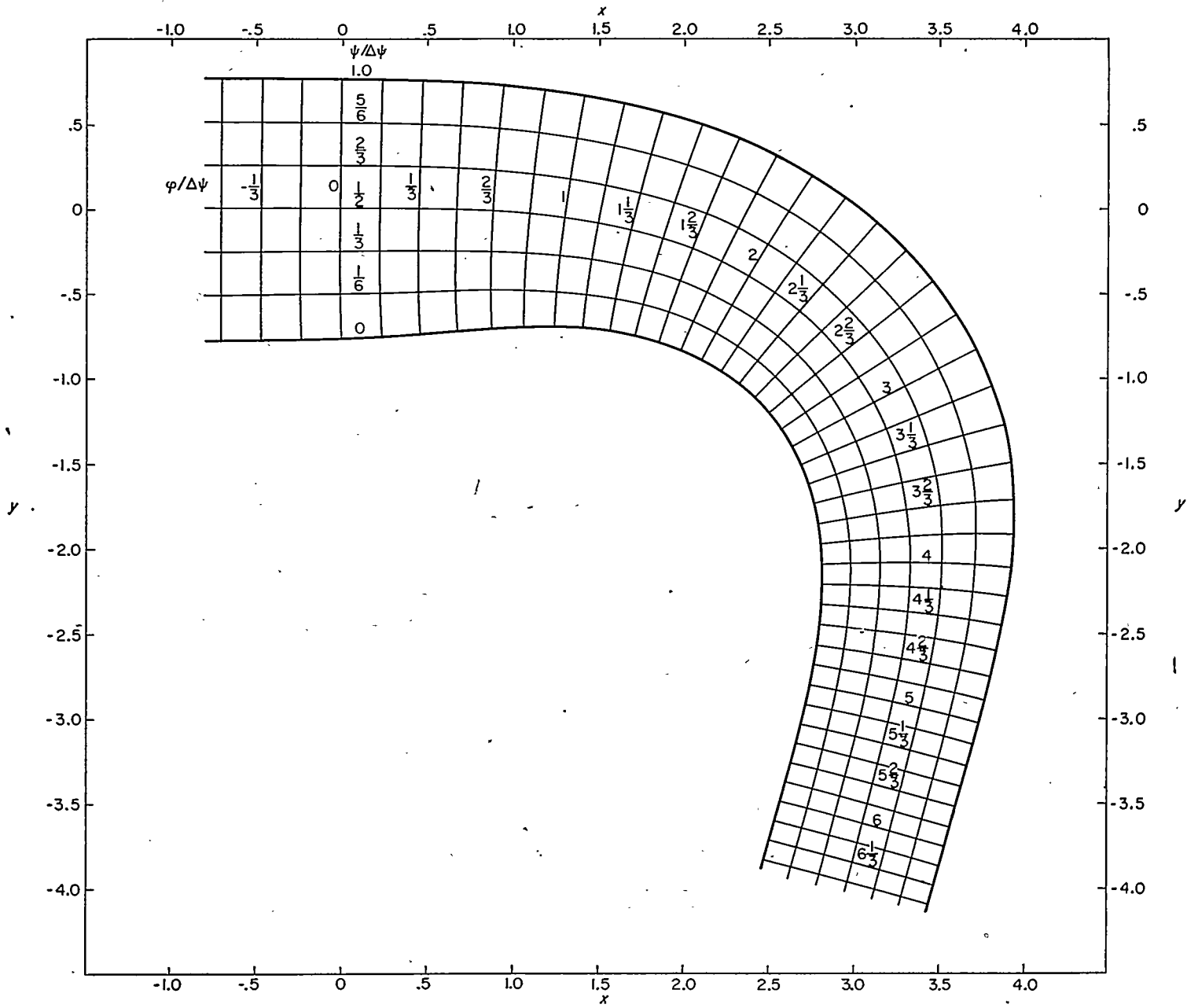


FIGURE 20.—Streamlines and velocity-potential lines in physical  $xy$ -plane for example V. Compressible flow ( $\gamma=1.4$ ); prescribed velocity as function of arc length along channel walls same as for examples III and IV (fig. 2) but with  $q_2$  equal to 0.79927.

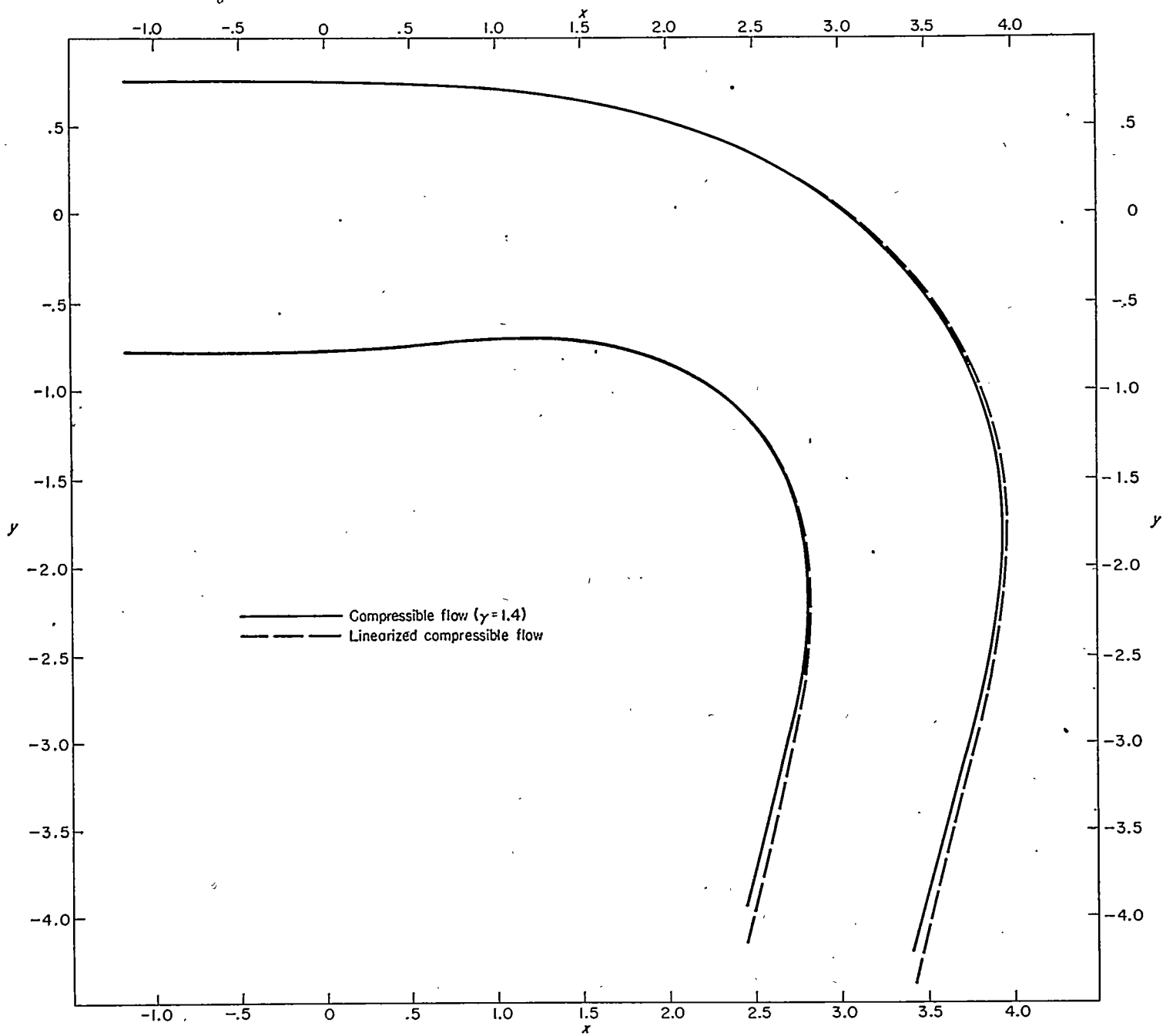


FIGURE 21.—Comparison of channel-wall shapes for compressible flow (example V) with  $\gamma$  equal to 1.4 and for linearized compressible flow (example IV) for same prescribed velocity as function of arc length along channel walls (fig. 2).

and for linearized compressible flow

$$d\Phi = \frac{\pi}{2} \frac{d\psi^*}{\Delta\psi^*} \quad (40b)$$

**Channel-wall coordinates.**—From part I the distribution of channel-wall coordinates  $x$  and  $y$  along the boundaries of constant  $\Psi$  equal to 0 and  $\pi/2$  in the transformed  $\Phi\Psi$ -plane is given by

$$x = \frac{2}{\pi} \Delta\psi^* \int_{\Psi} \frac{\cos \theta}{q^*} d\Phi \quad (41a)$$

and

$$y = \frac{2}{\pi} \Delta\psi^* \int_{\Psi} \frac{\sin \theta}{q^*} d\Phi \quad (41b)$$

for linearized compressible flow, and for incompressible flow is given by

$$x = \frac{2}{\pi} \int_{\Psi} \frac{\cos \theta}{Q} d\Phi \quad (42a)$$

and

$$y = \frac{2}{\pi} \int_{\Psi} \frac{\sin \theta}{Q} d\Phi \quad (42b)$$

where the constants of integration are selected to give known (specified) values of  $x$  or  $y$  at one value of  $\Phi$  along each boundary. Because  $q^*$  and  $Q$  are known functions of  $\Phi$  from the prescribed velocity as a function of arc length along the channel walls, the shape of the channel walls in the physical  $xy$ -plane is given by equation (41) or (42) if  $\theta$  is determined as a function of  $\Phi$  along the channel walls. In part II the solution for  $\theta$  as a function of  $\Phi$  along the channel walls in the  $\Phi\Psi$ -plane is obtained by Green's function.

#### SOLUTION BY GREEN'S FUNCTION

**Continuity.**—From part I the continuity equation becomes in the transformed  $\Phi\Psi$ -plane

$$\frac{\partial \log_e V}{\partial \Phi} + \frac{\partial \theta}{\partial \Psi} = 0 \quad (43a)$$

where for incompressible flow

$$V = Q \quad (43b)$$

and for linearized compressible flow

$$V = \frac{q^*}{1 + \sqrt{1 + q^{*2}}} \quad (43c)$$

**Irrotational motion.**—From part I the equation for irrotational motion becomes in the transformed  $\Phi\Psi$ -plane

$$\frac{\partial \log_e V}{\partial \Psi} - \frac{\partial \theta}{\partial \Phi} = 0 \quad (44)$$

**Integral equation for  $\theta(\Phi_o, \Psi_o)$ .**—From equations (43a) and (44)

$$\frac{\partial^2 \theta}{\partial \Phi^2} + \frac{\partial^2 \theta}{\partial \Psi^2} = 0 \quad (45)$$

so that from appendix E the value of  $\theta$  at a point  $(\Phi_o, \Psi_o)$

within, or on, the channel walls in the transformed  $\Phi\Psi$ -plane is given by the integral equation

$$\theta(\Phi_o, \Psi_o) = \frac{-1}{2\pi} \int_{-\infty}^{\infty} \left[ \left( G \frac{\partial \log_e V}{\partial \Phi} \right)_{\frac{\pi}{2}} - \left( G \frac{\partial \log_e V}{\partial \Phi} \right)_0 \right] d\Phi \quad (46)$$

where the subscripts 0 and  $\frac{\pi}{2}$  refer to the channel-wall boundaries along which  $\Psi$  is 0 and  $\frac{\pi}{2}$ , respectively, and  $G$  is the Green's function of the second kind for the channel, which is an infinite strip of width  $\frac{\pi}{2}$  extending in the  $\Phi$ -direction to  $\pm \infty$ .

**Green's function  $G$ .**—The Green's function of the second kind  $G$  for the infinite channel in the  $\Phi\Psi$ -plane is given along the channel-wall boundaries ( $\Psi$  equals 0 and  $\frac{\pi}{2}$ ) by (appendix F)

$$G_{0 \text{ or } \frac{\pi}{2}} = -\log_e [\cosh^2(\Phi - \Phi_o) - \cos^2(\Psi - \Psi_o)] \quad (47)$$

where  $(\Phi, \Psi)$  is any point on the channel-wall boundary and  $(\Phi_o, \Psi_o)$  is the point in the channel or on the boundary at which  $\theta$  is to be determined.

**Numerical integration for  $\theta(\Phi_o, \Psi_o)$ .**—From equations (46) and (47)

$$2\pi\theta(\Phi_o, \Psi_o) = \int_{-\infty}^{\infty} \left\{ \frac{\partial \log_e V}{\partial \Phi} \log_e [\cosh^2(\Phi - \Phi_o) - \sin^2 \Psi_o] \right\}_{\frac{\pi}{2}} d(\Phi - \Phi_o) - \int_{-\infty}^{\infty} \left\{ \frac{\partial \log_e V}{\partial \Phi} \log_e [\cosh^2(\Phi - \Phi_o) - \cos^2 \Psi_o] \right\}_0 d(\Phi - \Phi_o) \quad (48)$$

in which the independent variable of integration has been changed from  $d\Phi$  to  $d(\Phi - \Phi_o)$  so that the origin, for purposes of integration, lies at  $\Phi_o$  rather than  $\Phi = 0$ . If for small changes in  $(\Phi - \Phi_o)$ , that is, for small  $\Delta\Phi$ , the term  $\frac{\partial \log_e V}{\partial \Phi}$  may be considered constant and equal to its average value over the interval  $\Delta\Phi$ , then

$$\frac{\partial \log_e V}{\partial \Phi} = \frac{\Delta \log_e V}{\Delta \Phi}$$

and equation (48) becomes

$$2\pi\theta(\Phi_o, \Psi_o) = \sum_{(\Phi - \Phi_o) = -\infty}^{\infty} \left\{ \frac{\Delta \log_e V}{\Delta \Phi} \int_{(\Phi - \Phi_o)}^{(\Phi - \Phi_o) + \Delta \Phi} \log_e [\cosh^2(\Phi - \Phi_o) - \sin^2 \Psi_o] d(\Phi - \Phi_o) \right\}_{\frac{\pi}{2}} - \sum_{(\Phi - \Phi_o) = -\infty}^{\infty} \left\{ \frac{\Delta \log_e V}{\Delta \Phi} \int_{(\Phi - \Phi_o)}^{(\Phi - \Phi_o) + \Delta \Phi} \log_e [\cosh^2(\Phi - \Phi_o) - \cos^2 \Psi_o] d(\Phi - \Phi_o) \right\}_0 \quad (49)$$

where the summation sign is understood to mean that the quantity within the braces is summed over the entire range of  $(\Phi - \Phi_0)$  between  $\pm \infty$ .

Equation (49) determines  $\theta$  at any point in the flow field (channel). For a point  $(\Phi_0, \Psi_0)$  on the channel walls  $\Psi_0$  is equal to 0 or  $\pi/2$  and the integrands in equation (49) become

$$2 \log_e \cosh |(\Phi - \Phi_0)|$$

or

$$2 \log_e \sinh |(\Phi - \Phi_0)|$$

so that equation (49) becomes

$$\pi \theta(\Phi_0, \Psi_0) = \sum_{(\Phi - \Phi_0) = -\infty}^{\infty} \left[ \left( \frac{\Delta \log_e V}{\Delta \Phi} \Delta I \right)_{\frac{\pi}{2}} - \left( \frac{\Delta \log_e V}{\Delta \Phi} \Delta I \right)_0 \right] \quad (50a)$$

where

$$\Delta I = I_{(\Phi - \Phi_0) + \Delta \Phi} - I_{(\Phi - \Phi_0)} \quad (50b)$$

$$\left. \begin{aligned} I_{\frac{\pi}{2}} &= \alpha \text{ if } \Psi_0 = 0 \\ I_{\frac{\pi}{2}} &= \beta \text{ if } \Psi_0 = \frac{\pi}{2} \\ I_0 &= \alpha \text{ if } \Psi_0 = \frac{\pi}{2} \\ I_0 &= \beta \text{ if } \Psi_0 = 0 \end{aligned} \right\} \quad (50c)$$

where

$$\alpha = \pm \int_0^{|\Phi - \Phi_0|} \log_e \cosh |(\Phi - \Phi_0)| d |(\Phi - \Phi_0)| \quad (50d)$$

$$\beta = \pm \int_0^{|\Phi - \Phi_0|} \log_e \sinh |(\Phi - \Phi_0)| d |(\Phi - \Phi_0)| \quad (50e)$$

where the + signs apply for positive values of  $(\Phi - \Phi_0)$  and the - signs apply for negative values of  $(\Phi - \Phi_0)$ . Methods of evaluating  $\alpha$  and  $\beta$  are given in appendix G, and tabulated values are given for a wide range of  $|(\Phi - \Phi_0)|$  in table VII. Equation (50a) determines  $\theta(\Phi_0, \Psi_0)$  at any point on the channel-wall boundaries. Thus from equations (41a) and (41b) or (42a) and (42b) the coordinates for the channel-wall shape in the physical  $xy$ -plane can be determined.

#### NUMERICAL PROCEDURE

The numerical procedure for the channel design solution by Green's function is the same, except for minor details, for incompressible and linearized compressible flow. The stepwise procedure is outlined as follows:

(1) For incompressible flow the velocity  $Q$  and for linearized compressible flow the velocity  $q$ , or which is the same thing the velocity  $Q$  and the constant downstream velocity  $q_a$ , are specified as functions of arc length along the channel walls

$$Q = Q(s) \quad (51a)$$

or

$$q = q(s) \quad (51b)$$

where  $s$  is arbitrarily equal to 0 at that point along one channel wall where the velocity first begins to vary.

(2) Compute  $V$  as a function of  $s$  from equations (43b) and (51a) for incompressible flow or from equations (13b), (14b), (43c), and (51b) for linearized compressible flow

$$V = V(s) \quad (52)$$

(3) Compute  $\Phi$  as a function of  $s$  from equations (4) and (40a) for incompressible flow or from equations (16), (32), (40b), and (51b) for linearized compressible flow. In equation (32)  $\rho_a^*$  is obtained from equations (8a), (13a), and (14a). For arbitrary distributions of  $Q$  or  $q$  equation (40a) or (40b) is integrated numerically by using, for example, Simpson's one-third rule. Thus

$$\Phi = \Phi(s) \quad (53)$$

(4) From equations (52) and (53)  $V$  and  $\Phi$  are known functions of  $s$  so that

$$V = V(\Phi) \quad (54)$$

Thus  $V$  is a known function of  $\Phi$  along the channel-wall boundaries in the transformed  $\Phi\Psi$ -plane.

(5) If the prescribed velocity distribution along one wall is different from that along the other, the channel will, in general, turn the flow. This turning angle  $\Delta\theta$  is given by equation (H5) in appendix H. If the turning angle is unsatisfactory, a new distribution of velocity as a function of  $s$  (eqs. (51a) and (51b)) is prescribed and steps (1) to (5) repeated until the desired value of  $\Delta\theta$  is obtained. Equation (H5) is integrated numerically by using Simpson's one-third rule, for example, and equation (54).

(6) The channel-wall boundaries are straight parallel lines of constant  $\Psi$  equal to 0 and  $\pi/2$ , and extending to  $\pm \infty$  in the  $\Phi$ -direction. Along these boundaries of constant  $\Psi$ , a series of equally spaced points are located at each of which the flow direction  $\theta$  and the  $x, y$ -coordinates of the channel walls will be determined by numerical integration. In order to use the tables of  $\alpha$  and  $\beta$  presented in this report, the point spacing  $\Delta\Phi$  must be an even multiple of  $\pi/24$ . Thus the smallest point spacing  $\pi/24$  is equal to  $1/2$  of the channel width ( $\pi/2$ ). For a particular prescribed velocity distribution along the channel walls the accuracy of the solution increases, and so does the amount of computing, as the point spacing is reduced. The error for a given point spacing depends on the prescribed velocity distribution, and its order of magnitude is given by the leading term of the error series of the formula used for numerical integration (table VIII, ref. 4, for example). For the numerical example presented in part II of this report the point spacing  $\Delta\Phi$  was  $\pi/12$ . From equation (54)

$$\frac{\Delta \log_e V}{\Delta \Phi} = \frac{(\log_e V)_{\Phi + \Delta \Phi} - (\log_e V)_{\Phi}}{\Delta \Phi} \quad (55)$$

where the subscripts  $\Phi$  and  $\Phi + \Delta\Phi$  refer to adjacent points along the channel boundaries.

(7) The value of  $\theta$  at each point  $(\Phi_0, \Psi_0)$  on the channel-wall boundaries is obtained from equation (50a) in which  $(\Delta \log_e V)/\Delta\Phi$  is given by equation (55) and  $\Delta I$  is given by equations (50b), (50c), and table VII. Note that in equation

(50a) the origin has been moved to  $\Phi_0$  by changing from  $\Phi$  to  $(\Phi - \Phi_0)$ . Thus the value of  $(\Delta \log_e V)/\Delta\Phi$  for a given value of  $(\Phi - \Phi_0)$  varies with  $\Phi_0$ .

(8) The physical  $x, y$ -coordinates at each point on the channel-wall boundaries are obtained by the numerical integration of equations (42a) and (42b) for incompressible flow, or equations (41a) and (41b) for linearized compressible flow where  $\Delta\psi^*$  is given by equation (32). The constants of integration in equations (41) and (42) are selected to give known values of  $x$  and  $y$  at upstream or downstream positions where flow conditions can be considered uniform.

#### NUMERICAL EXAMPLE

The channel design method of part II has been applied to the design of an elbow for the same conditions as example IV of part I. The design is for an accelerating elbow with no local decelerations of the prescribed velocities along the channel walls and with linearized compressible flow.

**Prescribed velocity distribution.**—The prescribed velocity distribution along the channel walls is the same as that for example IV of part I. The prescribed velocity as a function of  $\Phi$  is plotted in figure 22.

**Results.**—As indicated in table VIII, the elbow design resulting from the prescribed velocities given in figure 22 is the same as that obtained by relaxation methods (fig. 21) for the same prescribed conditions (example IV, part I).

The solution obtained by Green's function (part II) required one experienced computer 3 days, whereas the solution by relaxation methods (part I) required about 10 days. The relaxation solutions provide additional information, such as the distribution of velocity across the channel; but for the most part this additional information is of secondary importance, and the design of channels by Green's function is more rapid and therefore to be preferred over the design by relaxation methods.

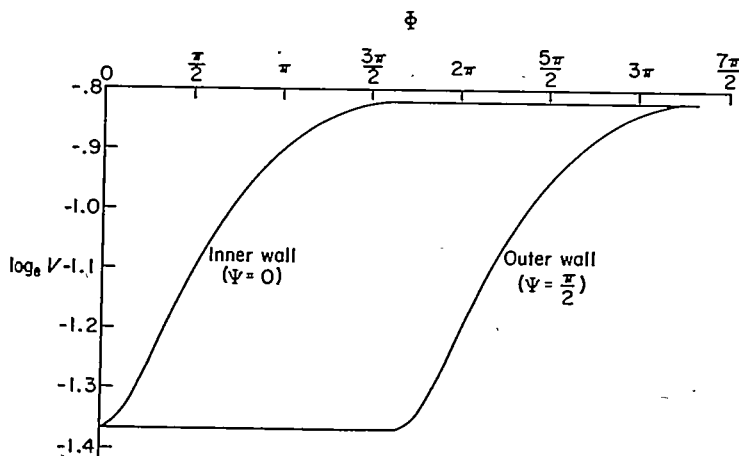


FIGURE 22.—Variation in prescribed values of  $\log_e V$  with  $\Phi$  along channel walls of numerical example in part II.

#### SUMMARY OF RESULTS AND CONCLUSIONS

A general method of design is developed for two-dimensional unbranched channels with prescribed velocities as a function of arc length along the channel walls. The method is developed for both compressible and incompressible, irrotational, nonviscous flow and applies to the design of elbows, diffusers, nozzles, and so forth. Two types of compressible flow are considered: the general type with arbitrary value for the ratio of specific heats  $\gamma$  (1.4, for example) and the linearized type in which  $\gamma$  is equal to  $-1.0$ . In part I solutions are obtained by relaxation methods on a transformed plane the coordinates of which are the streamlines and velocity-potential lines in the physical plane; in part II solutions are obtained by a Green's function. The method of solution in part I gives complete information concerning the flow throughout the channel, whereas the method of solution in part II gives the channel-wall coordinates only.

Five numerical examples are given in part I and the results are presented by (1) lines of constant velocity and flow direction or lines of constant physical coordinates in the transformed plane and (2) streamlines and velocity-potential lines or lines of constant velocity and flow direction in the physical plane. Among the five examples are three elbow designs for the same prescribed velocity as a function of arc length along the channel walls but with incompressible, linearized compressible, and compressible flow. The numerical results of these three elbow designs are tabulated to enable a detailed comparison of the three designs.

The shapes of the elbows for compressible flow and for linearized compressible flow are very nearly the same; and it is concluded that, if a nonviscous gas with arbitrary  $\gamma$  (1.4, for example) were to flow through a channel designed for linearized compressible flow ( $\gamma = -1.0$ ), the resulting velocity distribution along the channel walls would be nearly the velocity distribution prescribed for the linearized compressible flow. This conclusion is important because the design method for linearized compressible flow is considerably faster than that for compressible flow.

One numerical example is presented in part II for an accelerating elbow with linearized compressible flow. The elbow shape obtained from the solution by Green's function in part II is the same as that obtained from a solution by relaxation methods in part I for the same prescribed conditions. The time required for the calculations was considerably less for the solution by Green's function.

LEWIS FLIGHT PROPULSION LABORATORY  
NATIONAL ADVISORY COMMITTEE FOR AERONAUTICS  
CLEVELAND, OHIO, July 25, 1951

## APPENDIX A

## SYMBOLS

The following symbols are used in this report:

$A, B, C, D$	coefficients, equation (29)	$\theta$	flow direction in physical $xy$ -plane (measured in counterclockwise direction from positive $x$ -axis)
$A, B$	arbitrary constants, equation (C1a)	$\Delta\theta$	channel turning angle, equation (12)
$B_1, B_2, \dots$	Bernoulli's numbers	$\rho$	density (expressed as ratio of stagnation density)
$c$	constant, equation (E3)	$\rho^*$	density in linearized compressible flow and related to $\rho$ by equation (13a)
$G$	Green's function of the second kind, equations (E2) and (47)	$\Phi$	velocity potential used as Cartesian coordinate in transformed $\Phi\Psi$ -plane and related to $\varphi$ or $\varphi^*$ by equation (40a) or (40b), respectively
$I$	integral ( $\alpha$ or $\beta$ )	$\varphi$ and $\varphi^*$	velocity potential for incompressible and linearized compressible flow, respectively, equations (4) and (16)
$k_1$	coefficient, equation (14a)	$\Psi$	stream function used as Cartesian coordinate in transformed $\Phi\Psi$ -plane and related to $\psi$ or $\psi^*$ by equation (39a) or (39b), respectively
$k_2$	coefficient, equation (14b)	$\psi$ and $\psi^*$	stream function for incompressible and linearized compressible flow, respectively, equations (3) and (15)
$l$	length of closed boundary	$\Delta\psi^*$	boundary value of $\psi^*$ , for linearized compressible flow, along left channel wall when faced in the direction of flow, equation (32)
$n$	distance in $xy$ -plane measured normal to direction of flow (expressed as ratio of characteristic length equal to channel width downstream at infinity)	$\omega$	any harmonic function in $\Phi\Psi$ -plane
$p$	static pressure (expressed as ratio of stagnation density multiplied by stagnation speed of sound squared)	Subscripts:	
$Q$	velocity (expressed as ratio of characteristic velocity equal to constant channel velocity downstream at infinity)	$a, b$	quantities related to two velocities ( $q_a$ and $q_b$ , respectively) for which density given by equation (8a) is equal to density $\rho$ given by equations (13), (13a), and (13b)
$q$	velocity (expressed as ratio of stagnation speed of sound)	$d$	conditions downstream at infinity
$q^*$	velocity used in linearized compressible flow and related to $q$ by equation (13b)	$o$	point in $\Phi\Psi$ -plane at which $\theta$ is determined
$r$	distance from any point in $\Phi\Psi$ -plane to point $(\Phi_o, \Psi_o)$ at which logarithmic singularity exists	$u$	conditions upstream at infinity
$s$	distance in $xy$ -plane measured along direction of flow (expressed as ratio of characteristic length equal to channel width downstream at infinity)	$\Delta\psi^*$	left channel wall, when faced in direction of flow, along which $\psi^*$ is equal to $\Delta\psi^*$
$u$	velocity parameter related to $q^*$ by equation (18)	$(\Phi - \Phi_o)$	point at $(\Phi - \Phi_o)$ on either channel-wall boundary
$V$	velocity parameter defined by equations (43b) and (43c) for incompressible and linearized compressible flow, respectively	$(\Phi - \Phi_o) + \Delta\Phi$	point at $[(\Phi - \Phi_o) + \Delta\Phi]$ on either channel-wall boundary
$w, w_1, w_2$	complex functions defined by equations (F3), (F1a), and (F2a), respectively	$\varphi, \psi, \varphi^*, \psi^*$	along lines of constant $\varphi, \psi, \varphi^*$ , and $\psi^*$ , respectively
$x, y$	Cartesian coordinates in physical plane (expressed as ratios of characteristic length equal to channel width downstream at infinity)	0	right channel wall, when faced in direction of flow, along which $\Psi, \psi$ , or $\psi^*$ is equal to 0
$z$	complex coordinate, equation (F1b)	1.0	left channel wall, when faced in direction of flow, along which $\psi$ is equal to 1.0
$\bar{z}$	conjugate of $z$	$\frac{\pi}{2}$	left channel wall, when faced in direction of flow, along which $\Psi$ is equal to $\frac{\pi}{2}$
$\alpha$	integral, equation (50d)		
$\beta$	integral, equation (50e)		
$\gamma$	ratio of specific heats		
$\Delta$	finite increment		
$\delta$	increment of		

## APPENDIX B

EQUATIONS OF CONTINUITY AND IRROTATIONAL FLUID MOTION IN TERMS OF TRANSFORMED  $\varphi, \psi$ -COORDINATES

Consider the two-dimensional irrotational motion of a fluid particle in the physical  $xy$ -plane. The fluid particle is defined by adjacent streamlines (constant  $\psi$ ) and velocity-potential lines (constant  $\varphi$ ) spaced  $\delta n$  and  $\delta s$  apart as indicated in figure 23. The velocity  $Q$  is parallel to the streamlines and normal to the velocity-potential lines.

Continuity.—From continuity considerations of the fluid particle in figure 23

$$\frac{\partial}{\partial s} (\rho Q \delta n) = 0$$

or

$$\frac{\partial \log_e \rho}{\partial s} + \frac{\partial \log_e Q}{\partial s} + \frac{1}{\delta n} \frac{\partial(\delta n)}{\partial s} = 0 \quad (B1)$$

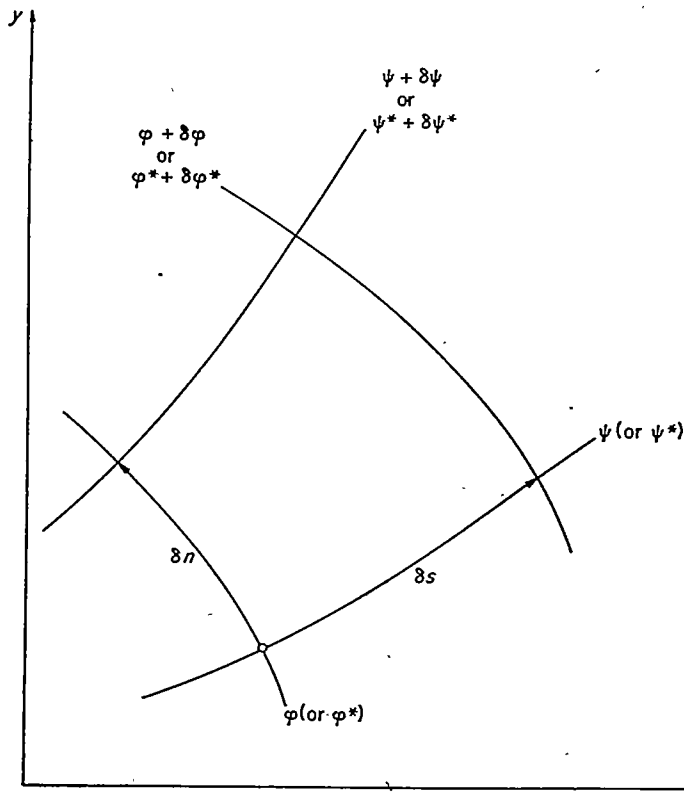


FIGURE 23.—Fluid particle bounded by streamlines and velocity-potential lines in physical  $xy$ -plane.

But, from geometrical considerations (ref. 5, p. 167, for example)

$$\frac{1}{\delta n} \frac{\partial(\delta n)}{\partial s} = \frac{\partial \theta}{\partial n} \quad (B2a)$$

and

$$\frac{1}{\delta s} \frac{\partial(\delta s)}{\partial n} = -\frac{\partial \theta}{\partial s} \quad (B2b)$$

so that equation (B1) becomes

$$\frac{\partial \log_e \rho}{\partial s} + \frac{\partial \log_e Q}{\partial s} + \frac{\partial \theta}{\partial n} = 0$$

or

$$\frac{\partial \log_e \rho}{\partial \varphi} \frac{d\varphi}{ds} + \frac{\partial \log_e Q}{\partial \varphi} \frac{d\varphi}{ds} + \frac{\partial \theta}{\partial \psi} \frac{d\psi}{dn} = 0$$

which, combined with equations (3) and (4), becomes

$$\frac{1}{\rho} \left( \frac{\partial \log_e \rho}{\partial \varphi} + \frac{\partial \log_e Q}{\partial \varphi} \right) + \frac{\partial \theta}{\partial \psi} = 0 \quad (5)$$

Equation (5) is the continuity equation expressed in terms of  $\varphi, \psi$ -coordinates.

Irrotational fluid motion.—For irrotational motion of the fluid particle in figure 23

$$\frac{\partial}{\partial n} (Q \delta s) = 0$$

or

$$\frac{\partial \log_e Q}{\partial n} + \frac{1}{\delta s} \frac{\partial(\delta s)}{\partial n} = 0 \quad (B3)$$

But, from equations (B2b) and (B3)

$$\frac{\partial \log_e Q}{\partial n} - \frac{\partial \theta}{\partial s} = 0$$

or

$$\frac{\partial \log_e Q}{\partial \psi} \frac{d\psi}{dn} - \frac{\partial \theta}{\partial \varphi} \frac{d\varphi}{ds} = 0$$

which, combined with equations (3) and (4), becomes

$$\rho \frac{\partial \log_e Q}{\partial \psi} - \frac{\partial \theta}{\partial \varphi} = 0 \quad (6)$$

Equation (6) is the equation for irrotational fluid motion expressed in terms of the  $\varphi, \psi$ -coordinates.

## APPENDIX C

## RELATION BETWEEN VELOCITY AND DENSITY, ASSUMING LINEAR VARIATION IN PRESSURE WITH SPECIFIC VOLUME

The approximate, linear relation between pressure  $p$  and specific volume  $1/\rho$  first suggested by Chaplygin (ref. 6) is given by

$$p = A - \frac{B}{\rho} \quad (C1a)$$

from which

$$\frac{dp}{d\rho} = \frac{B}{\rho^2} \quad (C1b)$$

where  $A$  and  $B$  are arbitrary constants.

If  $p$  denotes the static pressure expressed as a ratio of the stagnation density multiplied by the stagnation speed of sound squared, Bernoulli's equation is

$$\frac{dp}{\rho} + q dq = 0$$

which combined with equation (C1b) integrates to give the approximate relation between velocity and density

$$\frac{B}{2\rho^2} - \frac{q^2}{2} = \text{constant} \quad (\text{C2})$$

For convenience equation (C2) can be written as

$$\frac{1}{\rho^{*2}} - q^{*2} = 1$$

or

$$\rho^* = (1 + q^{*2})^{-1/2} \quad (\text{13})$$

where

$$\rho^* = k_1 \rho \quad (\text{13a})$$

and

$$q^* = k_2 q \quad (\text{13b})$$

The constants  $k_1$  and  $k_2$  replace the two arbitrary constants in equation (C2), and their values are determined so that for any two arbitrary values of  $q$  (designated by  $q_a$  and  $q_b$ ) the values of  $\rho$  given by equation (13) equal the values of  $\rho$  given by equation (8a). Thus the values of  $\rho$  given by equation (13) for  $q$  equal to  $q_a$  or  $q_b$  are correct; for all other values of  $q$  the values of  $\rho$  are approximate. The constants  $k_1$  and  $k_2$  are determined from the conditions

$$\left. \begin{aligned} \rho_a^* &= k_1 \rho_a \\ q_a^* &= k_2 q_a \\ \rho_b^* &= k_1 \rho_b \\ q_b^* &= k_2 q_b \end{aligned} \right\} \quad (\text{C3})$$

From equation (13) and the conditions given by equation (C3)

$$k_1 = \frac{1}{\rho_a} \sqrt{\frac{1 - \left(\frac{\rho_a q_a}{\rho_b q_b}\right)^2}{1 - \left(\frac{q_a}{q_b}\right)^2}} \quad (\text{14a})$$

and

$$k_2 = \frac{1}{q_b} \sqrt{\frac{\left(\frac{\rho_a}{\rho_b}\right)^2 - 1}{1 - \left(\frac{\rho_a q_a}{\rho_b q_b}\right)^2}} \quad (\text{14b})$$

where  $\rho_a$  and  $\rho_b$  are determined by equation (8a) for the selected values of  $q_a$  and  $q_b$ , respectively.

The values of  $q_a$  and  $q_b$  might, for example, be selected to equal the maximum and minimum values of  $q$  (which values of  $q$  must occur on the channel walls and are therefore known). Also, the values of  $q_a$  and  $q_b$  might be selected to equal the upstream and downstream velocities  $q_u$  and  $q_d$ . In this case the upstream and downstream channel widths would then satisfy continuity for a gas with the correct value of  $\gamma$  (1.4, for example). If the upstream and downstream velocities are equal, their value and the value of some other velocity (the maximum or minimum velocity, for example) can be selected for  $q_a$  and  $q_b$ ; or, if desired,  $q_a$  can be equal to  $q_b$ , in which case if

$$q_a = q + \epsilon \text{ where } \epsilon \rightarrow 0$$

$$q_b = q$$

it can be shown from equations (14a) and (14b) that

$$k_1 = \frac{1}{\rho} \sqrt{\frac{1 - \frac{\gamma+1}{2} q^2}{1 - \frac{\gamma-1}{2} q^2}} \quad (\text{C4a})$$

and

$$k_2 = \sqrt{\frac{1}{1 - \frac{\gamma+1}{2} q^2}} \quad (\text{C4b})$$

This latter case, in which  $q_a = q_b = q$ , corresponds to the method used by Chaplygin (ref. 6) and Kármán-Tsien (ref. 8) in which the correct relation between  $p$  and  $\frac{1}{\rho}$  is replaced by a straight line (eq. (C1a)) that is tangent to the correct relation at one point (where  $q_a = q_b$ ).

## APPENDIX D

### EQUATIONS OF CONTINUITY AND IRROTATIONAL FLUID MOTION IN TERMS OF TRANSFORMED $\varphi^*$ , $\psi^*$ -COORDINATES

Consider the two-dimensional irrotational motion of a fluid particle in the physical  $xy$ -plane. The fluid particle is defined by adjacent streamlines (constant  $\psi^*$ ) and velocity-potential lines (constant  $\varphi^*$ ) spaced  $\delta n$  and  $\delta s$  apart as indicated in figure 23. The velocity  $q^*$  is parallel to the streamlines and normal to the velocity-potential lines.

**Continuity.**—From continuity considerations of the fluid particle in figure 23

$$\frac{\partial}{\partial s} (\rho^* q^* \delta n) = 0$$

or

$$\frac{\partial \log_e \rho^*}{\partial s} + \frac{\partial \log_e q^*}{\partial s} + \frac{1}{\delta n} \frac{\partial(\delta n)}{\partial s} = 0$$

which combined with equation (B2a) becomes

$$\frac{\partial \log_e \rho^*}{\partial \varphi^*} \frac{d\varphi^*}{ds} + \frac{\partial \log_e q^*}{\partial \varphi^*} \frac{d\varphi^*}{ds} + \frac{\partial \theta}{\partial \psi^*} \frac{d\psi^*}{dn} = 0$$

or, from equations (15) and (16)

$$\frac{1}{\rho^*} \left( \frac{\partial \log_e \rho^*}{\partial \varphi^*} + \frac{\partial \log_e q^*}{\partial \varphi^*} \right) + \frac{\partial \theta}{\partial \psi^*} = 0 \quad (\text{D1})$$

But, from equation (13)

$$\frac{1}{\rho^*} \frac{\partial \log_e \rho^*}{\partial \varphi^*} = \frac{-q^{*2}}{\sqrt{1+q^{*2}}} \frac{\partial \log_e q^*}{\partial \varphi^*}$$

so that equation (D1) becomes

$$\frac{1}{\sqrt{1+q^{*2}}} \frac{\partial \log_e q^*}{\partial \varphi^*} + \frac{\partial \theta}{\partial \psi^*} = 0 \quad (\text{D2})$$

Finally, if

$$u = \frac{q^*}{1 + \sqrt{1 + q^{*2}}} \quad (18)$$

then

$$\frac{\partial \log_e q^*}{\sqrt{1 + q^{*2}}} = \partial \log_e u \quad (D3)$$

so that equation (D2) becomes

$$\frac{\partial \log_e u}{\partial \varphi^*} + \frac{\partial \theta}{\partial \psi^*} = 0 \quad (17)$$

Equation (17) is the continuity equation expressed in terms of  $\varphi^*$ ,  $\psi^*$ -coordinates and  $\log_e u$ .

Irrotational fluid motion.—For irrotational motion of the fluid particle in figure 23

$$\frac{\partial}{\partial n} (q^* \delta s) = 0$$

or

$$\frac{\partial \log_e q^*}{\partial n} + \frac{1}{\delta s} \frac{\partial (\delta s)}{\partial n} = 0$$

which combined with equation (B2b) becomes

$$\frac{\partial \log_e q^*}{\partial \psi^*} \frac{d\psi^*}{dn} - \frac{\partial \theta}{\partial \varphi^*} \frac{d\varphi^*}{ds} = 0$$

or, from equations (13), (15), and (16)

$$\frac{1}{\sqrt{1 + q^{*2}}} \frac{\partial \log_e q^*}{\partial \psi^*} - \frac{\partial \theta}{\partial \varphi^*} = 0 \quad (D4)$$

Finally, from equations (D3) and (D4)

$$\frac{\partial \log_e u}{\partial \psi^*} - \frac{\partial \theta}{\partial \varphi^*} = 0 \quad (20)$$

Equation (20) is the equation for irrotational fluid motion expressed in terms of  $\varphi^*$ ,  $\psi^*$ -coordinates and  $\log_e u$ .

## APPENDIX E

### INTEGRAL EQUATION FOR $\theta(\Phi, \Psi_0)$

If the distribution of the angle  $\theta(\Phi, \Psi)$  in the transformed  $\Phi\Psi$ -plane is harmonic, that is, satisfies equation (45) within and on the channel walls ( $\Psi$  equals 0 and  $\frac{\pi}{2}$ ), then from Green's theorem and the theorem of mean value it can be shown that the value of  $\theta$  at a point  $(\Phi_0, \Psi_0)$  within (or on) the channel walls is given by (ref. 9, p. 204, for example)

$$\theta(\Phi_0, \Psi_0) = \frac{1}{2\pi} \left[ \int_{-\infty}^{\infty} \left( \theta \frac{\partial G}{\partial \Psi} - G \frac{\partial \theta}{\partial \Psi} \right)_0 d\Phi - \int_{-\infty}^{\infty} \left( -\theta \frac{\partial G}{\partial \Psi} + G \frac{\partial \theta}{\partial \Psi} \right)_{\frac{\pi}{2}} d\Phi \right] \quad (E1)$$

where the two integrals on the right side of equation (E1) represent the line integral around the channel walls in the counterclockwise direction with the signs adjusted so that  $\frac{\partial}{\partial \Psi}$  represents the inner normal to the path of integration.

The function  $G(\Phi, \Psi)$  in equation (E1) is of the form (ref. 9, p. 204)

$$G(\Phi, \Psi) = \log_e \frac{1}{r} + \omega(\Phi, \Psi) \quad (E2)$$

where  $r$  is the distance from any point  $(\Phi, \Psi)$  to the point  $(\Phi_0, \Psi_0)$  and where  $\omega(\Phi, \Psi)$  is an arbitrary function that is harmonic within and on the channel walls. (Thus from equation (E2),  $G(\Phi, \Psi)$  is harmonic within and on the channel walls except at the point  $(\Phi_0, \Psi_0)$  where a logarithmic singularity exists.) Because the harmonic function  $\omega(\Phi, \Psi)$  is arbitrary, the function  $G(\Phi, \Psi)$  can be selected so that along

the channel-wall boundaries ( $\Psi$  equals 0 and  $\frac{\pi}{2}$ )  $\frac{\partial G}{\partial \Psi}$  is a constant  $c$  given by the following equation (obtained from notes presented by Tamarkin and Feller in the 1941 Summer Session for Advanced Instruction and Research in Mechanics at Brown Univ.):

$$c = \frac{2\pi}{l} \quad (E3)$$

where  $l$  is the length of the path along which the line integral is taken. For the path under consideration  $l$  is infinite and therefore  $G(\Phi, \Psi)$  can be selected so that  $\frac{\partial G}{\partial \Psi}$  is zero along the channel walls. A function with this property is a Green's function of the second kind. Equation (E1) becomes

$$\theta(\Phi_0, \Psi_0) = \frac{1}{2\pi} \int_{-\infty}^{\infty} \left[ \left( G \frac{\partial \theta}{\partial \Psi} \right)_{\frac{\pi}{2}} - \left( G \frac{\partial \theta}{\partial \Psi} \right)_0 \right] d\Phi$$

or, combined with equation (43a)

$$\theta(\Phi_0, \Psi_0) = \frac{-1}{2\pi} \int_{-\infty}^{\infty} \left[ \left( G \frac{\partial \log_e V}{\partial \Phi} \right)_{\frac{\pi}{2}} - \left( G \frac{\partial \log_e V}{\partial \Phi} \right)_0 \right] d\Phi \quad (46)$$

Along the channel walls  $\frac{\partial \log_e V}{\partial \Phi}$  is known from the prescribed velocity distribution so that, after the proper Green's function  $G$  has been determined (appendix F), equation (46) determines the value of  $\theta$  at any point  $(\Phi_0, \Psi_0)$ . The value of  $\theta(\Phi_0, \Psi_0)$  given by equation (46) can be adjusted by an arbitrary constant of integration to give a specified value of  $\theta$  at one point in the flow field.

## APPENDIX F

## GREEN'S FUNCTION OF SECOND KIND

From appendix E Green's function of the second kind  $G$  satisfies the condition

$$\frac{\partial G}{\partial \Psi} = 0$$

along the channel walls, which are straight and parallel boundaries ( $\Psi$  equals 0 and  $\frac{\pi}{2}$ ) extending to  $\pm \infty$  in the  $\Phi$ -direction, and satisfies the equation

$$\frac{\partial^2 G}{\partial \Phi^2} + \frac{\partial^2 G}{\partial \Psi^2} = 0$$

everywhere in the channel except at the point  $(\Phi_o, \Psi_o)$  where  $G$  has a logarithmic pole. For these conditions the Green's function  $G$  can be obtained by analogy from the velocity potential for incompressible flow into a point sink at  $(\Phi_o, \Psi_o)$  between straight parallel boundaries at  $\Psi$  equal to 0 and  $\frac{\pi}{2}$ . The logarithmic pole for  $G$  at  $(\Phi_o, \Psi_o)$  corresponds to the point sink, and the condition  $\frac{\partial G}{\partial \Psi} = 0$  at the boundaries corresponds to zero velocity, that is, no flow normal to the boundaries.

The velocity potential for fluid flow with the boundary conditions just described is obtained from two infinite series of point sinks with the sinks of each series spaced  $\pi$  distance apart in the  $\Psi$ -direction, and the two series arranged by the method of images in such a manner that no flow crosses the boundaries, that is,  $\frac{\partial G}{\partial \Psi} = 0$ . This arrangement of point sinks is shown in figure 24.

The complex function  $w_1$  for the first infinite series of point sinks is given by (ref. 10, p. 112, for example)

$$w_1 = -\log_e \sinh (z - z_o) \quad (\text{F1a})$$

where

$$z = \Phi + i\Psi \quad (\text{F1b})$$

The complex function  $w_2$  for the second infinite series of point sinks (mirror image of the first series in order to prevent flow across the boundaries  $\Psi$  equals 0 and  $\frac{\pi}{2}$ ) is given by

$$w_2 = -\log_e \sinh (z - \bar{z}_o) \quad (\text{F2a})$$

where

$$\bar{z} = \Phi - i\Psi \quad (\text{F2b})$$

The complex function  $w$  for the combined flow becomes from equations (F1a) to (F2b)

$$w = w_1 + w_2 = -\log_e \sinh [(\Phi - \Phi_o) + i(\Psi - \Psi_o)] - \log_e \sinh [(\Phi - \Phi_o) + i(\Psi + \Psi_o)] \quad (\text{F3})$$

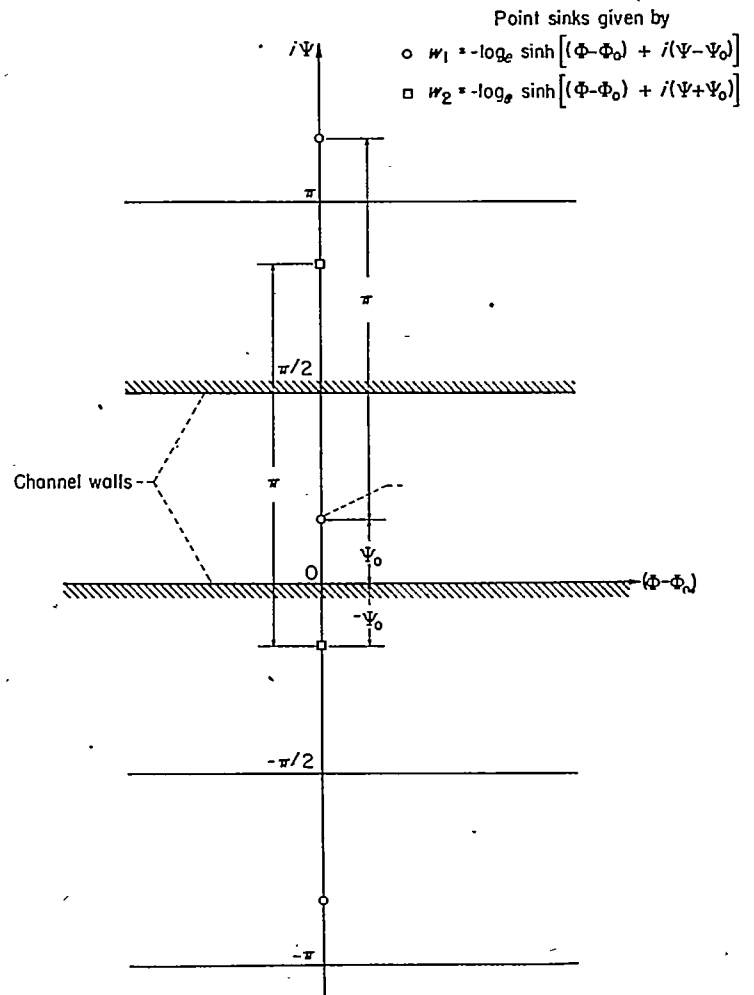


FIGURE 24.—Two infinite series of point sinks required in the development of Green's function of the second kind  $G$ .

The Green's function of the second kind  $G$  corresponds to the velocity potential for the incompressible flow and is therefore given by the real part of equation (F3)

$$G = -\frac{1}{2} \log_e [\cosh^2 (\Phi - \Phi_o) - \cos^2 (\Psi - \Psi_o)] [\cosh^2 (\Phi - \Phi_o) - \cos^2 (\Psi + \Psi_o)] \quad (\text{F4})$$

But along the channel walls  $\Psi$  is equal to 0 or  $\frac{\pi}{2}$  so that

$$\cos^2 (\Psi + \Psi_o) = \cos^2 (\Psi - \Psi_o)$$

and equation (F4) becomes

$$G_{\text{on } \frac{\pi}{2}} = -\log_e [\cosh^2 (\Phi - \Phi_o) - \cos^2 (\Psi - \Psi_o)] \quad (47)$$

Equation (47) gives the Green's function of the second kind along the channel walls (straight parallel lines of constant  $\Psi$  equal to 0 and  $\frac{\pi}{2}$  and extending to  $\pm \infty$  in the  $\Phi$ -direction).

## APPENDIX G

EVALUATION OF  $\alpha$  AND  $\beta$ 

Several techniques, depending on the magnitude of the upper limit  $|(\Phi-\Phi_0)|$ , were used to evaluate the integrals  $\alpha$  and  $\beta$  given by equations (50d) and (50e). Each integral is treated separately in this appendix, and the values of  $(\Phi-\Phi_0)$  for the upper limit  $|(\Phi-\Phi_0)|$  are considered positive. For negative values of  $(\Phi-\Phi_0)$  the magnitudes of  $I$  (that is, of  $\alpha$  or  $\beta$ ) are equal for corresponding values of  $|(\Phi-\Phi_0)|$  but opposite in sign. As a result the values of  $\Delta I$  have the same sign.

INTEGRAL  $\alpha$ 

Small and medium values of  $(\Phi-\Phi_0)$ .—For small and medium values of the upper limit of integration  $(\Phi-\Phi_0)$  in equation (50d), that is, for  $0 \leq (\Phi-\Phi_0) \leq 60\pi/24$ , the integral  $\alpha$  is evaluated by Simpson's one-third rule using increments of  $(\Phi-\Phi_0)$  equal to  $\pi/48$ .

Large values of  $(\Phi-\Phi_0)$ .—For large values of  $(\Phi-\Phi_0)$ , that is, for  $(\Phi-\Phi_0) > 60\pi/24$ , the integrand in equation (50d) becomes

$$\log_e \cosh (\Phi-\Phi_0) \approx (\Phi-\Phi_0) - \log_e 2 \quad (G1)$$

so that equation (50d) becomes

$$\begin{aligned} \alpha &\approx \int_0^{60\pi/24} \log_e \cosh (\Phi-\Phi_0) d(\Phi-\Phi_0) + \\ &\int_{60\pi/24}^{(\Phi-\Phi_0)} [(\Phi-\Phi_0) - \log_e 2] d(\Phi-\Phi_0) \\ &\approx 25.809782 + \left[ \frac{(\Phi-\Phi_0)^2}{2} - 0.693147(\Phi-\Phi_0) - 25.398552 \right] \\ &\approx 0.411230 - 0.693147(\Phi-\Phi_0) + \frac{1}{2}(\Phi-\Phi_0)^2 \quad (G2) \end{aligned}$$

Equation (G2) gives values of  $\alpha$  for values of  $(\Phi-\Phi_0)$  equal to or greater than  $60\pi/24$ . Values of the integral  $\alpha$  are tabulated in table VII for a range of  $|(\Phi-\Phi_0)|$  between 0 and  $100\pi/24$  in increments of  $\pi/24$ . For negative values of  $(\Phi-\Phi_0)$  the sign of  $\alpha$  is negative.

INTEGRAL  $\beta$ 

Small values of  $(\Phi-\Phi_0)$ .—For  $(\Phi-\Phi_0)$  equal to zero the integrand of equation (50e) becomes infinite so that Simpson's one-third rule cannot be used to evaluate  $\beta$  in this region of  $(\Phi-\Phi_0)$ , as was done for  $\alpha$ . However, equation (50e) integrates by parts to give

$$\int_0^{(\Phi-\Phi_0)} \log_e \sinh (\Phi-\Phi_0) d(\Phi-\Phi_0) = (\Phi-\Phi_0) \log_e \sinh (\Phi-\Phi_0) - \int_0^{(\Phi-\Phi_0)} (\Phi-\Phi_0) \operatorname{ctnh} (\Phi-\Phi_0) d(\Phi-\Phi_0) \quad (G3)$$

where the integrand  $(\Phi-\Phi_0) \operatorname{ctnh} (\Phi-\Phi_0)$  on the right side of equation (G3) can be expanded in the following series form:

$$\begin{aligned} (\Phi-\Phi_0) \operatorname{ctnh} (\Phi-\Phi_0) &= 1 + \frac{2^2 B_1 (\Phi-\Phi_0)^2}{2!} - \frac{2^4 B_3 (\Phi-\Phi_0)^4}{4!} + \\ &\frac{2^6 B_5 (\Phi-\Phi_0)^6}{6!} - \frac{2^8 B_7 (\Phi-\Phi_0)^8}{8!} + \frac{2^{10} B_9 (\Phi-\Phi_0)^{10}}{10!} - \\ &\frac{2^{12} B_{11} (\Phi-\Phi_0)^{12}}{12!} + \dots \quad (G4) \end{aligned}$$

where  $B_1, B_3$ , and so forth, are Bernoulli's numbers (ref. 11, p. 90, for example). From equations (G3) and (G4)

$$\begin{aligned} \beta &= (\Phi-\Phi_0) \log_e \sinh (\Phi-\Phi_0) - (\Phi-\Phi_0) - \frac{(\Phi-\Phi_0)^3}{9} + \frac{(\Phi-\Phi_0)^5}{225} - \\ &\frac{2(\Phi-\Phi_0)^7}{6615} + \frac{(\Phi-\Phi_0)^9}{42,525} - \frac{2(\Phi-\Phi_0)^{11}}{1,029,105} + \frac{1382(\Phi-\Phi_0)^{13}}{8,300,667,375} - \dots \quad (G5) \end{aligned}$$

Equation (G5) was used to obtain  $\beta$  as a function of  $(\Phi-\Phi_0)$  for  $0 \leq (\Phi-\Phi_0) \leq 8\pi/24$ .

Medium values of  $(\Phi-\Phi_0)$ .—For medium values of the upper limit of integration  $(\Phi-\Phi_0)$  in equation (50e), that is, for  $8\pi/24 < (\Phi-\Phi_0) \leq 60\pi/24$ , the integral  $\beta$  is evaluated by Simpson's one-third rule as was done for  $\alpha$ .

Large values of  $(\Phi-\Phi_0)$ .—For large values of  $(\Phi-\Phi_0)$ , that is, for  $(\Phi-\Phi_0) > 60\pi/24$ , the integrand in equation (50e) becomes

$$\log_e \sinh (\Phi-\Phi_0) \approx (\Phi-\Phi_0) - \log_e 2 \quad (G6)$$

so that equation (50e) becomes

$$\begin{aligned} \beta &\approx \int_0^{60\pi/24} \log_e \sinh (\Phi-\Phi_0) d(\Phi-\Phi_0) + \\ &\int_{60\pi/24}^{(\Phi-\Phi_0)} [(\Phi-\Phi_0) - \log_e 2] d(\Phi-\Phi_0) \\ &\approx 24.576082 + \left[ \frac{(\Phi-\Phi_0)^2}{2} - 0.693147(\Phi-\Phi_0) - 25.398552 \right] \\ &\approx -0.822470 - 0.693147(\Phi-\Phi_0) + \frac{1}{2}(\Phi-\Phi_0)^2 \quad (G7) \end{aligned}$$

Equation (G7) gives values of  $\beta$  for values of  $(\Phi-\Phi_0)$  equal to or greater than  $60\pi/24$ . Values of the integral  $\beta$  are tabulated in table VII for a range of  $|(\Phi-\Phi_0)|$  between 0 and  $100\pi/24$  in increments of  $\pi/24$ . For negative values of  $(\Phi-\Phi_0)$ , the sign of  $\beta$  changes.

## APPENDIX H

## CHANNEL TURNING ANGLE

If the prescribed velocity distribution along one channel wall differs from the distribution along the other wall, then in general the channel deflects an amount  $\Delta\theta$ , which is the difference in flow direction far downstream and far upstream

of the region in which the prescribed velocity distribution varies. Thus,

$$\Delta\theta = \theta_d - \theta_u \quad (H1)$$

For large values of  $|(\Phi - \Phi_0)|$  such as occur far upstream and far downstream of the region in which the prescribed velocity varies along the channel walls

$$\cosh^2(\Phi - \Phi_0) \gg \cos^2(\Psi - \Psi_0)$$

so that from equation (47)

$$G_0 = G_{\frac{\pi}{2}} = -2[|(\Phi - \Phi_0)| - \log_e 2] \quad (\text{H2})$$

Far upstream  $\Phi_0 < \Phi$  so that

$$|(\Phi - \Phi_0)| = (\Phi - \Phi_0)$$

and because  $V$  is harmonic

$$\int_{-\infty}^{\infty} \left[ \left( \frac{\partial \log_e V}{\partial \Phi} \right)_{\frac{\pi}{2}} - \left( \frac{\partial \log_e V}{\partial \Phi} \right)_0 \right] d\Phi = 0$$

so that equation (H2) substituted into equation (46) gives

$$\theta_u = \frac{1}{\pi} \int_{-\infty}^{\infty} \Phi \left[ \left( \frac{\partial \log_e V}{\partial \Phi} \right)_{\frac{\pi}{2}} - \left( \frac{\partial \log_e V}{\partial \Phi} \right)_0 \right] d\Phi \quad (\text{H3})$$

Likewise, far downstream  $\Phi_0 > \Phi$  so that

$$|(\Phi - \Phi_0)| = -(\Phi - \Phi_0)$$

and equation (H2) substituted into equation (46) gives

$$\theta_d = \frac{-1}{\pi} \int_{-\infty}^{\infty} \Phi \left[ \left( \frac{\partial \log_e V}{\partial \Phi} \right)_{\frac{\pi}{2}} - \left( \frac{\partial \log_e V}{\partial \Phi} \right)_0 \right] d\Phi \quad (\text{H4})$$

From equations (H1), (H3), and (H4)

$$\Delta\theta = \frac{-2}{\pi} \int_{-\infty}^{\infty} \Phi \left[ \left( \frac{\partial \log_e V}{\partial \Phi} \right)_{\frac{\pi}{2}} - \left( \frac{\partial \log_e V}{\partial \Phi} \right)_0 \right] d\Phi \quad (\text{H5})$$

Equation (H5) determines the channel turning angle  $\Delta\theta$ .

#### REFERENCES

- Carrier, G. F.: Elbows for Accelerated Flow. *Jour. Appl. Mech.*, vol. 14, no. 2, June 1947, pp. A-108-A-112.
- Lighthill, M. J.: A New Method of Two-Dimensional Aerodynamic Design. *R. & M. No. 2112*, British A. R. C., 1945.
- Clauser, Francis H.: Two-Dimensional Compressible Flows Having Arbitrarily Specified Pressure Distributions for Gases with Gamma Equal to Minus One. *Rep. NOLR 1132*, Symposium on Theoretical Compressible Flow, U. S. Naval Ordnance Lab., June 28, 1949, pp. 1-33.
- Southwell, R. V.: *Relaxation Methods in Theoretical Physics*. Clarendon Press (Oxford), 1946.
- Liepmann, Hans Wolfgang, and Puckett, Allen E.: *Introduction to Aerodynamics of a Compressible Fluid*. John Wiley & Sons, Inc., 1947.
- Chaplygin, S.: *Gas Jets*. NACA TM 1063, 1944.
- Emmons, Howard W.: The Numerical Solution of Partial Differential Equations. *Quart. Appl. Math.*, vol. II, no. 3, Oct. 1944, pp. 173-195.
- Tsien, Hsue-Shen: Two-Dimensional Subsonic Flow of Compressible Fluids. *Jour. Aero. Sci.*, vol. 6, no. 10, Aug. 1939, pp. 399-407.
- Osgood, William Fogg: *Functions of a Complex Variable*. G. E. Stechert & Co. (New York), 1942.
- Streeter, Victor L.: *Fluid Dynamics*. McGraw-Hill Book Co., Inc. (New York), 1948.
- Peirce, B. O.: *A Short Table of Integrals*. Third ed., Ginn and Company (Boston), 1929.

TABLE I—DISTRIBUTION OF VELOCITY  $Q$  AND FLOW DIRECTION  $\theta$  IN TRANSFORMED  $\psi$ -PLANE FOR EXAMPLE III (ELBOW WITH INCOMPRESSIBLE FLOW)

[Prescribed variation in  $Q$  with arc length  $s$  along channel walls plotted in fig. 2;  $Q_w=0.5$ ,  $Q_d=1.0$ ,  $\Delta\theta=89.36^\circ$ ]

$\psi$	0		0.125		0.250		0.375		0.500		0.625		0.750		0.875		1.000			
	$Q$	$\theta$																		
-2.000	0.5000	0	0.5000	0	0.5000	0	0.5000	0	0.5000	0	0.5000	0	0.5000	0	0.5000	0	0.5000	0	0.5000	0
-1.875	.5000	.01	.5000	.01	.5000	.00	.5000	.00	.5000	.00	.5000	.00	.5000	.00	.5000	.00	.5000	.01	.5000	.01
-1.750	.5000	.01	.5000	.01	.5000	.01	.5000	.00	.5000	.00	.5000	.00	.5000	.00	.5000	.01	.5000	.01	.5000	.01
-1.625	.5000	.01	.5000	.01	.5000	.01	.5001	.01	.5001	.01	.5001	.01	.5001	.01	.5001	.01	.5000	.01	.5000	.01
-1.500	.5000	.02	.5001	.03	.5001	.01	.5001	.01	.5001	.00	.5001	.00	.5001	.01	.5001	.01	.5001	.02	.5000	.02
-1.375	.5000	.03	.5001	.03	.5002	.02	.5002	.01	.5002	.00	.5002	.00	.5002	.01	.5002	.02	.5001	.03	.5000	.03
-1.250	.5000	.04	.5001	.04	.5002	.03	.5003	.02	.5003	.02	.5003	.02	.5002	.03	.5002	.03	.5001	.04	.5000	.04
-1.125	.5000	.06	.5002	.06	.5004	.04	.5005	.03	.5005	.00	.5005	.00	.5004	.03	.5004	.05	.5002	.06	.5000	.06
-1.000	.5000	.09	.5003	.08	.5006	.07	.5007	.04	.5008	.00	.5007	.04	.5005	.07	.5005	.07	.5003	.08	.5000	.09
-.875	.5000	.14	.5005	.12	.5009	.10	.5011	.05	.5012	.00	.5011	.06	.5008	.10	.5004	.12	.5004	.12	.5000	.14
-.750	.5000	.20	.5007	.18	.5013	.14	.5016	.08	.5017	.01	.5016	.09	.5012	.14	.5006	.18	.5006	.18	.5000	.20
-.625	.5000	.30	.5011	.27	.5019	.21	.5025	.11	.5026	.01	.5023	.13	.5018	.21	.5009	.27	.5009	.27	.5000	.30
-.500	.5000	.45	.5016	.40	.5029	.30	.5037	.16	.5038	.02	.5034	.19	.5026	.31	.5014	.40	.5014	.40	.5000	.45
-.375	.5000	.69	.5025	.60	.5044	.50	.5055	.24	.5056	.04	.5050	.28	.5037	.45	.5010	.60	.5010	.60	.5000	.69
-.250	.5000	1.04	.5039	.89	.5068	.65	.5082	.32	.5083	.09	.5072	.43	.5053	.67	.5028	.89	.5028	.89	.5000	1.04
-.125	.5000	1.63	.5065	1.34	.5107	.94	.5124	.44	.5123	.17	.5103	.64	.5074	.98	.5039	1.10	.5039	1.10	.5000	1.63
0	.5000	2.73	.5115	2.04	.5171	1.30	.5187	.60	.5175	.36	.5145	.99	.5103	1.44	.5053	1.71	.5053	1.71	.5000	2.73
.125	.5097	5.06	.5226	3.21	.5276	1.64	.5278	.34	.5249	.70	.5200	1.50	.5139	2.07	.5071	2.41	.5071	2.41	.5000	5.06
.250	.5354	6.83	.5424	4.02	.5433	1.73	.5402	.03	.5344	1.27	.5289	2.24	.5184	2.93	.5093	3.34	.5093	3.34	.5000	6.83
.375	.5715	7.36	.5682	4.02	.5637	1.32	.5557	.75	.5460	2.18	.5361	3.29	.5236	4.07	.5118	4.64	.5118	4.64	.5000	7.36
.500	.6134	6.69	.6006	3.19	.5874	.33	.5736	1.89	.5592	3.46	.5444	4.66	.5285	5.51	.5146	6.01	.5146	6.01	.5000	6.69
.625	.6576	4.95	.6344	1.62	.6132	-1.31	.5980	-3.55	.5735	5.19	.5544	6.43	.5357	7.31	.5176	7.83	.5176	7.83	.5000	4.95
.750	.7018	2.40	.6690	-.82	.6399	-3.52	.6132	-5.89	.5853	7.33	.5647	8.57	.5422	9.45	.5207	9.97	.5207	9.97	.5000	2.40
.875	.7448	-.81	.7030	-3.76	.6663	-6.26	.6334	-8.31	.6032	9.89	.5761	11.09	.5487	11.95	.5237	12.46	.5237	12.46	.5000	-.81
1.000	.7855	-4.82	.7350	-7.18	.6919	-9.46	.6530	-11.34	.6177	12.84	.5822	13.98	.5450	14.79	.5207	15.27	.5207	15.27	.5000	-4.82
1.125	.8235	-8.64	.7662	-11.01	.7162	-13.05	.6717	-14.76	.6316	16.14	.5949	17.20	.5511	17.98	.5296	18.41	.5296	18.41	.5000	-8.64
1.250	.8598	-13.05	.7945	-15.16	.7387	-16.97	.6891	-18.51	.6446	19.76	.6041	20.74	.5608	21.49	.5323	22.00	.5323	22.00	.5000	-13.05
1.375	.8998	-17.77	.8202	-19.59	.7583	-21.17	.7052	-22.53	.6597	22.66	.6126	24.62	.5721	25.19	.5348	25.68	.5348	25.68	.5000	-17.77
1.500	.9177	-22.07	.8432	-24.22	.7778	-25.00	.7189	-26.78	.6678	27.81	.6204	29.62	.5771	29.29	.5371	29.60	.5371	29.60	.5000	-22.07
1.625	.9418	-27.72	.8638	-29.03	.7944	-30.20	.7331	-31.25	.6779	32.16	.6278	32.90	.5817	33.44	.5393	33.77	.5393	33.77	.5000	-27.72
1.750	.9620	-32.88	.8809	-33.95	.8089	-34.64	.7450	-35.84	.6873	35.67	.6347	37.37	.5862	37.89	.5414	38.21	.5414	38.21	.5000	-32.88
1.875	.9782	-38.10	.8949	-38.94	.8215	-39.73	.7558	-40.84	.6962	41.32	.6415	42.01	.5908	42.63	.5437	42.86	.5437	42.86	.5000	-38.10
2.000	.9901	-43.30	.9065	-43.91	.8325	-44.58	.7659	-45.28	.7050	46.04	.6488	46.78	.5959	47.35	.5463	47.73	.5463	47.73	.5000	-43.30
2.125	.9975	-48.43	.9163	-48.83	.8422	-49.38	.7757	-50.02	.7143	50.80	.6569	51.66	.6023	52.35	.5499	52.56	.5499	52.56	.5000	-48.43
2.250	1.0000	-53.34	.9218	-53.57	.8510	-54.00	.7858	-54.65	.7249	55.51	.6671	56.56	.6112	57.49	.5560	58.32	.5560	58.32	.5000	-53.34
2.375	1.0000	-57.83	.9271	-58.01	.8596	-58.44	.7968	-59.14	.7374	60.11	.6805	61.28	.6248	62.03	.5686	64.31	.5686	64.31	.5000	-57.83
2.500	1.0000	-62.00	.9321	-62.16	.8687	-62.63	.8091	-63.40	.7494	64.48	.6977	65.83	.6442	67.05	.5905	69.98	.5905	69.98	.5000	-62.00
2.625	1.0000	-65.84	.9374	-66.01	.8785	-66.51	.8223	-67.35	.7697	68.62	.7188	70.02	.6689	72.14	.6200	74.88	.6200	74.88	.5000	-65.84
2.750	1.0000	-69.39	.9429	-69.55	.8890	-70.07	.8378	-70.96	.7891	72.20	.7424	73.82	.6876	76.07	.6544	78.95	.6544	78.95	.5000	-69.39
2.875	1.0000	-72.57	.9487	-72.74	.8999	-73.27	.8637	-74.17	.8097	75.44	.7680	77.11	.7285	79.37	.6915	82.21	.6915	82.21	.5000	-72.57
3.000	1.0000	-75.43	.9544	-75.59	.9111	-76.12	.8699	-77.02	.8309	78.27	.7943	79.92	.7603	82.10	.7292	84.80	.7292	84.80	.5000	-75.43
3.125	1.0000	-77.93	.9601	-78.10	.9221	-78.60	.8860	-79.46	.8521	80.67	.8205	82.26	.7918	84.30	.7603	86.80	.7603	86.80	.5000	-77.93
3.250	1.0000	-80.11	.9656	-80.27	.9327	-80.75	.9016	-81.55	.8726	82.69	.8460	84.17	.8222	86.05	.8018	88.32	.8018	88.32	.5000	-80.11
3.375	1.0000	-81.97	.9708	-82.11	.9427	-82.56	.9164	-83.30	.8920	84.35	.8700	85.71	.8508	87.41	.8351	89.44	.8351	89.44	.5000	-81.97
3.500	1.0000	-83.54	.9755	-83.67	.9521	-84.07	.9301	-84.74	.9100	85.69	.8923	86.92	.8773	88.43	.8668	90.25	.8668	90.25	.5000	-83.54
3.625	1.0000	-84.84	.9798	-84.96	.9605	-85.32	.9426	-85.91	.9264	86.75	.9125	87.83	.9014	89.16	.8936	90.72	.8936	90.72	.5000	-84.84
3.750	1.0000	-85.90	.9837	-86.01	.9680	-86.32	.9537	-86.84	.9410	87.57	.9305	88.51	.9225	89.65	.9183	90.99	.9183	90.99	.5000	-85.90
3.875	1.0000	-86.75	.9870	-86.84	.9746	-87.11	.9634	-87.56	.9538	88.18	.9462	88.98	.9414	89.94	.9397	91.06	.9397	91.06	.5000	-86.75
4.000	1.0000	-87.43	.9898	-87.50	.9802	-87.73	.9717	-88.10	.9646	88.62	.9596	89.28	.9571	90.07	.9577	90.98	.9577	90.98	.5000	-87.43
4.125	1.0000	-87.95	.9922	-88.01	.9849	-88.20	.9786	-88.50	.9738	88.92	.9705	89.45	.9698	90.07	.9722	90.78	.9722	90.78	.5000	-87.95
4.250	1.0000	-88.34	.9942	-88.39	.9889	-88.54	.9842	-88.78	.9808	89.11	.9792	89.53	.9798	89.99	.9831	90.50	.9831	90.50	.5000	-88.34
4.375	1.0000	-88.64	.9957	-88.68	.9917	-88.79	.9886	-88.98	.9864	89.23	.9867	89.55	.9880	89.87	.9905	90.19	.9905	90.19	.5000	-88.64
4.500	1.0000	-88.85	.9969	-88.88	.9941	-88.97	.9910	-89.10	.9905	89.29	.9904	89.53	.9917	89.73	.9948	89.90	.9948	89.90	1.0000	-88.85
4.625	1.0000	-89.01	.9978	-89.03	.9958	-89.09	.9943	-89.19	.9935	89.33	.9935	89.49	.9946	89.62	.9969	89.72	.9969	89.72	1.0000	-89.01
4.750	1.0000	-89.11	.9984	-89.13	.9971	-89.18	.9961	-89.25	.9956	89.34	.9957	89.45	.9965	89.64	.9980	89.60	.9980	89.60	1.0000	-89.11
4.875	1.0000	-89.19	.9989	-89.21	.9980	-89.24	.9973	-89.29	.9970	89.35	.9971	89.43	.9977	89.48	.9987	89.52	.9987	89.52	1.0000	-89.19
5.000	1.0000	-89.24	.9993	-89.25	.9986	-89.28	.9982	-89.31	.9980	89.36	.9981	89.41	.9985	89.44	.9992	89.47	.9992	89.47	1.0000	-89.24
5.125	1.0000	-89.28	.9995	-89.29	.9991	-89.30	.9988	-89.33	.9986	89.36	.9987	89.39	.9990	89.42	.9995	89.43	.9995	89.43	1.0000	-89.28
5.250	1.0000	-89.31	.9997	-89.31	.9994	-89.32	.9992	-89.34	.9991	89.36	.9992	89.38	.9994	89.40	.9997	89.41	.9997	89.41	1.0000	-89.31
5.375	1.0000	-89.32	.9998	-89.33	.9996	-89.33	.9995	-89.35	.9994	89.36	.9995	89								

TABLE II—DISTRIBUTION OF PHYSICAL COORDINATES  $x$  AND  $y$  IN TRANSFORMED  $\psi$ -PLANE FOR EXAMPLE III (ELBOW WITH INCOMPRESSIBLE FLOW)

[Prescribed variation in  $Q$  with arc length  $s$  along channel walls plotted in fig. 2;  $Q_0=0.5$ ,  $Q_d=1.0$ ,  $\Delta\theta=89.36^\circ$ ]

$\psi$	0		0.125		0.250		0.375		0.500		0.625		0.750		0.875		1.000	
	$x$	$y$	$x$	$y$														
-2.000	-3.978	-0.998	-3.978	-0.748	-3.978	-0.498	-3.978	-0.248	-3.978	0.002	-3.978	0.252	-3.978	0.502	-3.978	0.752	-3.978	1.002
-1.875	-3.727	-0.998	-3.728	-0.748	-3.728	-0.498	-3.728	-0.248	-3.728	0.002	-3.728	0.252	-3.728	0.502	-3.728	0.752	-3.728	1.002
-1.750	-3.477	-0.998	-3.478	-0.748	-3.478	-0.498	-3.478	-0.248	-3.478	0.002	-3.478	0.252	-3.478	0.502	-3.478	0.752	-3.478	1.002
-1.625	-3.227	-0.998	-3.228	-0.748	-3.228	-0.498	-3.228	-0.248	-3.228	0.002	-3.228	0.252	-3.228	0.502	-3.228	0.752	-3.228	1.002
-1.500	-2.977	-0.998	-2.978	-0.748	-2.978	-0.498	-2.978	-0.248	-2.978	0.002	-2.978	0.252	-2.978	0.502	-2.978	0.752	-2.978	1.002
-1.375	-2.727	-0.998	-2.728	-0.748	-2.728	-0.498	-2.728	-0.248	-2.728	0.002	-2.728	0.252	-2.728	0.502	-2.728	0.752	-2.728	1.002
-1.250	-2.477	-0.997	-2.478	-0.747	-2.478	-0.498	-2.478	-0.248	-2.478	0.002	-2.478	0.252	-2.478	0.502	-2.478	0.752	-2.478	1.002
-1.125	-2.227	-0.997	-2.228	-0.747	-2.228	-0.497	-2.228	-0.248	-2.228	0.002	-2.228	0.252	-2.228	0.502	-2.228	0.752	-2.228	1.002
-1.000	-1.977	-0.997	-1.978	-0.747	-1.978	-0.497	-1.978	-0.247	-1.978	0.002	-1.978	0.252	-1.978	0.501	-1.978	0.751	-1.978	1.001
-0.875	-1.727	-0.996	-1.728	-0.747	-1.728	-0.497	-1.728	-0.247	-1.728	0.002	-1.728	0.252	-1.728	0.501	-1.728	0.751	-1.728	1.001
-0.750	-1.477	-0.996	-1.478	-0.746	-1.478	-0.496	-1.478	-0.247	-1.478	0.002	-1.478	0.251	-1.478	0.501	-1.478	0.751	-1.478	1.000
-0.625	-1.227	-0.995	-1.229	-0.746	-1.230	-0.496	-1.230	-0.247	-1.230	0.002	-1.230	0.251	-1.230	0.500	-1.230	0.750	-1.230	999
-0.500	-0.977	-0.993	-0.979	-0.743	-0.981	-0.495	-0.982	-0.246	-0.982	0.002	-0.982	0.250	-0.982	0.499	-0.979	0.748	-0.977	997
-0.375	-0.727	-0.990	-0.730	-0.741	-0.733	-0.493	-0.734	-0.245	-0.735	0.002	-0.734	0.249	-0.732	0.497	-0.730	0.746	-0.727	995
-0.250	-0.478	-0.987	-0.482	-0.738	-0.485	-0.491	-0.487	-0.244	-0.488	0.002	-0.487	0.248	-0.484	0.495	-0.481	0.743	-0.478	992
-0.125	-0.228	-0.981	-0.235	-0.733	-0.239	-0.487	-0.242	-0.242	-0.243	0.001	-0.241	0.246	-0.238	0.491	-0.233	0.739	-0.228	987
0	0.022	-0.972	0.011	-0.726	0.004	-0.482	0.000	-0.240	0.000	0.000	0.003	0.242	0.006	0.488	0.015	0.732	0.023	981
0.125	0.270	-0.955	0.254	-0.715	0.243	-0.476	0.289	-0.239	0.240	-0.002	0.245	0.237	0.252	0.479	0.261	0.724	0.273	971
0.250	0.510	-0.930	0.489	-0.700	0.477	-0.469	0.472	-0.238	0.476	-0.006	0.484	0.229	0.494	0.463	0.507	0.711	0.522	958
0.375	0.754	-0.901	0.713	-0.684	0.702	-0.463	0.700	-0.239	0.707	-0.013	0.719	0.218	0.734	0.454	0.751	0.695	0.772	941
0.500	0.942	-0.875	0.925	-0.670	0.918	-0.460	0.921	-0.244	0.933	-0.024	0.950	0.202	0.970	0.434	0.994	0.672	1.021	917
0.625	1.139	-0.855	1.120	-0.662	1.128	-0.461	1.136	-0.254	1.153	-0.041	1.177	0.180	1.204	0.408	1.234	0.643	1.269	886
0.750	1.322	-0.843	1.321	-0.660	1.327	-0.470	1.343	-0.271	1.367	-0.054	1.398	0.161	1.433	0.375	1.472	0.607	1.516	848
0.875	1.495	-0.840	1.502	-0.668	1.518	-0.486	1.542	-0.295	1.575	-0.095	1.614	0.113	1.658	0.332	1.707	0.560	1.761	798
1.000	1.658	-0.848	1.675	-0.684	1.701	-0.511	1.734	-0.328	1.776	-0.135	1.824	0.067	1.879	0.279	1.938	0.503	2.003	738
1.125	1.812	-0.866	1.840	-0.710	1.875	-0.545	1.918	-0.370	1.969	-0.245	2.028	0.010	2.094	0.216	2.165	0.435	2.242	665
1.250	1.958	-0.893	1.995	-0.747	2.041	-0.590	2.094	-0.423	2.156	-0.345	2.225	-0.068	2.302	0.142	2.386	0.354	2.477	578
1.375	2.098	-0.931	2.143	-0.793	2.198	-0.644	2.262	-0.485	2.334	-0.316	2.415	-0.137	2.504	0.055	2.601	0.260	2.705	477
1.500	2.226	-0.979	2.282	-0.849	2.348	-0.709	2.422	-0.558	2.504	-0.398	2.596	-0.228	2.697	-0.044	2.807	0.162	2.927	361
1.625	2.347	-1.038	2.418	-0.914	2.488	-0.783	2.572	-0.642	2.665	-0.491	2.768	-0.330	2.882	-0.156	3.005	0.030	3.139	229
1.750	2.461	-1.102	2.535	-0.989	2.621	-0.867	2.713	-0.735	2.816	-0.594	2.930	-0.444	3.055	-0.281	3.192	-0.106	3.341	082
1.875	2.566	-1.177	2.649	-1.073	2.741	-0.960	2.844	-0.838	2.957	-0.708	3.081	-0.569	3.218	-0.418	3.368	-0.255	3.531	-091
2.000	2.662	-1.260	2.763	-1.164	2.853	-1.061	2.964	-0.950	3.086	-0.831	3.219	-0.705	3.367	-0.587	3.529	-0.418	3.706	-259
2.125	2.749	-1.350	2.847	-1.264	2.956	-1.170	3.074	-1.070	3.202	-0.953	3.344	-0.850	3.501	-0.727	3.675	-0.594	3.865	-451
2.250	2.828	-1.447	2.932	-1.369	3.047	-1.286	3.172	-1.197	3.307	-1.102	3.455	-1.002	3.620	-0.895	3.803	-0.780	4.004	-658
2.375	2.899	-1.550	3.008	-1.481	3.128	-1.407	3.258	-1.339	3.398	-1.247	3.550	-1.160	3.721	-1.070	3.910	-0.977	4.119	-880
2.500	2.961	-1.650	3.075	-1.608	3.199	-1.633	3.332	-1.466	3.476	-1.395	3.631	-1.322	3.803	-1.249	3.994	-1.177	4.203	-1105
2.625	3.016	-1.771	3.134	-1.718	3.260	-1.663	3.396	-1.605	3.541	-1.546	3.697	-1.485	3.869	-1.428	4.056	-1.374	4.259	-1324
2.750	3.064	-1.888	3.184	-1.841	3.313	-1.794	3.450	-1.746	3.595	-1.697	3.751	-1.648	3.919	-1.604	4.100	-1.565	4.294	-1532
2.875	3.105	-2.005	3.227	-1.966	3.357	-1.927	3.494	-1.887	3.638	-1.847	3.792	-1.803	3.956	-1.775	4.130	-1.748	4.314	-1727
3.000	3.139	-2.125	3.263	-2.092	3.393	-2.060	3.530	-2.028	3.673	-1.996	3.824	-1.985	3.983	-1.941	4.160	-1.923	4.334	-1911
3.125	3.168	-2.246	3.292	-2.219	3.423	-2.193	3.559	-2.167	3.700	-2.142	3.848	-2.119	4.002	-2.101	4.162	-2.089	4.328	-2094
3.250	3.191	-2.369	3.317	-2.347	3.447	-2.326	3.582	-2.305	3.721	-2.285	3.876	-2.267	4.015	-2.266	4.168	-2.249	4.328	-2247
3.375	3.211	-2.493	3.337	-2.475	3.466	-2.457	3.600	-2.411	3.737	-2.426	3.899	-2.413	4.024	-2.405	4.171	-2.401	4.323	-2402
3.500	3.227	-2.617	3.362	-2.602	3.481	-2.588	3.614	-2.576	3.749	-2.564	3.888	-2.555	4.029	-2.549	4.173	-2.548	4.317	-2551
3.625	3.239	-2.741	3.365	-2.729	3.493	-2.719	3.624	-2.709	3.758	-2.700	3.894	-2.693	4.032	-2.690	4.171	-2.690	4.311	-2693
3.750	3.249	-2.865	3.375	-2.856	3.503	-2.848	3.633	-2.840	3.764	-2.834	3.898	-2.829	4.033	-2.827	4.169	-2.828	4.305	-2832
3.875	3.257	-2.990	3.383	-2.983	3.510	-2.976	3.639	-2.971	3.769	-2.965	3.901	-2.962	4.033	-2.961	4.166	-2.962	4.299	-2966
4.000	3.264	-3.115	3.389	-3.109	3.516	-3.104	3.644	-3.100	3.773	-3.096	3.903	-3.093	4.033	-3.093	4.164	-3.094	4.294	-3097
4.125	3.269	-3.240	3.394	-3.235	3.520	-3.231	3.648	-3.228	3.776	-3.225	3.905	-3.223	4.033	-3.222	4.162	-3.223	4.290	-3226
4.250	3.273	-3.365	3.398	-3.361	3.524	-3.358	3.651	-3.355	3.778	-3.352	3.906	-3.351	4.033	-3.350	4.160	-3.351	4.287	-3353
4.375	3.276	-3.490	3.401	-3.487	3.527	-3.484	3.653	-3.482	3.780	-3.480	3.907	-3.478	4.033	-3.478	4.160	-3.478	4.286	-3478
4.500	3.279	-3.615	3.404	-3.612	3.529	-3.610	3.655	-3.608	3.781	-3.606	3.908	-3.605	4.034	-3.604	4.159	-3.603	4.285	-3603
4.625	3.281	-3.740	3.406	-3.738	3.531	-3.736	3.657	-3.734	3.783	-3.732	3.909	-3.731	4.034	-3.730	4.160	-3.729	4.285	-3729
4.750	3.283	-3.865	3.408	-3.863	3.533	-3.861	3.659	-3.859	3.784	-3.858	3.910	-3.856	4.035	-3.855	4.161	-3.854	4.286	-3853
4.875	3.285	-3.990	3.410	-3.988	3.535	-3.986	3.660	-3.985	3.786	-3.983	3.911	-3.982	4.036	-3.981	4.162	-3.979	4.287	-3978
5.000	3.287	-4.115	3.412	-4.113	3.537	-4.111	3.662	-4.110	3.787	-4.108	3.912	-4.107	4.038	-4.106	4.163	-4.105	4.288	-4103
5.125	3.288	-4.240	3.413	-4.238	3.538	-4.237	3.663	-4.235	3.788	-4.234	3.914	-4.232	4.039	-4.231	4.164	-4.230	4.289	-4226
5.250	3.290	-4.365	3.415	-4.363	3.540	-4.362	3.665	-4.360	3.790	-4.359	3.915	-4.356	4.040	-4.356	4.165	-4.355	4.290	-4353
5.375	3.291	-4.490	3.416	-4.488	3.541	-4.487	3.666	-4.485	3.791	-4.484	3.916	-4.482	4.041	-4.481	4.166	-4.480	4.292	-4478
5.500	3.293	-4.615	3.418	-4.613	3.543	-4.612	3.668	-4.610	3.793	-4.609	3.918	-4.6						

TABLE III—DISTRIBUTION OF VELOCITY  $q$  AND FLOW DIRECTION  $\theta$  IN TRANSFORMED  $\psi^*$ - $\Delta\psi^*$ -PLANE FOR EXAMPLE IV (ELBOW WITH LINEARIZED COMPRESSIBLE FLOW)

[Prescribed variation in  $Q$  with arc length  $s$  along channel walls plotted in fig. 2;  $Q_0=0.5$ ,  $Q_2=1.0$ ,  $q_2=0.80176$ ,  $\Delta\psi^*=0.73782$ ,  $\Delta\theta=104.07^\circ$ ]

$\frac{\psi^*}{\Delta\psi^*}$	0		$\frac{1}{4}$		$\frac{1}{2}$		$\frac{3}{4}$		$\frac{5}{8}$		$\frac{5}{6}$		1.0	
	$q$	$\theta$	$q$	$\theta$	$q$	$\theta$	$q$	$\theta$	$q$	$\theta$	$q$	$\theta$	$q$	$\theta$
-11/8	0.4009	0	0.4009	0	0.4009	0	0.4009	0	0.4009	0	0.4009	0	0.4009	0
-10/8	.4009	.01	.4009	.01	.4009	.00	.4009	.00	.4009	.00	.4009	-.01	.4009	-.01
-9/8	.4009	.01	.4009	.01	.4010	.01	.4010	.00	.4010	-.01	.4009	-.01	.4009	-.01
-8/8	.4009	.02	.4010	.02	.4010	.01	.4010	.00	.4010	-.01	.4010	-.02	.4009	-.02
-7/8	.4009	.03	.4010	.03	.4011	.01	.4011	.00	.4011	-.01	.4010	-.02	.4009	-.03
-6/8	.4009	.05	.4011	.04	.4012	.02	.4013	.00	.4012	-.02	.4011	-.04	.4009	-.05
-5/8	.4009	.08	.4012	.07	.4015	.04	.4015	.00	.4014	-.04	.4012	-.07	.4009	-.08
-4/8	.4009	.14	.4015	.12	.4019	.07	.4020	.00	.4018	-.07	.4014	-.11	.4009	-.13
-3/8	.4009	.24	.4019	.20	.4025	.11	.4027	-.01	.4024	-.11	.4017	-.18	.4009	-.21
-2/8	.4009	.40	.4026	.33	.4037	.17	.4039	-.03	.4033	-.20	.4022	-.31	.4009	-.35
-1/8	.4009	.70	.4041	.57	.4057	.27	.4059	-.05	.4048	-.33	.4030	-.50	.4009	-.60
0	.4009	1.31	.4070	.96	.4093	.36	.4090	-.17	.4071	-.58	.4042	-.84	.4009	-.92
1/8	.4272	2.82	.4141	1.49	.4155	.43	.4139	-.40	.4104	-.99	.4058	-1.34	.4009	-1.45
2/8	.4243	3.88	.4268	1.77	.4251	.24	.4207	-.87	.4148	-1.63	.4080	-2.07	.4009	-2.22
3/8	.4489	4.00	.4444	1.46	.4377	-.38	.4295	-1.70	.4202	-2.59	.4106	-3.11	.4009	-3.28
4/8	.4780	3.17	.4654	.60	.4626	-1.49	.4626	-2.92	.4285	-3.90	.4135	-4.46	.4009	-4.55
5/8	.5094	1.44	.4882	-1.17	.4689	-3.16	.4606	-4.62	.4333	-5.63	.4167	-6.21	.4009	-6.41
6/8	.5415	-.88	.5118	-3.43	.4857	-5.34	.4621	-6.76	.4403	-7.75	.4200	-8.33	.4009	-8.52
7/8	.5732	-4.00	.5352	-6.23	.5024	-8.01	.4734	-9.35	.4472	-10.29	.4232	-10.85	.4009	-11.04
8/8	.6038	-7.48	.5578	-9.48	.5186	-11.10	.4844	-12.34	.4539	-13.22	.4262	-13.74	.4009	-13.91
9/8	.6329	-11.35	.5793	-13.12	.5340	-14.57	.4947	-16.70	.4601	-18.49	.4291	-16.97	.4009	-17.13
10/8	.6602	-15.52	.5994	-17.09	.5482	-18.37	.5043	-19.38	.4699	-20.09	.4317	-20.52	.4009	-20.67
11/8	.6855	-19.96	.6178	-21.33	.5613	-22.46	.5131	-23.34	.4712	-23.98	.4341	-24.37	.4009	-24.49
12/8	.7086	-24.62	.6346	-25.80	.5732	-26.79	.5210	-27.66	.4769	-28.12	.4362	-28.46	.4009	-28.58
13/8	.7293	-29.46	.6496	-30.47	.5837	-31.32	.5281	-32.00	.4801	-32.49	.4381	-32.79	.4009	-32.98
14/8	.7477	-34.45	.6629	-35.31	.5931	-36.03	.5343	-36.02	.4838	-37.05	.4398	-37.40	.4009	-37.40
15/8	.7636	-39.56	.6744	-40.27	.6013	-40.89	.5398	-41.39	.4872	-41.77	.4413	-46.85	.4009	-46.83
16/8	.7769	-44.76	.6842	-45.34	.6084	-45.86	.5447	-45.30	.4902	-46.64	.4427	-51.63	.4009	-51.63
17/8	.7875	-50.02	.6924	-50.47	.6146	-50.90	.5492	-51.30	.4931	-51.63	.4440	-56.98	.4009	-56.98
18/8	.7963	-55.27	.6991	-55.01	.6202	-55.88	.5537	-55.36	.4961	-55.72	.4456	-62.28	.4009	-62.44
19/8	.8001	-60.49	.7045	-60.72	.6257	-61.06	.5580	-61.47	.4999	-61.01	.4477	-67.79	.4009	-67.79
20/8	.8018	-65.65	.7091	-65.68	.6315	-66.03	.5617	-66.83	.5035	-67.13	.4495	-73.46	.4009	-73.46
21/8	.8018	-70.32	.7135	-70.45	.6365	-70.85	.5647	-71.49	.5068	-72.37	.4508	-78.91	.4009	-78.91
22/8	.8018	-74.81	.7186	-74.96	.6411	-75.43	.5678	-76.29	.5098	-77.36	.4515	-83.79	.4009	-83.79
23/8	.8018	-78.97	.7245	-83.01	.6456	-83.59	.5708	-84.67	.5124	-88.02	.4519	-88.01	.4009	-88.01
24/8	.8018	-82.82	.7311	-86.48	.6496	-87.07	.5733	-88.08	.5149	-92.57	.4525	-94.48	.4009	-94.48
25/8	.8018	-86.39	.7382	-92.25	.6532	-92.81	.5758	-93.75	.5168	-95.10	.4529	-98.83	.4009	-98.83
26/8	.8018	-89.37	.7452	-96.54	.6564	-95.09	.5783	-95.97	.5187	-97.21	.4533	-100.39	.4009	-100.39
27/8	.8018	-92.07	.7523	-100.67	.6592	-97.02	.5808	-97.82	.5206	-98.94	.4537	-101.63	.4009	-101.63
28/8	.8018	-94.40	.7591	-101.57	.6617	-98.62	.5823	-99.34	.5221	-100.34	.4540	-102.59	.4009	-102.59
29/8	.8018	-96.39	.7666	-102.26	.6642	-101.01	.5837	-101.51	.5235	-101.46	.4543	-103.31	.4009	-103.31
30/8	.8018	-98.05	.7733	-102.80	.6667	-102.51	.5852	-102.34	.5249	-102.33	.4546	-103.83	.4009	-103.83
31/8	.8018	-99.44	.7798	-103.20	.6692	-103.37	.5867	-103.01	.5263	-103.47	.4549	-104.18	.4009	-104.18
32/8	.8018	-100.56	.7855	-103.59	.6717	-103.90	.5882	-103.64	.5277	-104.11	.4552	-104.30	.4009	-104.30
33/8	.8018	-101.47	.7911	-104.06	.6742	-104.37	.5897	-104.06	.5291	-104.01	.4555	-104.48	.4009	-104.48
34/8	.8018	-102.18	.7966	-104.51	.6767	-104.82	.5912	-104.12	.5305	-104.12	.4558	-104.49	.4009	-104.49
35/8	.8018	-102.73	.8021	-104.92	.6792	-105.09	.5927	-104.02	.5319	-104.16	.4561	-104.33	.4009	-104.33
36/8	.8018	-103.14	.8076	-105.37	.6817	-105.37	.5942	-104.06	.5333	-104.14	.4564	-104.23	.4009	-104.23
37/8	.8018	-103.45	.8131	-105.82	.6842	-105.64	.5957	-104.06	.5347	-104.11	.4567	-104.16	.4009	-104.16
38/8	.8018	-103.66	.8186	-106.27	.6867	-105.91	.5972	-104.06	.5361	-104.09	.4570	-104.12	.4009	-104.12
39/8	.8018	-103.81	.8241	-106.72	.6892	-106.18	.5987	-104.06	.5375	-104.08	.4573	-104.08	.4009	-104.08
40/8	.8018	-103.90	.8296	-107.17	.6917	-106.45	.5999	-104.06	.5389	-104.07	.4576	-104.07	.4009	-104.07
41/8	.8018	-103.97	.8351	-107.62	.6942	-106.72	.6014	-104.06	.5403	-104.07	.4579	-104.07	.4009	-104.07
42/8	.8018	-104.00	.8406	-108.07	.6967	-107.00	.6029	-104.06	.5417	-104.07	.4582	-104.07	.4009	-104.07
43/8	.8018	-104.03	.8461	-108.52	.6992	-107.27	.6044	-104.06	.5431	-104.07	.4585	-104.07	.4009	-104.07
44/8	.8018	-104.04	.8516	-108.97	.7017	-107.54	.6059	-104.06	.5445	-104.07	.4588	-104.07	.4009	-104.07
45/8	.8018	-104.05	.8571	-109.42	.7042	-107.81	.6074	-104.06	.5459	-104.07	.4591	-104.07	.4009	-104.07
46/8	.8018	-104.06	.8626	-109.87	.7067	-108.08	.6089	-104.06	.5473	-104.07	.4594	-104.07	.4009	-104.07
47/8	.8018	-104.06	.8681	-110.32	.7092	-108.35	.6104	-104.06	.5487	-104.07	.4597	-104.07	.4009	-104.07
48/8	.8018	-104.06	.8736	-110.77	.7117	-108.62	.6119	-104.06	.5501	-104.07	.4600	-104.07	.4009	-104.07
49/8	.8018	-104.06	.8791	-111.22	.7142	-108.89	.6134	-104.06	.5515	-104.07	.4603	-104.07	.4009	-104.07
50/8	.8018	-104.06	.8846	-111.67	.7167	-109.16	.6149	-104.06	.5529	-104.07	.4606	-104.07	.4009	-104.07

TABLE IV—DISTRIBUTION OF PHYSICAL COORDINATES  $x$  AND  $y$  IN TRANSFORMED  $\varphi^*\psi^*$ -PLANE FOR EXAMPLE IV (ELBOW WITH LINERARIZED COMPRESSIBLE FLOW)

[Prescribed variation in  $Q$  with arc length  $s$  along channel walls plotted in fig. 2;  $Q_1=0.5$ ,  $Q_2=1.0$ ,  $g_1=0.80176$ ,  $\Delta\psi^*=0.73782$ ,  $\Delta\theta=104.07^\circ$ ]

$\frac{\psi^*}{\Delta\psi^*}$	0		$\frac{1}{6}$		$\frac{1}{3}$		$\frac{1}{2}$		$\frac{2}{3}$		$\frac{5}{6}$		1.0	
	$x$	$y$	$x$	$y$	$x$	$y$	$x$	$y$	$x$	$y$	$x$	$y$	$x$	$y$
-11/6	-2.466	-0.769	-2.466	-0.512	-2.466	-0.256	-2.466	0.001	-2.466	0.257	-2.466	0.513	-2.466	0.770
-10/6	-2.241	-0.769	-2.241	-0.512	-2.241	-0.256	-2.241	0.001	-2.241	0.257	-2.241	0.513	-2.241	0.770
-9/6	-2.016	-0.769	-2.016	-0.512	-2.016	-0.256	-2.016	0.001	-2.016	0.257	-2.016	0.513	-2.016	0.770
-8/6	-1.791	-0.769	-1.791	-0.512	-1.791	-0.256	-1.791	0.001	-1.791	0.257	-1.791	0.513	-1.791	0.770
-7/6	-1.566	-0.768	-1.566	-0.512	-1.566	-0.256	-1.566	0.001	-1.566	0.257	-1.566	0.513	-1.566	0.770
-6/6	-1.341	-0.768	-1.341	-0.512	-1.341	-0.256	-1.341	0.001	-1.341	0.257	-1.341	0.513	-1.341	0.769
-5/6	-1.116	-0.768	-1.116	-0.512	-1.117	-0.256	-1.117	0.001	-1.117	0.257	-1.116	0.513	-1.116	0.769
-4/6	-0.891	-0.768	-0.892	-0.511	-0.892	-0.255	-0.892	0.001	-0.892	0.256	-0.892	0.513	-0.891	0.769
-3/6	-0.666	-0.767	-0.667	-0.511	-0.668	-0.255	-0.668	0.001	-0.668	0.256	-0.667	0.512	-0.666	0.768
-2/6	-0.441	-0.766	-0.443	-0.510	-0.444	-0.254	-0.444	0.001	-0.444	0.256	-0.443	0.511	-0.441	0.767
-1/6	-0.216	-0.763	-0.219	-0.508	-0.221	-0.254	-0.221	0.000	-0.220	0.255	-0.219	0.510	-0.216	0.765
0	0.008	-0.760	0.003	-0.505	0.000	-0.252	0.000	0.000	0.002	0.253	0.005	0.507	0.009	0.763
1/6	0.233	-0.752	0.223	-0.500	0.219	-0.251	0.219	0.001	0.222	0.250	0.228	0.503	0.234	0.758
2/6	0.450	-0.739	0.438	-0.494	0.434	-0.249	0.436	0.003	0.441	0.245	0.449	0.496	0.459	0.751
3/6	0.668	-0.724	0.645	-0.488	0.643	-0.250	0.648	0.008	0.657	0.237	0.670	0.486	0.684	0.740
4/6	0.851	-0.712	0.844	-0.485	0.846	-0.253	0.855	0.016	0.870	0.225	0.888	0.472	0.908	0.725
5/6	1.033	-0.704	1.033	-0.485	1.042	-0.261	1.057	0.029	1.079	0.208	1.104	0.452	1.132	0.703
6/6	1.205	-0.703	1.213	-0.492	1.230	-0.274	1.254	0.049	1.284	0.184	1.318	0.425	1.355	0.674
7/6	1.368	-0.710	1.386	-0.507	1.411	-0.295	1.445	0.076	1.485	0.152	1.529	0.389	1.577	0.636
8/6	1.519	-0.725	1.548	-0.529	1.586	-0.325	1.630	0.111	1.681	0.112	1.737	0.344	1.797	0.587
9/6	1.663	-0.749	1.704	-0.560	1.753	-0.363	1.809	0.166	1.871	0.061	1.940	0.288	2.013	0.527
10/6	1.788	-0.781	1.852	-0.600	1.913	-0.410	1.981	0.210	2.056	0.000	2.138	0.221	2.226	0.455
11/6	1.926	-0.822	1.992	-0.649	2.065	-0.466	2.146	0.274	2.235	-0.072	2.331	0.142	2.434	0.368
12/6	2.046	-0.871	2.124	-0.706	2.209	-0.532	2.304	0.349	2.406	-0.156	2.517	0.050	2.635	0.268
13/6	2.157	-0.928	2.247	-0.772	2.346	-0.608	2.453	0.435	2.580	-0.251	2.694	-0.055	2.829	0.153
14/6	2.261	-0.993	2.363	-0.847	2.473	-0.693	2.593	0.530	2.723	-0.357	2.862	-0.173	3.013	0.024
15/6	2.358	-1.064	2.489	-0.930	2.591	-0.787	2.723	0.636	2.866	-0.475	3.020	-0.304	3.186	-0.120
16/6	2.443	-1.143	2.587	-1.020	2.700	-0.889	2.843	0.751	2.999	-0.604	3.166	-0.447	3.346	-0.278
17/6	2.521	-1.228	2.655	-1.117	2.798	-1.000	2.952	0.875	3.118	-0.743	3.298	-0.601	3.492	-0.449
18/6	2.590	-1.318	2.732	-1.220	2.885	-1.117	3.049	1.007	3.225	-0.890	3.416	-0.766	3.623	-0.632
19/6	2.650	-1.414	2.800	-1.330	2.960	-1.240	3.132	1.146	3.317	-1.046	3.518	-0.940	3.736	-0.826
20/6	2.701	-1.514	2.858	-1.443	3.024	-1.369	3.203	1.290	3.395	-1.208	3.603	-1.122	3.830	-1.030
21/6	2.743	-1.619	2.905	-1.561	3.076	-1.501	3.259	1.438	3.456	-1.374	3.669	-1.309	3.901	-1.242
22/6	2.777	-1.726	2.942	-1.681	3.117	-1.635	3.303	1.588	3.501	-1.541	3.715	-1.496	3.947	-1.455
23/6	2.803	-1.836	2.970	-1.803	3.147	-1.770	3.333	1.737	3.531	-1.707	3.743	-1.680	3.969	-1.661
24/6	2.820	-1.947	2.990	-1.926	3.167	-1.905	3.353	1.885	3.548	-1.869	3.755	-1.858	3.974	-1.856
25/6	2.831	-2.059	3.001	-2.048	3.177	-2.038	3.362	2.030	3.554	-2.026	3.756	-2.027	3.966	-2.038
26/6	2.835	-2.171	3.005	-2.169	3.181	-2.169	3.363	2.171	3.552	-2.177	3.747	-2.189	3.950	-2.209
27/6	2.834	-2.283	3.003	-2.290	3.177	-2.297	3.357	2.308	3.542	-2.322	3.732	-2.342	3.927	-2.369
28/6	2.827	-2.396	2.996	-2.409	3.163	-2.423	3.345	2.440	3.527	-2.461	3.712	-2.487	3.900	-2.520
29/6	2.817	-2.508	2.984	-2.527	3.155	-2.547	3.330	2.570	3.508	-2.596	3.688	-2.626	3.871	-2.663
30/6	2.803	-2.619	2.969	-2.643	3.139	-2.668	3.311	2.695	3.485	-2.725	3.662	-2.760	3.841	-2.799
31/6	2.788	-2.731	2.951	-2.758	3.119	-2.787	3.289	2.818	3.461	-2.851	3.635	-2.888	3.809	-2.929
32/6	2.769	-2.841	2.931	-2.872	3.097	-2.904	3.266	2.938	3.435	-2.973	3.606	-3.012	3.777	-3.055
33/6	2.744	-2.952	2.908	-2.985	3.074	-3.019	3.241	3.055	3.409	-3.093	3.577	-3.133	3.746	-3.176
34/6	2.721	-3.062	2.885	-3.097	3.049	-3.133	3.215	3.171	3.381	-3.209	3.548	-3.260	3.714	-3.294
35/6	2.697	-3.172	2.860	-3.209	3.024	-3.246	3.188	3.294	3.353	-3.324	3.518	-3.366	3.683	-3.409
36/6	2.672	-3.281	2.834	-3.319	2.998	-3.358	3.161	3.397	3.325	-3.437	3.489	-3.479	3.653	-3.522
37/6	2.646	-3.391	2.808	-3.430	2.971	-3.469	3.134	3.509	3.297	-3.549	3.460	-3.591	3.623	-3.633
38/6	2.620	-3.500	2.782	-3.540	2.944	-3.579	3.107	3.619	3.269	-3.660	3.432	-3.701	3.594	-3.744
39/6	2.593	-3.609	2.755	-3.649	2.917	-3.689	3.079	3.730	3.241	-3.770	3.403	-3.811	3.565	-3.853
40/6	2.566	-3.719	2.728	-3.759	2.890	-3.799	3.052	3.839	3.214	-3.880	3.376	-3.921	3.537	-3.962
41/6	2.539	-3.828	2.701	-3.868	2.862	-3.908	3.024	3.949	3.186	-3.990	3.348	-4.030	3.510	-4.071
42/6	2.512	-3.937	2.673	-3.977	2.835	-4.018	2.997	4.058	3.159	-4.089	3.320	-4.139	3.482	-4.180
43/6	2.484	-4.046	2.646	-4.087	2.808	-4.127	2.970	4.168	3.131	-4.208	3.293	-4.249	3.455	-4.289
44/6	2.457	-4.155	2.619	-4.196	2.780	-4.236	2.942	4.277	3.104	-4.317	3.266	-4.358	3.427	-4.388
45/6	2.430	-4.264	2.591	-4.305	2.753	-4.345	2.915	4.386	3.077	-4.426	3.238	-4.467	3.400	-4.507
46/6	2.402	-4.374	2.564	-4.414	2.726	-4.455	2.887	4.495	3.049	-4.536	3.211	-4.576	3.372	-4.617
47/6	2.375	-4.483	2.537	-4.523	2.698	-4.564	2.860	4.604	3.022	-4.645	3.183	-4.635	3.345	-4.726
48/6	2.348	-4.592	2.509	-4.632	2.671	-4.673	2.833	4.713	2.994	-4.754	3.156	-4.794	3.318	-4.835
49/6	2.320	-4.701	2.482	-4.741	2.644	-4.782	2.805	4.822	2.967	-4.863	3.129	-4.903	3.290	-4.944
50/6	2.293	-4.810	2.455	-4.851	2.616	-4.891	2.778	4.932	2.940	-4.972	3.101	-5.013	3.263	-5.053

TABLE V—DISTRIBUTION OF VELOCITY  $q$  AND FLOW DIRECTION  $\theta$  IN TRANSFORMED  $\varphi\psi$ -PLANE FOR EXAMPLE V (ELBOW WITH COMPRESSIBLE FLOW ( $\gamma=1.4$ ))

[Prescribed variation in  $Q$  with arc length  $s$  along channel walls plotted in fig. 2;  $Q_a=0.5$ ,  $Q_b=1.0$ ,  $q_a=0.79927$ ,  $\Delta\psi=0.71054$ ,  $\Delta\theta=105.31^\circ$ ]

$\frac{\psi}{\Delta\psi}$	0		$\frac{1}{4}$		$\frac{1}{2}$		$\frac{3}{4}$		$\frac{5}{8}$		$\frac{3}{2}$		1.0	
	$q$	$\theta$	$q$	$\theta$	$q$	$\theta$	$q$	$\theta$	$q$	$\theta$	$q$	$\theta$	$q$	$\theta$
-12/8	0.3996	0	0.3996	0	0.3996	0	0.3996	0	0.3996	0	0.3996	0	0.3996	0
-11/8	.3996	.00	.3997	.00	.3997	.00	.3997	.00	.3997	.00	.3997	.00	.3997	.00
-10/8	.3996	.01	.3997	.01	.3997	.00	.3997	.00	.3997	.00	.3997	.00	.3997	.01
-9/8	.3996	.01	.3997	.01	.3997	.01	.3997	.01	.3997	.00	.3997	.01	.3997	.01
-8/8	.3996	.02	.3997	.02	.3998	.01	.3998	.01	.3998	.00	.3998	.01	.3997	.02
-7/8	.3996	.03	.3998	.03	.3999	.02	.3999	.02	.3999	.00	.3998	.02	.3998	.03
-6/8	.3996	.05	.3998	.04	.4000	.03	.4000	.00	.4000	.00	.4000	.03	.3998	.05
-5/8	.3996	.09	.4000	.08	.4002	.04	.4003	.00	.4002	.00	.4002	.04	.4000	.09
-4/8	.3996	.15	.4002	.13	.4006	.07	.4008	.00	.4006	.00	.4006	.07	.4002	.15
-3/8	.3996	.25	.4007	.22	.4014	.12	.4015	.01	.4012	.00	.4005	.12	.3996	.25
-2/8	.3996	.43	.4015	.39	.4026	.18	.4028	.03	.4022	.00	.4011	.22	.3996	.43
-1/8	.3996	.77	.4030	.62	.4047	.30	.4049	.06	.4038	.00	.4019	.36	.3996	.77
0	.3996	1.45	.4062	1.06	.4086	.39	.4082	.19	.4062	.00	.4031	.64	.3996	1.45
1/8	.4066	3.13	.4137	1.64	.4162	.46	.4134	.45	.4097	.00	.4019	1.45	.4066	3.13
2/8	.4253	4.28	.4276	1.93	.4255	.24	.4207	.98	.4144	.00	.4072	2.30	.4253	4.28
3/8	.4519	4.31	.4464	1.54	.4389	.45	.4300	1.92	.4202	.00	.4099	3.46	.4519	4.31
4/8	.4830	3.26	.4637	.40	.4547	1.74	.4408	3.30	.4268	.00	.4131	4.87	.4830	3.26
5/8	.5162	1.21	.4928	-1.53	.4719	-3.64	.4524	-5.21	.4340	.00	.4164	-6.82	.5162	1.21
6/8	.5498	-1.61	.5175	-4.11	.4895	-6.10	.4645	-7.61	.4413	.00	.4198	-9.28	.5498	-1.61
7/8	.5823	-3.05	.5419	-7.27	.5079	-9.09	.4782	-10.50	.4485	.00	.4231	-12.03	.5823	-3.05
8/8	.6144	-4.99	.5652	-10.92	.5236	-12.55	.4975	-13.82	.4554	.00	.4263	-15.29	.6144	-4.99
9/8	.6441	-13.32	.5871	-14.98	.5393	-16.40	.4981	-17.84	.4618	.00	.4292	-18.68	.6441	-13.32
10/8	.6717	-17.98	.6074	-19.38	.5538	-20.61	.5078	-21.61	.4677	.00	.4319	-22.79	.6717	-17.98
11/8	.6970	-22.89	.6258	-24.06	.5669	-25.12	.5166	-25.98	.4730	.00	.4343	-27.02	.6970	-22.89
12/8	.7197	-28.02	.6424	-28.98	.5788	-29.87	.5245	-30.62	.4777	.00	.4361	-31.18	.7197	-28.02
13/8	.7399	-33.31	.6589	-34.09	.5899	-34.84	.5314	-35.48	.4818	.00	.4383	-35.96	.7399	-33.31
14/8	.7573	-38.74	.6698	-39.35	.5978	-39.98	.5375	-40.82	.4855	.00	.4400	-41.20	.7573	-38.74
15/8	.7719	-44.26	.6803	-44.74	.6056	-45.25	.5428	-45.72	.4888	.00	.4415	-46.33	.7719	-44.26
16/8	.7836	-49.84	.6891	-50.20	.6123	-50.62	.5478	-51.03	.4918	.00	.4429	-51.37	.7836	-49.84
17/8	.7922	-55.44	.6963	-55.70	.6182	-56.04	.5522	-56.43	.4951	.00	.4446	-57.07	.7922	-55.44
18/8	.7975	-60.96	.7019	-61.13	.6238	-61.44	.5573	-61.85	.4990	.00	.4463	-62.69	.7975	-60.96
19/8	.7993	-66.35	.7066	-66.45	.6297	-66.76	.5635	-67.25	.5047	.00	.4467	-68.57	.7993	-66.35
20/8	.7993	-71.43	.7110	-71.53	.6367	-71.88	.5720	-72.51	.5138	.00	.4469	-74.59	.7993	-71.43
21/8	.7993	-76.19	.7163	-76.31	.6456	-76.73	.5835	-77.50	.5274	.00	.4473	-80.35	.7993	-76.19
22/8	.7993	-80.67	.7224	-80.80	.6562	-81.27	.5979	-82.14	.5453	.00	.4469	-85.45	.7993	-80.67
23/8	.7993	-84.69	.7292	-84.83	.6684	-85.33	.6145	-86.27	.5662	.00	.4453	-89.70	.7993	-84.69
24/8	.7993	-88.32	.7366	-88.47	.6816	-88.97	.6327	-89.92	.5892	.00	.4438	-93.41	.7993	-88.32
25/8	.7993	-91.55	.7442	-91.69	.6952	-92.17	.6616	-93.06	.6129	.00	.4415	-96.29	.7993	-91.55
26/8	.7993	-94.33	.7516	-94.46	.7087	-94.90	.6705	-95.72	.6386	.00	.4400	-98.06	.7993	-94.33
27/8	.7993	-96.70	.7587	-96.81	.7219	-97.21	.6888	-97.94	.6597	.00	.4377	-100.62	.7993	-96.70
28/8	.7993	-98.08	.7653	-98.78	.7342	-99.14	.7062	-99.77	.6815	.00	.4367	-100.72	.7993	-98.08
29/8	.7993	-100.31	.7714	-100.40	.7456	-100.71	.7223	-101.25	.7019	.00	.4349	-103.13	.7993	-100.31
30/8	.7993	-101.64	.7769	-101.73	.7559	-101.97	.7370	-102.43	.7205	.00	.4330	-103.10	.7993	-101.64
31/8	.7993	-102.68	.7817	-102.76	.7651	-102.97	.7502	-103.34	.7373	.00	.4309	-104.61	.7993	-102.68
32/8	.7993	-103.48	.7858	-103.54	.7731	-103.72	.7617	-104.03	.7520	.00	.4287	-105.05	.7993	-103.48
33/8	.7993	-104.09	.7893	-104.14	.7800	-104.28	.7716	-104.53	.7648	.00	.4263	-105.33	.7993	-104.09
34/8	.7993	-104.53	.7922	-104.58	.7856	-104.67	.7799	-104.87	.7754	.00	.4246	-105.49	.7993	-104.53
35/8	.7993	-104.83	.7945	-104.88	.7901	-104.95	.7855	-105.09	.7830	.00	.4229	-105.54	.7993	-104.83
36/8	.7993	-105.04	.7962	-105.05	.7935	-105.11	.7914	-105.21	.7903	.00	.4215	-105.56	.7993	-105.04
37/8	.7993	-105.16	.7975	-105.17	.7959	-105.21	.7948	-105.28	.7945	.00	.4200	-105.56	.7993	-105.16
38/8	.7993	-105.22	.7983	-105.24	.7974	-105.26	.7969	-105.30	.7970	.00	.4187	-105.54	.7993	-105.22
39/8	.7993	-105.26	.7987	-105.27	.7983	-105.28	.7981	-105.31	.7982	.00	.4173	-105.53	.7993	-105.26
40/8	.7993	-105.29	.7990	-105.29	.7988	-105.30	.7987	-105.31	.7987	.00	.4160	-105.53	.7993	-105.29
41/8	.7993	-105.30	.7991	-105.30	.7990	-105.30	.7990	-105.31	.7990	.00	.4149	-105.53	.7993	-105.30
42/8	.7993	-105.31	.7992	-105.31	.7992	-105.31	.7991	-105.31	.7992	.00	.4139	-105.51	.7993	-105.31
43/8	.7993	-105.31	.7993	-105.31	.7992	-105.31	.7992	-105.31	.7992	.00	.4131	-105.51	.7993	-105.31
44/8	.7993	-105.31	.7993	-105.31	.7993	-105.31	.7993	-105.31	.7993	.00	.4125	-105.51	.7993	-105.31

TABLE VI—DISTRIBUTION OF PHYSICAL COORDINATES  $x$  AND  $y$  IN TRANSFORMED  $\varphi\psi$ -PLANE FOR EXAMPLE V (ELBOW WITH COMPRESSIBLE FLOW ( $\gamma=1.4$ ))

[Prescribed variation in  $Q$  with arc length  $s$  along channel walls plotted in fig. 2;  $Q_u=0.5$ ,  $Q_d=1.0$ ,  $g_u=0.79927$ ,  $\Delta\psi=0.71054$ ,  $\Delta\theta=105.31^\circ$ ]

$\frac{\psi}{\Delta\psi}$	0		$\frac{1}{6}$		$\frac{1}{3}$		$\frac{1}{2}$		$\frac{2}{3}$		$\frac{5}{6}$		1.0	
	$x$	$y$	$x$	$y$	$x$	$y$	$x$	$y$	$x$	$y$	$x$	$y$	$x$	$y$
-12/6	-2.832	-0.770	-2.832	-0.513	-2.832	-0.256	-2.832	0.001	-2.832	0.258	-2.832	0.514	-2.832	0.771
-11/6	-2.695	-0.770	-2.695	-0.513	-2.695	-0.256	-2.695	0.001	-2.695	0.258	-2.695	0.514	-2.695	0.771
-10/6	-2.358	-0.770	-2.358	-0.513	-2.358	-0.256	-2.358	0.001	-2.358	0.258	-2.358	0.514	-2.358	0.771
-9/6	-2.122	-0.770	-2.122	-0.513	-2.122	-0.256	-2.122	0.001	-2.122	0.258	-2.122	0.514	-2.122	0.771
-8/6	-1.885	-0.770	-1.885	-0.513	-1.885	-0.256	-1.885	0.001	-1.885	0.258	-1.885	0.514	-1.885	0.771
-7/6	-1.648	-0.770	-1.648	-0.513	-1.648	-0.256	-1.648	0.001	-1.648	0.257	-1.648	0.514	-1.648	0.771
-6/6	-1.411	-0.769	-1.411	-0.513	-1.411	-0.256	-1.411	0.001	-1.411	0.257	-1.411	0.514	-1.411	0.771
-5/6	-1.174	-0.769	-1.175	-0.512	-1.175	-0.256	-1.175	0.001	-1.175	0.257	-1.175	0.514	-1.174	0.771
-4/6	-0.937	-0.769	-0.938	-0.512	-0.939	-0.256	-0.939	0.001	-0.938	0.257	-0.938	0.513	-0.937	0.770
-3/6	-0.701	-0.768	-0.702	-0.511	-0.702	-0.255	-0.703	0.001	-0.702	0.257	-0.702	0.513	-0.701	0.769
-2/6	-0.464	-0.767	-0.466	-0.510	-0.467	-0.255	-0.467	0.001	-0.467	0.256	-0.465	0.512	-0.464	0.768
-1/6	-0.227	-0.764	-0.230	-0.508	-0.232	-0.254	-0.233	0.001	-0.232	0.255	-0.230	0.510	-0.227	0.766
0	0.009	-0.760	0.004	-0.605	0.000	-0.252	0.000	0.000	0.002	0.253	0.005	0.607	-0.010	0.763
1/6	0.245	-0.750	0.235	-0.499	0.230	-0.250	0.230	-0.001	0.234	0.250	0.240	0.602	0.247	0.768
2/6	0.473	-0.735	0.460	-0.492	0.456	-0.249	0.458	-0.004	0.463	0.244	0.473	0.495	0.484	0.749
3/6	0.688	-0.719	0.677	-0.485	0.675	-0.249	0.680	-0.009	0.690	0.235	0.704	0.483	0.720	0.737
4/6	0.891	-0.705	0.884	-0.482	0.887	-0.253	0.897	-0.019	0.913	0.220	0.934	0.466	0.956	0.719
5/6	1.080	-0.697	1.081	-0.483	1.091	-0.263	1.109	-0.035	1.132	0.200	1.161	0.443	1.182	0.693
6/6	1.257	-0.698	1.268	-0.492	1.285	-0.279	1.314	-0.058	1.347	0.173	1.385	0.411	1.426	0.669
7/6	1.424	-0.707	1.446	-0.510	1.476	-0.304	1.513	-0.089	1.556	0.135	1.605	0.369	1.659	0.615
8/6	1.631	-0.726	1.616	-0.537	1.658	-0.338	1.705	-0.130	1.760	0.088	1.822	0.317	1.888	0.558
9/6	1.729	-0.755	1.775	-0.574	1.828	-0.383	1.890	-0.182	1.953	0.029	2.033	0.252	2.115	0.488
10/6	1.867	-0.794	1.926	-0.620	1.992	-0.438	2.067	-0.245	2.149	-0.042	2.239	0.174	2.336	0.403
11/6	1.997	-0.842	2.069	-0.677	2.148	-0.503	2.236	-0.320	2.332	-0.125	2.437	0.082	2.550	0.303
12/6	2.117	-0.899	2.202	-0.743	2.295	-0.579	2.396	-0.406	2.507	-0.221	2.627	-0.024	2.767	0.187
13/6	2.229	-0.966	2.326	-0.820	2.432	-0.666	2.546	-0.503	2.671	-0.330	2.806	-0.145	2.953	0.055
14/6	2.331	-1.040	2.441	-0.905	2.558	-0.763	2.686	-0.612	2.824	-0.452	2.974	-0.270	3.137	-0.094
15/6	2.424	-1.122	2.545	-0.999	2.674	-0.869	2.814	-0.732	2.965	-0.585	3.129	-0.428	3.308	-0.268
16/6	2.506	-1.211	2.638	-1.100	2.778	-0.984	2.929	-0.862	3.092	-0.730	3.270	-0.589	3.463	-0.436
17/6	2.579	-1.306	2.720	-1.209	2.870	-1.108	3.031	-1.000	3.205	-0.886	3.394	-0.762	3.601	-0.629
18/6	2.642	-1.407	2.791	-1.325	2.949	-1.238	3.118	-1.147	3.301	-1.050	3.501	-0.946	3.719	-0.834
19/6	2.694	-1.513	2.850	-1.445	3.015	-1.374	3.191	-1.299	3.381	-1.221	3.588	-1.138	3.816	-1.050
20/6	2.737	-1.624	2.898	-1.570	3.068	-1.514	3.248	-1.456	3.443	-1.396	3.654	-1.335	3.887	-1.274
21/6	2.770	-1.738	2.935	-1.697	3.107	-1.656	3.290	-1.614	3.486	-1.572	3.698	-1.533	3.928	-1.499
22/6	2.794	-1.854	2.961	-1.826	3.135	-1.799	3.319	-1.772	3.513	-1.747	3.722	-1.727	3.945	-1.714
23/6	2.809	-1.971	2.977	-1.956	3.152	-1.940	3.334	-1.927	3.527	-1.917	3.729	-1.912	3.944	-1.916
24/6	2.816	-2.089	2.985	-2.085	3.159	-2.081	3.339	-2.079	3.528	-2.081	3.724	-2.089	3.929	-2.106
25/6	2.816	-2.208	2.985	-2.212	3.157	-2.218	3.336	-2.226	3.520	-2.238	3.710	-2.256	3.906	-2.281
26/6	2.810	-2.326	2.978	-2.339	3.149	-2.353	3.325	-2.369	3.505	-2.389	3.689	-2.414	3.878	-2.446
27/6	2.799	-2.444	2.965	-2.463	3.135	-2.484	3.308	-2.507	3.484	-2.533	3.664	-2.564	3.846	-2.601
28/6	2.783	-2.561	2.948	-2.586	3.116	-2.613	3.287	-2.641	3.460	-2.672	3.635	-2.708	3.812	-2.748
29/6	2.763	-2.678	2.928	-2.708	3.094	-2.739	3.263	-2.771	3.433	-2.807	3.604	-2.845	3.777	-2.887
30/6	2.740	-2.794	2.904	-2.828	3.069	-2.862	3.236	-2.898	3.404	-2.936	3.573	-2.976	3.742	-3.021
31/6	2.715	-2.910	2.879	-2.947	3.043	-2.984	3.208	-3.022	3.374	-3.063	3.540	-3.105	3.707	-3.160
32/6	2.689	-3.025	2.851	-3.064	3.014	-3.104	3.178	-3.144	3.342	-3.186	3.507	-3.229	3.672	-3.274
33/6	2.660	-3.140	2.822	-3.181	2.985	-3.222	3.148	-3.264	3.311	-3.307	3.474	-3.351	3.637	-3.396
34/6	2.631	-3.255	2.793	-3.297	2.954	-3.339	3.117	-3.382	3.279	-3.425	3.441	-3.470	3.603	-3.515
35/6	2.601	-3.369	2.762	-3.412	2.924	-3.455	3.085	-3.498	3.247	-3.542	3.409	-3.587	3.570	-3.632
36/6	2.570	-3.484	2.731	-3.527	2.893	-3.571	3.054	-3.614	3.215	-3.658	3.376	-3.703	3.537	-3.748
37/6	2.540	-3.598	2.701	-3.642	2.862	-3.685	3.023	-3.729	3.184	-3.773	3.344	-3.818	3.505	-3.862
38/6	2.509	-3.712	2.669	-3.756	2.830	-3.800	2.991	-3.844	3.152	-3.888	3.313	-3.932	3.474	-3.977
39/6	2.477	-3.827	2.638	-3.871	2.799	-3.915	2.960	-3.959	3.121	-4.003	3.281	-4.047	3.442	-4.091
40/6	2.446	-3.941	2.607	-3.985	2.768	-4.029	2.929	-4.073	3.089	-4.117	3.250	-4.161	3.411	-4.205
41/6	2.415	-4.055	2.576	-4.099	2.736	-4.143	2.897	-4.187	3.058	-4.232	3.219	-4.275	3.380	-4.319
42/6	2.384	-4.169	2.544	-4.213	2.705	-4.257	2.866	-4.301	3.027	-4.345	3.187	-4.389	3.348	-4.433
43/6	2.352	-4.284	2.513	-4.328	2.674	-4.372	2.835	-4.416	2.996	-4.460	3.156	-4.504	3.317	-4.548
44/6	2.321	-4.398	2.482	-4.442	2.643	-4.486	2.803	-4.530	2.964	-4.574	3.125	-4.618	3.286	-4.662

TABLE VII—TABULATED VALUES OF THE INTEGRALS  $\alpha$  AND  $\beta$  FOR A RANGE OF  $|(\Phi-\Phi_0)|$   
 [Computational methods given in appendix G]

$ (\Phi-\Phi_0) $	$\alpha^{(1)}$	$\Delta I = \Delta \alpha$		$\beta^{(1)}$	$\Delta I = \Delta \beta$	
		$\Delta \alpha$ ( $\Delta \Phi = \pi/24$ )	$\Delta \alpha$ ( $\Delta \Phi = 2\pi/24$ )		$\Delta \beta$ ( $\Delta \Phi = \pi/24$ )	$\Delta \beta$ ( $\Delta \Phi = 2\pi/24$ )
0	0			0		
1( $\pi/24$ )	.000373	0.000373	0.002970	-.396937	-0.396937	-0.611660
2( $\pi/24$ )	.002970	.002970		-.611660	-.214723	
3( $\pi/24$ )	.009942	.006972	.020331	-.756406	-.144746	-.242791
4( $\pi/24$ )	.023301	.013359		-.854451	-.096045	
5( $\pi/24$ )	.044875	.021574	.052976	-.916486	-.062035	-.094079
6( $\pi/24$ )	.076277	.031402		-.948530	-.032044	
7( $\pi/24$ )	.118897	.042620	.097632	-.954346	-.005816	.012092
8( $\pi/24$ )	.173909	.055012		-.936438	.017908	
9( $\pi/24$ )	.242283	.068374	.150903	-.896542	.039896	.100542
10( $\pi/24$ )	.324812	.082529		-.835896	.060646	
11( $\pi/24$ )	.422136	.097324	.209951	-.755399	.080497	.180181
12( $\pi/24$ )	.534763	.112627		-.655715	.099684	
13( $\pi/24$ )	.663098	.128335	.272697	-.537338	.118377	.255075
14( $\pi/24$ )	.807460	.144362		-.400640	.136698	
15( $\pi/24$ )	.968096	.160636	.337741	-.245901	.154739	.327305
16( $\pi/24$ )	1.146201	.177105		-.073335	.172566	
17( $\pi/24$ )	1.338926	.193725	.404188	.116897	.190232	.398006
18( $\pi/24$ )	1.549389	.210463		.324671	.207774	
19( $\pi/24$ )	1.776679	.227290	.471478	.548892	.225221	.467817
20( $\pi/24$ )	2.020867	.244188		.792488	.242596	
21( $\pi/24$ )	2.282008	.261141	.539276	1.052403	.259915	.537106
22( $\pi/24$ )	2.560143	.278135		1.329594	.277191	
23( $\pi/24$ )	2.855304	.295161	.607373	1.624029	.294435	.606089
24( $\pi/24$ )	3.167516	.312212		1.935883	.311654	
25( $\pi/24$ )	3.496799	.329283	.675652	2.264536	.328853	.674890
26( $\pi/24$ )	3.843168	.346369		2.610573	.346037	
27( $\pi/24$ )	4.206633	.363465	.744035	2.973783	.363210	.743585
28( $\pi/24$ )	4.587203	.380570		3.354158	.380375	
29( $\pi/24$ )	4.984885	.397682	.812482	3.751689	.397531	.812215
30( $\pi/24$ )	5.399685	.414800		4.166373	.414684	
31( $\pi/24$ )	5.831607	.431922	.880967	4.598205	.431832	.880808
32( $\pi/24$ )	6.280652	.449045		5.047181	.448976	
33( $\pi/24$ )	6.746825	.466173	.949474	5.513301	.466120	.949380
34( $\pi/24$ )	7.230126	.483301		5.996561	.483260	
35( $\pi/24$ )	7.730557	.500431	1.017993	6.496961	.500400	1.017938
36( $\pi/24$ )	8.248119	.517562		7.014499	.517538	
37( $\pi/24$ )	8.782813	.534694	1.086521	7.549175	.534676	1.086488
38( $\pi/24$ )	9.334640	.551827		8.100887	.551812	
39( $\pi/24$ )	9.903690	.568960	1.155053	8.669936	.568949	1.155034
40( $\pi/24$ )	10.489693	.586093		9.256021	.586085	
41( $\pi/24$ )	11.092920	.603227	1.223588	9.859241	.603220	1.223576
42( $\pi/24$ )	11.713281	.620361		10.479597	.620356	
43( $\pi/24$ )	12.350777	.637496	1.292125	11.117089	.637492	1.292118
44( $\pi/24$ )	13.005406	.654629		11.771715	.654626	
45( $\pi/24$ )	13.677170	.671764	1.360662	12.443477	.671762	1.360658
46( $\pi/24$ )	14.366068	.688898		13.132273	.688896	
47( $\pi/24$ )	15.072101	.706033	1.429200	13.838405	.706032	1.429196
48( $\pi/24$ )	15.795268	.723167		14.561571	.723166	
49( $\pi/24$ )	16.535571	.740303	1.497739	15.301873	.740302	1.497738
		.757436			.757436	

<sup>(1)</sup> For negative values of  $(\Phi-\Phi_0)$  the signs of  $\alpha$  and  $\beta$  change, but the signs of  $\Delta\alpha$  and  $\Delta\beta$  remain unchanged.

TABLE VII—TABULATED VALUES OF THE INTEGRALS  $\alpha$  AND  $\beta$  FOR A RANGE OF  $|\Phi - \Phi_0|$ —Concluded.

[Computation methods given in appendix G.]

$ \Phi - \Phi_0 $	$\alpha^{(1)}$	$\Delta I = \Delta \alpha$		$\beta^{(1)}$	$\Delta I = \Delta \beta$	
		$\frac{\Delta \alpha}{(\Delta \Phi = \pi/24)}$	$\frac{\Delta \alpha}{(\Delta \Phi = 2\pi/24)}$		$\frac{\Delta \beta}{(\Delta \Phi = \pi/24)}$	$\frac{\Delta \beta}{(\Delta \Phi = 2\pi/24)}$
50( $\pi/24$ )	17.293007			16.059309		
51( $\pi/24$ )	18.067579	0.774572	1.566278	16.833880	0.774571	1.566276
52( $\pi/24$ )	18.859285	.791706		17.625585	.791705	
53( $\pi/24$ )	19.668125	.808840	1.634816	18.434426	.808841	1.634816
54( $\pi/24$ )	20.494101	.825976		19.260401	.825975	
55( $\pi/24$ )	21.337211	.843110	1.703355	20.103511	.843110	1.703354
56( $\pi/24$ )	22.197456	.860245		20.963755	.860244	
57( $\pi/24$ )	23.074835	.877379	1.771893	21.841135	.877380	1.771894
58( $\pi/24$ )	23.969349	.894514		22.735949	.894514	
59( $\pi/24$ )	24.880998	.911649	1.840433	23.647298	.911649	1.840433
60( $\pi/24$ )	25.809782	.928784		24.576082	.928784	
61( $\pi/24$ )	26.755694	.945912	1.908968	25.521994	.945912	1.908968
62( $\pi/24$ )	27.718750	.963056		26.485050	.963056	
63( $\pi/24$ )	28.698940	.980190	1.977507	27.465240	.980190	1.977507
64( $\pi/24$ )	29.696257	.997317		28.462557	.997317	
65( $\pi/24$ )	30.710717	1.014460	2.046044	29.477017	1.014460	2.046044
66( $\pi/24$ )	31.742311	1.031594		30.508611	1.031594	
67( $\pi/24$ )	32.791033	1.048722	2.114585	31.567333	1.048722	2.114585
68( $\pi/24$ )	33.856896	1.065863		32.623196	1.065863	
69( $\pi/24$ )	34.939895	1.082999	2.183123	33.706195	1.082999	2.183123
70( $\pi/24$ )	36.040029	1.100134		34.806329	1.100134	
71( $\pi/24$ )	37.157289	1.117280	2.251663	35.923589	1.117280	2.251663
72( $\pi/24$ )	38.291692	1.134403		37.057992	1.134403	
73( $\pi/24$ )	39.443230	1.151538	2.320201	38.209530	1.151538	2.320201
74( $\pi/24$ )	40.611893	1.168663		39.378193	1.168663	
75( $\pi/24$ )	41.797701	1.185808	2.388740	40.564001	1.185808	2.388740
76( $\pi/24$ )	43.000643	1.202942		41.766943	1.202942	
77( $\pi/24$ )	44.220710	1.220067	2.457279	42.987010	1.220067	2.457279
78( $\pi/24$ )	45.457922	1.237212		44.224222	1.237212	
79( $\pi/24$ )	46.712269	1.254347	2.525818	45.478569	1.254347	2.525818
80( $\pi/24$ )	47.983750	1.271481		46.750050	1.271481	
81( $\pi/24$ )	49.272356	1.288606	2.594357	48.038656	1.288606	2.594357
82( $\pi/24$ )	50.578107	1.305751		49.344407	1.305751	
83( $\pi/24$ )	51.900992	1.322885	2.662895	50.667292	1.322885	2.662895
84( $\pi/24$ )	53.241002	1.340010		52.007302	1.340010	
85( $\pi/24$ )	54.598168	1.357156	2.731435	53.364458	1.357156	2.731435
86( $\pi/24$ )	55.972447	1.374289		54.738747	1.374289	
87( $\pi/24$ )	57.363861	1.391414	2.799974	56.130161	1.391414	2.799973
88( $\pi/24$ )	58.772421	1.408560		57.538720	1.408560	
89( $\pi/24$ )	60.198115	1.425694	2.868512	58.964415	1.425694	2.868513
90( $\pi/24$ )	61.640933	1.442818		60.407233	1.442818	
91( $\pi/24$ )	63.100897	1.459964	2.937052	61.867197	1.459964	2.937052
92( $\pi/24$ )	64.577995	1.477098		63.344295	1.477098	
93( $\pi/24$ )	66.072228	1.494233	3.005590	64.838528	1.494233	3.005590
94( $\pi/24$ )	67.583535	1.511357		66.349885	1.511357	
95( $\pi/24$ )	69.112088	1.528503	3.074130	67.878388	1.528503	3.074130
96( $\pi/24$ )	70.657725	1.545637		69.424025	1.545637	
97( $\pi/24$ )	72.220486	1.562761	3.142668	70.986786	1.562761	3.142668
98( $\pi/24$ )	73.800393	1.579907		72.566893	1.579907	
99( $\pi/24$ )	75.397435	1.597042	3.211206	74.163735	1.597042	3.211206
100( $\pi/24$ ) <sup>(2)</sup>	77.011599	1.614164		75.777899	1.614164	

(1) For negative values of  $(\Phi - \Phi_0)$  the signs of  $\alpha$  and  $\beta$  change, but the signs of  $\Delta \alpha$  and  $\Delta \beta$  remain unchanged.  
 (2) For values of  $|\Phi - \Phi_0| > 100(\pi/24)$  use equation (G2) for  $\alpha$  and equation (G7) for  $\beta$ .

TABLE VIII—COMPARISON OF ELBOW DESIGNS OBTAINED FROM SOLUTIONS BY RELAXATION METHODS AND BY GREEN'S FUNCTION

[Linearized compressible flow; prescribed velocity distribution given in figs. 2 and 22.]

$\phi$	$\Psi=0$ (Inner wall)									$\Psi=\pi/2$ (Outer wall)								
	Q	q	Solution by relaxation methods (Part I)			Solution by Green's function (Part II)			Q	q	Solution by relaxation methods (Part I)			Solution by Green's function (Part II)				
			x	y	$\theta$ (deg)	x	y	$\theta$ (deg)			x	y	$\theta$ (deg)	x	y	$\theta$ (deg)		
-22( $\pi/24$ )	0.5000	0.4009	-2.466	-0.769	0	-2.466	-0.769	0	0.5000	0.4009	-2.466	0.770	0	-2.466	0.770	0		
-20( $\pi/24$ )	.5000	.4009	-2.241	-.769	.01	-2.241	-.769	.01	.5000	.4009	-2.241	.770	-.01	-2.241	.770	-.01		
-18( $\pi/24$ )	.5000	.4009	-2.016	-.769	.01	-2.016	-.769	.01	.5000	.4009	-2.016	.770	-.01	-2.016	.770	-.01		
-16( $\pi/24$ )	.5000	.4009	-1.791	-.769	.02	-1.791	-.769	.02	.5000	.4009	-1.791	.779	-.02	-1.791	.779	-.02		
-14( $\pi/24$ )	.5000	.4009	-1.566	-.768	.03	-1.566	-.768	.03	.5000	.4009	-1.566	.770	-.03	-1.566	.770	-.03		
-12( $\pi/24$ )	.5000	.4009	-1.341	-.768	.05	-1.341	-.768	.05	.5000	.4009	-1.341	.769	-.05	-1.341	.770	-.05		
-10( $\pi/24$ )	.5000	.4009	-1.116	-.768	.08	-1.116	-.768	.08	.5000	.4009	-1.116	.769	-.08	-1.116	.769	-.08		
-8( $\pi/24$ )	.5000	.4009	-.891	-.768	.14	-.891	-.768	.14	.5000	.4009	-.891	.769	-.13	-.891	.769	-.13		
-6( $\pi/24$ )	.5000	.4009	-.666	-.767	.24	-.666	-.767	.24	.5000	.4009	-.666	.768	-.21	-.666	.768	-.22		
-4( $\pi/24$ )	.5000	.4009	-.441	-.766	.40	-.441	-.766	.41	.5000	.4009	-.441	.767	-.35	-.441	.767	-.36		
-2( $\pi/24$ )	.5000	.4009	-.216	-.765	.70	-.216	-.765	.74	.5000	.4009	-.216	.765	-.56	-.216	.765	-.59		
0	.5000	.4009	.008	-.760	1.31	.010	-.759	1.52	.5000	.4009	.009	.763	-.92	.009	.762	-.91		
2( $\pi/24$ )	.5079	.4072	.255	-.752	2.82	.253	-.751	2.76	.5000	.4009	.224	.758	-1.45	.234	.758	-1.45		
4( $\pi/24$ )	.5283	.4243	.450	-.739	3.88	.449	-.738	3.76	.5000	.4009	.459	.751	-2.22	.459	.750	-2.21		
6( $\pi/24$ )	.5599	.4489	.656	-.724	4.00	.656	-.724	3.89	.5000	.4009	.684	.740	-3.28	.684	.740	-3.29		
8( $\pi/24$ )	.5932	.4780	.831	-.712	3.17	.850	-.713	3.07	.5000	.4009	.908	.725	-4.65	.908	.721	-4.68		
10( $\pi/24$ )	.6354	.5094	1.033	-.703	1.44	1.033	-.705	1.38	.5000	.4009	1.132	.703	-6.41	1.132	.702	-6.43		
12( $\pi/24$ )	.6754	.5415	1.205	-.703	-.88	1.205	-.704	-1.04	.5000	.4009	1.355	.674	-8.52	1.355	.673	-8.56		
14( $\pi/24$ )	.7149	.5732	1.386	-.710	-4.00	1.387	-.711	-4.04	.5000	.4009	1.577	.636	-11.04	1.577	.636	-11.06		
16( $\pi/24$ )	.7531	.6038	1.519	-.725	-7.48	1.519	-.727	-7.51	.5000	.4009	1.797	.587	-17.13	1.797	.588	-17.16		
18( $\pi/24$ )	.7894	.6329	1.663	-.749	-11.35	1.663	-.750	-11.37	.5000	.4009	2.013	.527	-20.67	2.013	.528	-20.69		
20( $\pi/24$ )	.8235	.6602	1.798	-.781	-15.52	1.799	-.783	-15.54	.5000	.4009	2.226	.455	-24.49	2.226	.453	-24.52		
22( $\pi/24$ )	.8550	.6855	1.928	-.822	-19.98	1.928	-.823	-19.98	.5000	.4009	2.434	.368	-29.49	2.434	.367	-29.52		
24( $\pi/24$ )	.8838	.7086	2.046	-.871	-24.62	2.046	-.871	-24.63	.5000	.4009	2.635	.268	-35.68	2.635	.266	-35.69		
26( $\pi/24$ )	.9097	.7293	2.157	-.928	-29.46	2.158	-.929	-29.47	.5000	.4009	2.829	.163	-42.89	2.828	.162	-42.90		
28( $\pi/24$ )	.9326	.7477	2.261	-.993	-34.45	2.261	-.994	-34.46	.5000	.4009	3.013	.094	-47.40	3.012	.092	-47.41		
30( $\pi/24$ )	.9524	.7636	2.356	-1.064	-39.56	2.356	-1.066	-39.57	.5000	.4009	3.186	-.120	-42.08	3.185	-.122	-42.09		
32( $\pi/24$ )	.9690	.7769	2.443	-1.143	-44.78	2.443	-1.144	-44.77	.5000	.4009	3.346	-.278	-46.93	3.346	-.279	-46.94		
34( $\pi/24$ )	.9822	.7875	2.521	-1.228	-50.02	2.521	-1.229	-50.01	.5000	.4009	3.492	-.449	-51.93	3.492	-.450	-51.94		
36( $\pi/24$ )	.9919	.7953	2.590	-1.318	-55.27	2.590	-1.320	-55.27	.5000	.4009	3.623	-.632	-57.08	3.623	-.633	-57.10		
38( $\pi/24$ )	.9979	.8001	2.650	-1.414	-60.49	2.650	-1.415	-60.47	.5000	.4009	3.736	-.826	-62.44	3.736	-.828	-62.49		
40( $\pi/24$ )	1.0000	.8018	2.701	-1.514	-65.56	2.701	-1.516	-65.51	.5000	.4009	3.830	-1.030	-68.16	3.829	-1.034	-68.37		
42( $\pi/24$ )	1.0000	.8018	2.743	-1.619	-70.32	2.744	-1.620	-70.29	.5079	.4072	3.901	-1.242	-74.80	3.901	-1.244	-74.75		
44( $\pi/24$ )	1.0000	.8018	2.777	-1.726	-74.81	2.777	-1.727	-74.78	.5283	.4243	3.947	-1.455	-81.03	3.945	-1.456	-81.01		
46( $\pi/24$ )	1.0000	.8018	2.803	-1.836	-78.97	2.803	-1.837	-78.96	.5599	.4489	3.969	-1.661	-88.33	3.969	-1.662	-88.23		
48( $\pi/24$ )	1.0000	.8018	2.820	-1.947	-82.82	2.821	-1.948	-82.80	.5932	.4780	3.974	-1.856	-96.69	3.975	-1.856	-96.69		
50( $\pi/24$ )	1.0000	.8018	2.831	-2.059	-86.28	2.831	-2.059	-86.26	.6354	.5094	3.966	-2.038	-94.16	3.967	-2.040	-94.19		
52( $\pi/24$ )	1.0000	.8018	2.835	-2.171	-89.37	2.836	-2.172	-89.34	.6754	.5415	3.950	-2.209	-96.63	3.951	-2.210	-96.68		
54( $\pi/24$ )	1.0000	.8018	2.834	-2.283	-92.07	2.834	-2.285	-92.04	.7149	.5732	3.927	-2.369	-99.11	3.928	-2.371	-99.07		
56( $\pi/24$ )	1.0000	.8018	2.827	-2.396	-94.40	2.828	-2.397	-94.37	.7531	.6038	3.900	-2.520	-100.83	3.901	-2.522	-100.80		
58( $\pi/24$ )	1.0000	.8018	2.817	-2.508	-96.39	2.817	-2.509	-96.36	.7894	.6329	3.871	-2.663	-102.17	3.872	-2.665	-102.14		
60( $\pi/24$ )	1.0000	.8018	2.803	-2.619	-98.05	2.803	-2.620	-98.03	.8235	.6602	3.841	-2.799	-103.19	3.842	-2.801	-103.17		
62( $\pi/24$ )	1.0000	.8018	2.786	-2.731	-99.44	2.786	-2.732	-99.42	.8550	.6855	3.809	-2.929	-103.95	3.810	-2.931	-103.91		
64( $\pi/24$ )	1.0000	.8018	2.766	-2.841	-100.56	2.767	-2.842	-100.55	.8838	.7086	3.777	-3.055	-104.49	3.778	-3.056	-104.48		
66( $\pi/24$ )	1.0000	.8018	2.744	-2.952	-101.47	2.745	-2.953	-101.45	.9097	.7293	3.746	-3.176	-104.84	3.746	-3.178	-104.83		
68( $\pi/24$ )	1.0000	.8018	2.721	-3.062	-102.18	2.722	-3.063	-102.17	.9226	.7477	3.714	-3.294	-105.03	3.715	-3.296	-105.03		
70( $\pi/24$ )	1.0000	.8018	2.697	-3.172	-102.73	2.698	-3.173	-102.72	.9524	.7636	3.683	-3.409	-105.10	3.684	-3.411	-105.09		
72( $\pi/24$ )	1.0000	.8018	2.672	-3.281	-103.14	2.672	-3.283	-103.14	.9690	.7769	3.653	-3.522	-105.05	3.654	-3.524	-105.01		
74( $\pi/24$ )	1.0000	.8018	2.646	-3.391	-103.45	2.647	-3.392	-103.44	.9822	.7875	3.623	-3.633	-104.91	3.624	-3.635	-104.91		
76( $\pi/24$ )	1.0000	.8018	2.620	-3.500	-103.66	2.620	-3.501	-103.66	.9919	.7953	3.594	-3.744	-104.71	3.595	-3.746	-104.72		
78( $\pi/24$ )	1.0000	.8018	2.593	-3.609	-103.81	2.594	-3.611	-103.79	.9979	.8001	3.565	-3.853	-104.49	3.566	-3.855	-104.49		
80( $\pi/24$ )	1.0000	.8018	2.566	-3.719	-103.90	2.567	-3.720	-103.90	1.0000	.8018	3.537	-3.962	-104.28	3.538	-3.964	-104.30		
82( $\pi/24$ )	1.0000	.8018	2.539	-3.828	-103.97	2.540	-3.829	-103.97	1.0000	.8018	3.510	-4.071	-104.18	3.510	-4.073	-104.19		